Framework
an urban + rural ecology

DELIVERABLE 18
Structural Testing

July 28, 2017

Report Deliverables:

A. Structural Test Results Summary
B. Test 1, 2, 3:
    1. CLT Crushing Test Report
    2. Bare CLT Wall Panel Test Report
    3. CLT In-Plane Shear Wall Test Report
C. Glulam Beam-Column Connection Test Report

Produced by: OSU, PSU

DISCLAIMERS REGARDING INSTRUMENTS OF SERVICE

By downloading or otherwise receiving the attached or enclosed information and/or document(s) (collectively, "Instruments of Service"), you ("Recipient") are deemed to agree to the following:

The Instruments of Service are provided solely for personal or non-commercial use. No part of the Instruments of Services may be reproduced, published, or transmitted for commercial purposes in any form or by any means, electronic, mechanical, photocopying, recording, or otherwise, whether or not in translated form, without the prior written permission of the owner of the rights in such Instruments of Service.

The Instruments of Service are provided without any representation, warranty, covenant or guaranty of any kind or nature, express or implied, and no liability or responsibility is assumed by any party (including without limitation the author, owner or distributor of the Instruments of Service) with respect to the use, application of, and/or reference to opinions, findings, conclusions, or recommendations included in the Instruments of Service. Recipient is responsible to verify all information. Accordingly, Recipient has no right to rely upon the Instruments of Service or any part thereof for any purpose or in any respect, including without limitation the accuracy, adequacy, quality, completeness or correctness thereof or its fitness for a particular purpose. The receipt and use of any Instruments of Service by Recipient is at Recipient's sole risk and without any liability whatsoever to any other party, including without limitation the author, owner, and distributor of the Instruments of Service.

Recipient acknowledges and agrees that the receipt of any Instruments of Service does not convey any property rights or licenses. All rights (including common law, statutory or other reserved rights) in the Instruments of Service shall remain with the party who owned such rights prior to receipt.

The author, owner, and distributor of the Instruments of Service have no obligation or liability whatsoever to Recipient with respect to the Instruments of Service or any information therein or use made thereof. To the fullest extent permitted by law, Recipient releases any and all claims of every kind or nature against the author, owner, and distributor of the Instruments of Service relating to or that arises in any manner out of Recipient's receipt or use of the Instruments of Service.

Recipient acknowledges that anomalies and errors can be introduced into electronic files when it is transferred or used in a different or incompatible computer systems. Further, if any translation of the information and data on electronic files occurs then Recipient acknowledges that such translation cannot be accomplished without the possible introduction of inexactitudes, anomalies, or errors. Recipient agrees and acknowledges that electronic files transferred to, used, altered or translated by Recipient may not necessarily show the same information and data, or in the same format, as the hard copy originals thereof. Recipient agrees to assume all risks associated with such transfer, use, alteration and translation of electronic files, and to the fullest extent permitted by applicable law, to release all claims of every kind against the author, owner or distributor arising from, related to, or in any manner in connection with the transfer, use, alteration and translation of electronic files to or by Recipient.

The Instruments of Service were developed as an element in the design of a specific project, is provided for information only, and therefore is not intended to provide professional advice with respect to any other project or activity. Recipient and users of the Instruments of Service are responsible for exercising independent professional knowledge and judgment in the application of this information.

REPORT DELIVERABLE 18-A:
Structural Test Results Summary

Structural Testing		
TEST	**DESCRIPTION**	**STATUS**
1	CLT Crushing Test (Oregon State University)	**Successful.** The objective of the cross-laminated timber (CLT) crushing tests is to determine the stress-strain relationship of the CLT walls out to ultimate failure (i.e., strain at which strength loss falls below 20% of peak strength). The purpose of this is to determine the stress-strain relationship of the CLT panels to be used in the project to aid in the design/modeling at the end, or "toe", of the rocking wall. Six bare panel specimens, (3) specimens with confining self-tapping screws, and (3) steel plated specimens were successfully tested under monotonic, quasi-static loading. The initial data from the tests has been received and are being evaluated to determine the appropriate amount of reinforcing/protection (if any) is required to limit damage to the toe of the rocking wall under the design basis and maximum considered earthquakes.
2	Bare CLT Wall Panel Test (Oregon State University)	**Successful.** The objective of the bare CLT wall panel tests is to assess the material properties of the CLT wall panels to be used in the building, specifically the equivalent linear flexural and shear stiffness of the bare CLT wall panels. This is required to accurately model and design the CLT wall panels, which is of particular importance for tall wood buildings in high seismic regions. Two 3-point bending tests of CLT9 wall panels (5ft x 20ft) under cyclic, quasi-static loading were successfully completed to obtain the material properties sought. The values determined are near the upper bound of preliminary predictions.
3	CLT In-Plane Shear Wall Test (Oregon State University)	**Successful. – Epoxy Dowel** **Successful. – Shear Key** **Unsuccessful. – Epoxy HSK** The objective of the CLT wall panel in-plane shear tests is to assess the capacity and stiffness (flexural and shear) of the splices to be used in the project. Three splice types were tested (2 each) under the same loading protocol as for the bare CLT wall panel tests. These include an epoxy doweled splice connection, a steel shear key splice connection and an epoxy HSK steel plate connection. The epoxy dowel and shear key splice options have been successfully completed and both demonstrated good performance, although there were some fabrication difficulties with the Shear Key splices. The HSK connection had fabrication issues and failed prematurely. Based upon the test results, costs, and fabrication difficulty the Epoxy Dowel splice connection was chosen for the project.

4	Glulam Beam – Column Connection Test (Portland State University)	**Successful.** The objective of the glulam timber (GLT) beam-to-column connection tests is to demonstrate that the proposed connection is capable of withstanding cyclic deformations out to the drifts expected in the building at the risk-targeted maximum considered earthquake without loss of gravity-carrying capacity. This is often referred to as a deformation-compatibility check. Three full scale, fully loaded, connections have been successfully tested under cyclic, quasi-static lateral loading, demonstrating that this objective has been achieved. The tests indicate that the connection is expected to sustain very little to no damage up to 2.5%, which exceeds the expected maximum considered earthquake (MCE) inter story drift of 2.2%. Damage up to 4.5% drift is limited to replaceable disc springs and damage at 6% (greater than 3x design displacement) is limited to the replaceable disc springs and minor localized crushing at the beam-to-column interface.

REPORT DELIVERABLE 18-B:
Test 1, 2, 3:
1. CLT Crushing Test Report
2. Bare CLT Wall Panel Test Report
3. CLT In-Plane Shear Wall Test Report

Structural Testing for the Framework Project

by

Andre Barbosa, Ph.D.,

Arijit Sinha, Ph.D.,

and

Christopher Higgins, Ph.D., P.E.

June 20, 2017

ACKNOWLEDGEMENTS

Financial support for this research was provided by the Framework Project sponsored by the U.S Tall Wood Building Competition a partnership between the USDA, Softwood Lumber Board, and the Binational Softwood Lumber Council. In addition, the Authors acknowledge the support of the Tall Wood Design Institute, which subsidized part of the faculty time for this effort. The findings and conclusions of this work are solely those of the authors.

ABSTRACT

A series of large-scale cross-laminated timber wall panels were tested in compression loading and under in-plane shear loading. The objective of the series of physical tests is to provide data on structural performance of building subassemblies for the Framework project and to increase the state of knowledge of mass-timber systems for building applications for use in the United States more broadly.

Cross-laminated timber (CLT) crushing tests were performed to determine the stress-strain relationship of the CLT walls out to ultimate failure (i.e., strain at which strength loss falls below 20% of peak strength). Testing included monotonic, quasi-static loading uniform compression tests developed on 18-inch-wide specimen of CLT5 (5-ply CLT) with a specimen length of 5 ft. The specimens were supported at mid-length to prevent buckling. Six (6) specimens of bare CLT5 and six (6) specimens of CLT5 with self-tapping screws with different arrangements were tested.

CLT wall panel tests were also performed to assess the material equivalent stiffness properties of a bare CLT wall panel, and splice configurations in the built-up CLT wall panels. More specifically, the following results are presented in this report: (1) the equivalent flexural and shear stiffness of the bare CLT wall panels, and (2) the splice flexural and shear stiffness. Results for four (4) specimen tests are reported, including two (2) 5'x20' bare CLT9 specimens, designated as "bare panel 1" and "bare panel 2", and two (2) 5'x20' CLT9 with project specific splices, designated as "epoxy rod splice 1" and "epoxy rod splice 2", respectively.

Table of Contents

List of Figures

List of Tables

1 Introduction

This document presents results on structural testing performed to generate data that supports the Performance-based Design of the Framework building project to be built in Portland, Oregon, namely in support of facilitating the design of rocking CLT walls, which is developed by KPFF Consulting Engineers. A series of large-scale cross-laminated timber panels were tested in compression loading and CLT wall panels were tested under in-plane shear loading. The objective of the series of physical tests is to provide data on structural performance of building subassemblies for the Framework project and to increase the state of knowledge of mass-timber systems for building applications for use in the United States more broadly.

The objective of the crushing tests was to characterize the stress-strain relationship of the CLT wall panels when subjected to failure loads. The panels were loaded beyond the peak load until strength loss stabilized or after the strength loss was greater than 20%. Specimens with and without strengthening mechanisms were tested to characterize the following: (1) point at which crushing commences; (2) point beginning of strength degradation, (3) point at which strength degradation stabilizes, and (4) point of ultimate strain.

The objective of the CLT wall panel tests was to assess the engineering properties of a bare CLT wall panel, and for a splice configuration in the built-up CLT wall panel. More specifically, the following are presented: (1) the equivalent linear flexural and shear stiffness of the bare CLT wall panels, and (2) the splice flexural and shear stiffness. The panels were loaded beyond the failure point in cyclic loading that followed and results presented reflect the performance of the panels beyond the strict objectives of the testing performed.

2 Experimental Program

2.1 Overview

Several experimental tests were conducted to evaluate the structural performance of CLT5 in compression and of CLT9 under in-plane shear loading. Tests reported in this document include:

1) CLT Crushing Tests: Twelve (12) CLT5 specimens. Six panels were tested as controls, while six other were tested with a strengthening mechanism installed to prevent buckling of the fiber ends of laminations and provide confinement at the ends of the panels.
2) CLT Wall Panel Tests: Four (4) CLT9 specimens. These are identified as (a) Bare Panel 1, (b) Bare Panel 2, (c) Epoxy Rod Panel 1, and Epoxy Rod Panel 2.

The CLT used in the specimens was CrossLam® produced by StructurLam of British Columbia, Canada, using MSR E-graded laminations. The timber in the panels consisted of spruce-pine-fir for all laminations. A water repellent was applied to then end grains in the shop. The CLT panels were fabricated to the required finished dimensions prior to shipping to the Structural Engineering Research Laboratory at Oregon State University (OSU).

Six (6) CLT control specimens for the compression testing were received and ready for testing, while the strengthening of six other specimens was assembled in the laboratory by specialized crew members from StructureCraft.

The CLT wall panels tested under in-plane shear loading that had splices were manufactured by StructureCraft and received at OSU ready for testing. Received specimens were stored in the laboratory under ambient conditions for testing. The specimens were then placed in different laboratory setups and tested.

Crushing tests were performed in the Wood Research Laboratory. CLT wall panel tests were performed at the Structural Engineering Research Laboratory. Details of the specimens and experimental methods are described in this chapter. Sketches of all CLT crushing specimens are shown in Appendix, as are all the reported CLT wall specimens. In addition, other wall specimens tested are also shown in Appendix, but results are not reported in this report, whose main objective is to report on the test results of the solutions used in support of the building performance-based design performed by KPFF Consulting Engineers.

2.2 CLT Crushing Tests

2.2.1 Specimen Descriptions

Twelve (12) CLT panels were received by Oregon State University for the CLT crushing tests. The panels were 18.0 inches wide, 6.9 inches in thickness, and 60 inches long. As received, the average moisture content of the panels was 15.5%, measured by a pin-type moisture meter. Six (6) panels were tested as controls, while six (6) others were tested with a strengthening mechanism installed to prevent buckling of the fiber ends and provide confinement at the ends. One mechanism used self-tapping screws (STS) drilled on the surface of the panels penetrating all the way through the thickness. The second mechanism used a steel U-plate installed at either ends of the panel along with the self-tapping screws (STS) on the surface of the panels.

2.2.2 Methods

The test set-up and instrumentation plan was peer-reviewed and approved prior to commencement of testing. The setup schematic for the compression testing and the instrumentation plan can be found in Appendix E1-E4. The compression tests were performed horizontally to ease the material handling process as well as for safety reasons. The setup is presented in Figure 2.1. The set up consisted of a 500-kip hydraulic actuator with a 20-in cylinder

travel attached to a reaction wall designed to withstand a moment of 3,000 kip-feet with allowable deflection of 0.01 in. The hydraulic actuator was laterally braced to prevent uplift that would in turn produce out-of-plane loads. The hydraulic actuator was fitted with a load cell to measure the applied force. A steel bulkhead was used as the base of the compression panel. The steel bulkhead was bolted to the strong floor using four anchor points. Each anchor point is a set of four (4), 1in diameter bolts. Each connection point is rated for 240 kip uplift (axial) and 360 kip lateral force. A steel plate was attached to the steel bulkhead, at the position where the base of the CLT panel rest against, to ensure an even surface for the panel to react against. The CLT panel was placed on 6-inch piece of plywood. A frictionless surface between the CLT panel and the plywood was provided using two greased high-density polyethylene sheets. On top of the panel and in line with the plywood, a buckling restraint mechanism consisting of C-channels and 0.75 in all threaded rods was installed. The details of buckling restraint along with schematic are found in Appendix E4. Alignment of the panels and the actuator load head was checked using a laser level.

A monotonic load was applied to the CLT panel using a steel plate between the head of the CLT panel and the actuator. The test was controlled by a constant rate of displacement of the hydraulic actuator. The rate of displacement of the actuator was 0.05 inch per minute until 80% of the post-peak load was achieved.

2.2.3 Instrumentation

Two linear variable differential transducers (LVDT) were used on either side of the panel to measure the compression along the panel's centerline. The scale of the LVDTs were +/- 2 inch with a resolution of 0.0002 inch and a gauge length of 48 inch. On either side of steel plates, LVDTs were used to measure the vertical displacement of the steel plates to ensure minimal slipping. In addition to LVDTs, the top surface of the panels was imaged and analyzed using digital

image correlation technique to obtain displacements and strain maps of the top surface. In DIC, two cameras take images of the specimen at a predetermined interval. These images taken when the specimen is under loading are correlated back to base image to form a strain and displacement profile of the surface. To ensure this tracking, the surface was painted black and speckled to provide unique pattern and contrast. Load, deflection of the load head, and LVDT deflection were continually monitored and logged using an automated data acquisition system. Using the monitored load and deflection data, load-deflection curves were generated for further analysis. DIC data was used to discern nuances in the data and support any observation.

2.3 CLT In-plane Shear Tests

2.3.1 Experimental Setup for CLT Wall Panels

All wall specimens were tested in a simply supported configuration on a 224 in. span length with a concentrated load applied at midspan. The loading frame with a typical specimen is shown schematically in Figure 2 and in Figure 3. A digital image of the setup is shown in Figure 4. Figure 5 shows a view of the setup from the south-east, including the "red beam" used to apply the axial load across the panels (see close-up in Figure 6). Since the test was performed under cyclic loading, the specimens were anchored down to the strong floor with four (4) 1.25 in. diameter A193-B7 threaded rods at each support location. The anchorages restricted uplift of the support ends, but provided negligible bending restraint. The threaded rods were hand tightened during assembly to bring surfaces into contact but not to produce initial compression loading. Prior to testing, the threaded rods were tied with wrenches to provide a tight fit and minimize initial testing slack.

To avoid crushing of the fibers at the supports, 16 in. x 16 in. steel plates were provided between the specimen and the top support beams that were anchored to the strong floor (see Figure 7) and bottom supports (see Figure 8a). Under the bottom supports, beams that were supported on

only one central point, that were installed to provide enough clearance for the experimental setup and instrumentation. The central point of the bottom support beams comprised of 2 in. diameter steel rollers that rested on a 1/2 in. thick steel strip to provide uniform contact across the concrete surface of the strong floor at the bearing location, as shown in Figure 8b.

2.3.2 Methods

Cyclic, quasi-static, loading in accordance with the abbreviated basic loading history in CUREE Publication No. W-02 were performed, except that trailing cycles were taken equal to the primary cycle (rather than 75% of it). The CUREE "delta" of 1.0 in. was set and maintained constant for all specimens for comparison purposes. Axial load was maintained constant at 135 kips. Following the CUREE protocol, the specimens were subjected to cyclic loading with increasing displacement amplitudes at a constant displacement rate of 0.01 in/sec until the target (CUREE "delta") displacement was achieved, at which point the displacement rate was increased to 0.025 in/sec until the end of the test.

Prior to testing, the moisture content was measured and recorded. The average measured moisture content for the test specimens at the time of each test ranged from 14.5 percent to 15.6 percent for all specimens.

2.3.3 Instrumentation Plan for CLT Wall Specimens

Thirty eight (38) sensors were used to monitor the behavior of each bare panel specimen during testing. This included three (3) displacement transducers to measure the vertical displacement of the specimen relative to the laboratory floor, thirty (30) displacement transducers to measure shear strains in different locations in the panels, two (2) LVDTs to measure diagonal strains in one of the panels, a load cell to measure the axial load applied with the hydraulic jack, a load cell to measure the applied actuator force, and lastly a displacement transducer to measure the actuator

displacement. For the splice specimens, forty seven (47) sensors were used. Typical instrument locations and channel reference labels are shown in Figure 9 and Figure 10, respectively. Other details are provided in appendix. In addition, the sensor and channel listings, as well as the raw data files were provided Excel files in BOX to KPFF due to the large size of the files.

The rigid body motion of the specimen (due to such things as non-conservative contact bearing at supports) was removed to provide the absolute specimen relative displacement by subtracting the support deformations. It is worth noting that the controlled displacement during testing was the absolute specimen relative displacement.

3 Experimental Results

The key results are reported here for four (4) experiments conducted in this research program. Results are reported in separate sections for each specimen configuration. Results were also provided in an electronic format and can be shared upon request and approval from KPFF Consulting Engineers due to the large size of the files.

3.1 CLT Crushing Tests

A summary of results is presented in Table 1. The average peak load for the control CLT panels was 387.6 kips with a coefficient of variation of 5%. The bulk modulus of elasticity (MOE) as calculated over 48" was 1.11 million psi. This calculation does not exclude the perpendicular laminations and hence it is reported as bulk MOE. The COV for bulk modulus is 7.2%. After strength modifications of the panels with STS and combination of STS and plates, the average ultimate load was 383.7 kips and 313.9 kips, respectively. There was no statistical difference between the maximum loads for the panels with two different treatments. However, a statistically significant difference in bulk MOE was observed between treatment with just STS and a combination of STS and end plates. The average bulk MOE with STS treatment was 1.05 million psi; with STS and end plates, the average bulk MOE was 1.17 million psi. When comparing the control specimen and the specimen with treatments (as a group) no significant difference is the bulk MOE was observed. The treatments did not contribute much in terms of peak load and bulk modulus.

Table 1 – Summary of CLT Crushing Test Results

Sample no.	Strengthening	As Tested MC (%)	RH (%)	Dimensions L (in)	W (in)	T (in)	Peak Load (kips)	Bulk MOE (10^6 Psi)	First onset of Yielding Load (kips)	Disp (in)	Onset of Buckling Load (kips)	Disp (in)	Delam. reaching 1' Load (kips)	Disp (in)
1	None	16.1	73	60	18.0	6.94	373.5	1.14	360	0.41	346	0.63	275	0.88
2	None	15.8	73	60	18.1	6.93	356.9	1.01	354	0.42	304	0.76	219	1.41
3	None	16.1	73	60	18.0	6.95	361.0	1.09	358	0.42	280	0.76	191	1.50
4	None	14.9	69	60	18.1	6.93	335.4	0.99	330	0.40	296	0.73	228	1.17
5	None	15.3	69	60	18.1	6.92	346.6	1.08	337	0.37	287	0.83	216	1.65
6	None	15.7	69	60	18.0	6.92	360.9	1.08	347	0.37	303	0.72	125	1.20
7	STS	14.8	81	60	18.0	6.93	382.9	1.12	376	1.53	348	2.30	97	2.11
8	STS	15.2	81	60	18.0	6.94	410.0	0.99	402	1.40	-	-	161	2.28
9	STS	15.5	79	60	18.1	6.93	358.2	1.04	354	1.03	296	1.69	97	2.52
10	STS and Steel plates	15.4	79	60	18.0	6.91	385.8	1.16	374	1.28	301	2.73	186	4.70
11	STS and Steel plates	16.0	79	60	18.0	6.94	383.2	1.19	379	1.00	297	2.40	152	3.50
12	STS and Steel plates	15.5	79	60	18.0	6.92	405.5	1.17	399	1.05	299	2.59	207	5.86

The contribution of treatment is vividly observed in shifting the load at which the first onset of yielding occurs. Moreover, the treatments affect the post peak behavior of the CLT panels. The panels with treatment were able to withstand high compressive deflection after ultimate load has been reached. Figure 11a and Figure 11b show the load deflection diagram of all the tests. Figure 11a shows the load-displacement curves for the six (6) specimens without any strengthening, while Figure 11b presents the load-deflection curve of the specimens with strengthening. As seen from Figure 11b, when there is connectivity through the thickness as provided by the STS, there is more added capacity in the panel before reaching post-peak 80% of the maximum load. The metal plates at the end further reinforce the post-peak behavior by providing added load carrying capacity for the same amount of deflection as compared to the samples with no treatment or with STS only. There is an additive effect from the metal plates, which is providing confinement to the wood fibers.

The treatments altered the failure progression in the CLT panels. The specimen without any treatment failed at random locations along the length. Since buckling was restrained, failure was mainly due to excessive crushing and ultimately leading to splitting of the fibers (or delamination) Figure 12a, b. This failure mode was completely absent in the specimen with treatments. The treatment with STS and steel plate forced the failure to occur near or within the steel plate (Figure 12d). The failure was due to crushing and localized buckling of the wood fiber. Wood continued to buckle as the testing progressed and in turn expanded the steel U plates as shown in Figure 12e. This was possible as the steel plate was unrestrained at one edge. The samples with STS only, also showed localized buckling failure (Figure 12c). The location of the visible failure was either at the end where the CLT panel is in contact with the steel plate or right below the buckling restraint.

Table 1 also presents the load at which first onset of yielding is observed, onset of buckling, as well as the load where delamination or separation of the fiber reach 1 inch. Corresponding strain values are also reported in Table 1. These observations were made after visual assessment of pictures and videos recorded during testing, DIC analysis, and corroborating those with testing notes. Additionally, visual estimates were checked against DIC data. The DIC tends to provide a lower bound for the onset of failure stresses and the corresponding strain when compared to those obtained from human observation. The definition of onset of failure that DIC uses is user dependent and if altered will provide different result. Since, there is no certain criteria for onset of failure, visual estimates are presented and relied upon. Using DIC strain maps can be created at different load points during the test as shown in Figure 14. These strain maps can provide valuable information about the condition of the specimen surface. A major limitation of DIC is that it only provides surface maps and state of the material inside specimen is subject to assumptions and interpretations. DIC analysis is ongoing and will be an integral part of manuscripts stemming from this work.

3.2 CLT Wall Tests

A summary of the key results is shown in this section for four (4) CLT wall specimens. Key results are the expected flexural and shear stiffness of the bare CLT panels as well as the expected flexural and shear stiffness of the spliced panels, which are obtained based on the physical testing of the large-scale CLT panels.

Figure 14 shows the moment-curvature results for the bare wall panel 1 for six (6) locations. The locations correspond to the locations of the center of the six instrumented regions (“panel zones” in Figure 9). A total of four (4) locations are reported for the east face of the panel, and two (2) locations for the west face of the panel. It can be seen that the tangent stiffness across the

instrumented panels are very similar across all locations. There are some jumps visible in the data; these correspond to instances when the instrumentation stopped recording useful data, due to loss of support of the instrumentation or due to local failure of the substrate laminations in shear at the specific locations where the sensors were installed.

Figure 15 summarizes the peak-to-peak effective flexural stiffness (EI) during the testing at six for the bare wall panel 1 for six (6) locations. The values of EI range from 10 x 10^8 to approximately 3 x 10^8.

Figure 16 shows the effective shear modulus results from CLT panel testing, where it can be observed that the effective shear modulus is a function of shear stress, with stiffness generally decreasing with increasing shear stress. It is worth noting that the tests were subjected to the constant axial compression during testing. The reduction of the peak-to-peak gross shear modulus versus shear stress is shown in Figure 17. It can be seen that the shear modulus ranges from about 110 ksi to 60 ksi. In addition, the general trend in reduction of the effective gross shear modulus as a function of increasing gross shear stress, the effect the increased number of cycles at the same level of stress reduces is only noticeable after approximately 0.45 the peak stresses reached. At this level of 0.45 the peak stress, the shear modulus is approximately equal to 78 ksi. At the highest levels of shear stress, a reduction of up 10% in the gross shear modulus was observed after three cycle of loading at the same values.

Figure 18 to Figure 21 show the moment-curvature results for the bare wall panel 2, peak-to-peak flexural stiffness versus curvatures, gross shear stress versus shear strains, and peak-to-peak shear modulus versus shear stress results for all locations in the panels. Trends shown in these figures are similar to the ones discussed in the results for the bare panel 1. It is worth noting that

results shown focus on the mainly linear range of the responses, to elucidate on trends of the responses of interest to approximately 50% to 60% of the peak loads achieved.

Figure 22 shows the moment versus rotation results at two splice locations of the epoxy rod splice panel specimen 1. It is worth noting that even though the specimen was symmetric with symmetric loading and both splices were at equal distances between supports and the loading point, minor asymmetries in strength and stiffness present in the splices, which are natural, highlight the fact that when one of the splines started accumulating damage, most of the nonlinearity of the specimen response was due to one splice only. In the epoxy rod splice panel 1 specimen, the damage concentrated over the north splice (shown as N-splice in the figure). It can be seen that the response was essentially linear up to a rotation of 0.002 rads, with minor change in stiffness at 50% of the peak moment achieved, which was at about 1000 kip-ft.

Figure 23 summarizes the peak-to-peak effective flexural stiffness (EI) during the testing at six for the epoxy rod splice wall panel 1 for six (6) locations, including the two splice locations and four locations that measured panel deformations in zones that did not cross the splices. The values of EI for regions outside the splices also range from 10×10^8 to approximately 3×10^8, which is similar to the range of values obtained for the bare panels. At about 5.0×10^{-5} (1/in.) curvature, the load in the testing was capped as the north splice started accumulating damage. At this level of deformation, it can be seen that the effective flexural stiffness across the splices is approximately two thirds of the effective flexural stiffness of the bare panels.

Figure 24 shows the shear force carried across the splice versus relative shear deformation between two adjacent faces of the splice, i.e. the relative shear deformation across the splice, at two splice locations of the epoxy rod splice panel 1. It can be seen that the splice response was essentially linear until approximately 0.10 to 0.15 in. and minor hysteresis was observed even at

0.2 in of relative deformation between both faces of the splice. The peak loaded exceeded 200 kips.

Figure 25 illustrates peak-to-peak gross shear modulus versus gross shear stress at the two splice locations and at three locations away from the splices, for the epoxy rod splice panel 1. The average results for the panels with the splices ("average splice") and the average results for locations at three locations away from the splices ("average bare") highlight the expected reduction of gross shear modulus due to the presence of the splices. In addition, it can be seen that the trend of the average curves is similar as the shear stress increases.

Figure 26 to Figure 29 show results the epoxy rod splice panel 1, similar to the ones shown in Figure 22 to Figure 25 that were discussed above for the epoxy rod splice panel 2. Results are very similar in terms of peak forces and deformations achieved. However, in the second epoxy rod splice panel specimen, the south splice accumulated damage instead of the north splice (see Figure 26). The trends in the peak-to-peak gross shear modulus versus gross shear strength are show a larger impact of the splice on the reduction of the shear modulus, whereby at peak load the shear modulus is reduced to nearly 40% of the shear modulus of the bare panels.

4 Conclusion

A series of tests were performed in support of the performance-based seismic design developed by KPFF Consulting Engineers for the Framework Project. The new benchmark data can be used for this project as well as for other projects that require similar data.

FIGURES

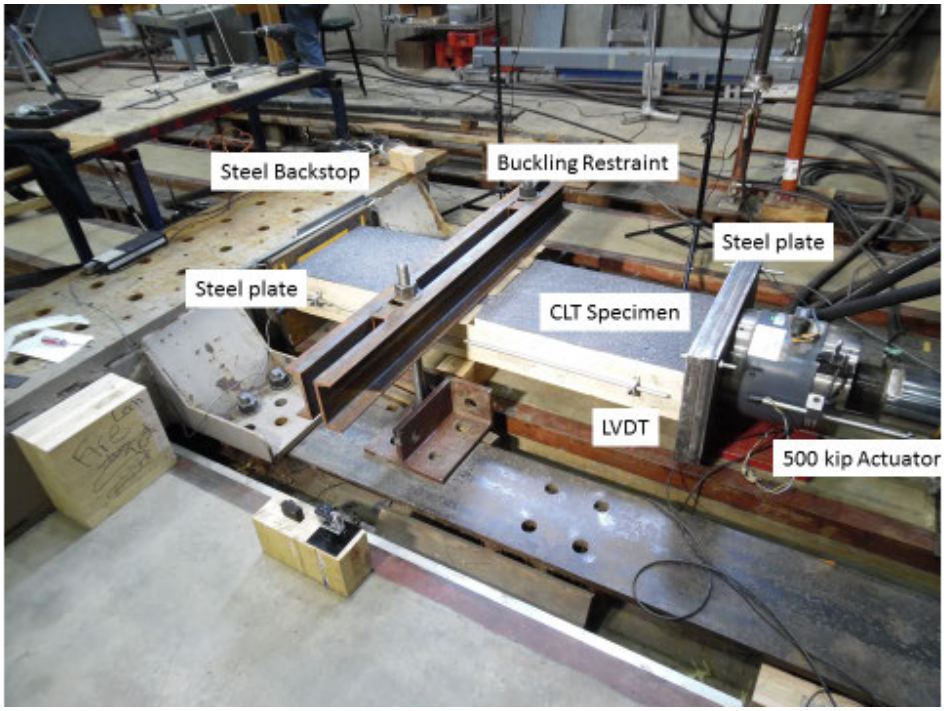

Figure 1 – CLT crushing test setup.

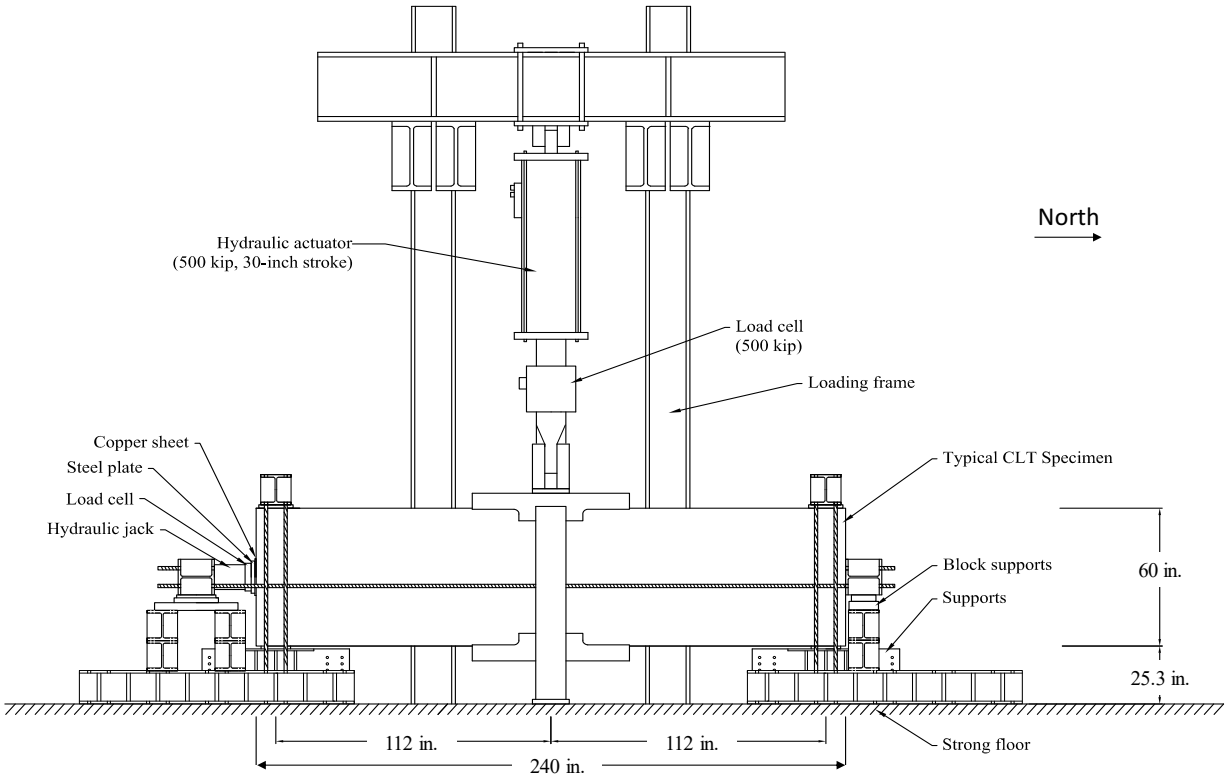

Figure 2 – Schematic elevation view of test setup with typical CLT9 wall specimen.

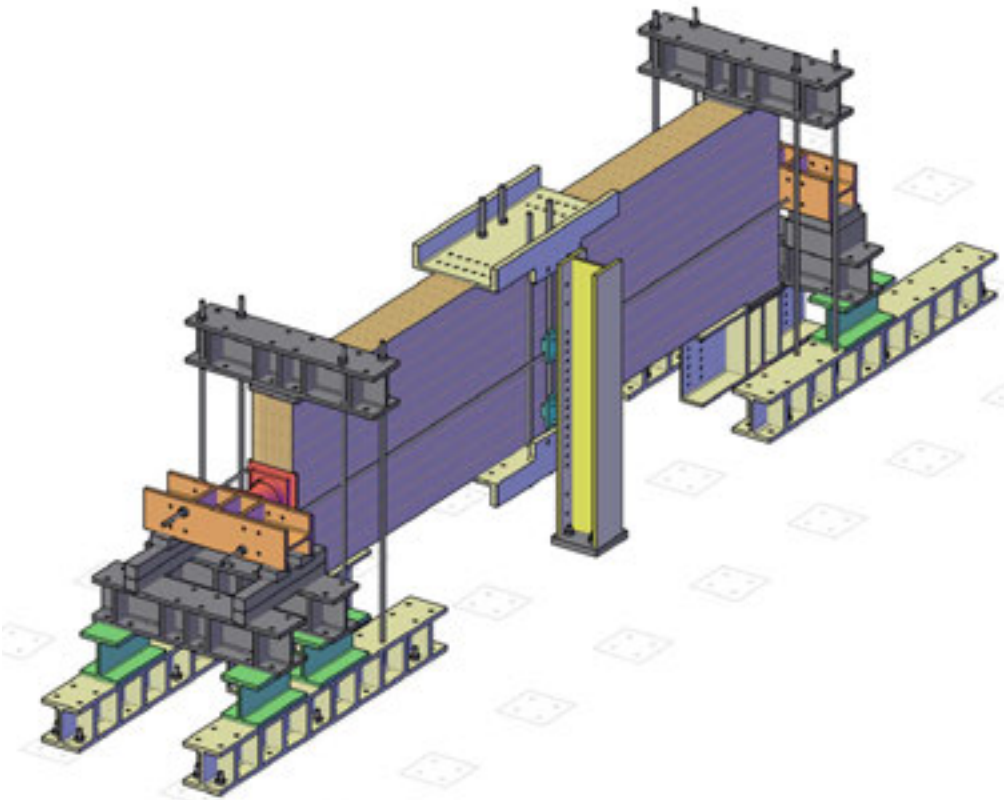

Figure 3 – Schematic 3-D view of test setup with typical CLT9 wall specimen.

Figure 4 – Overview of Test Setup for CLT9 Wall Specimens.

Figure 5 – View of Typical Specimen from the South-East.

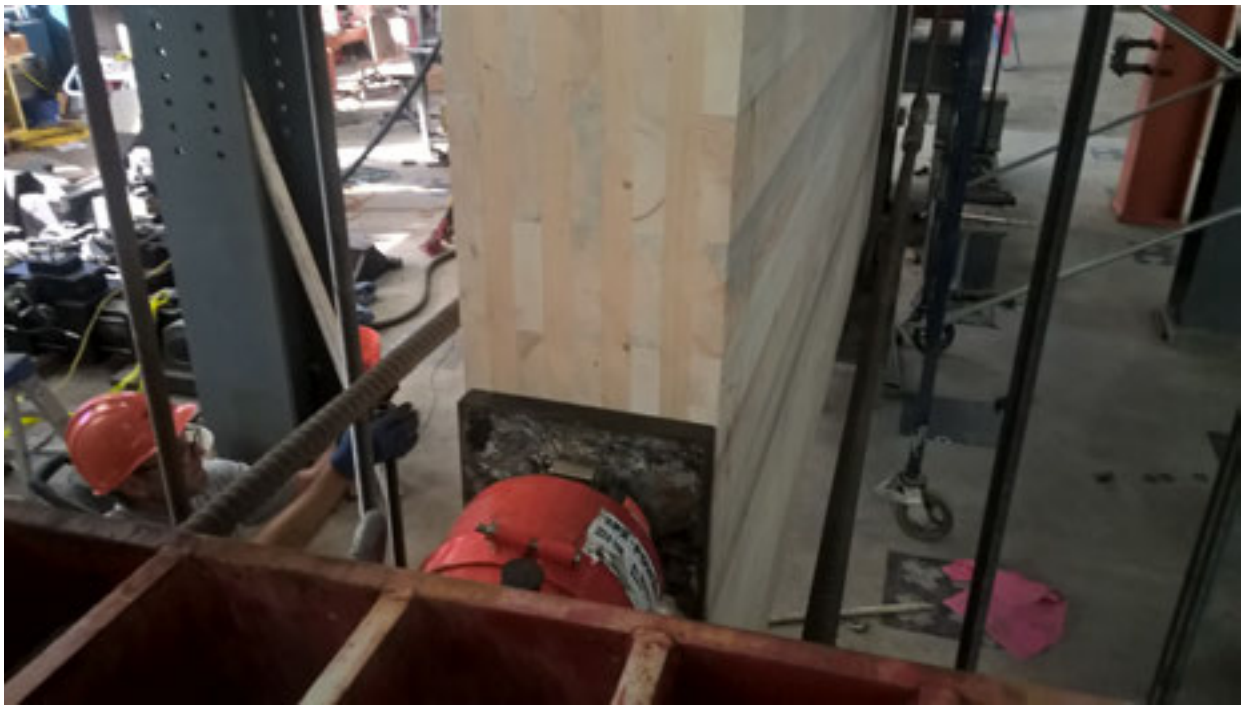

Figure 6 – Close-up of Axial-Load Jack and Load Cell (view from South).

Figure 7 – Close-up View of Top Support at the North End of the Specimen.

(a)

(b)

Figure 8 – Close-up View of Bottom Supports: (a) North support (view from east), (b) North support (view from the north) with one central roller visible under the support beam.

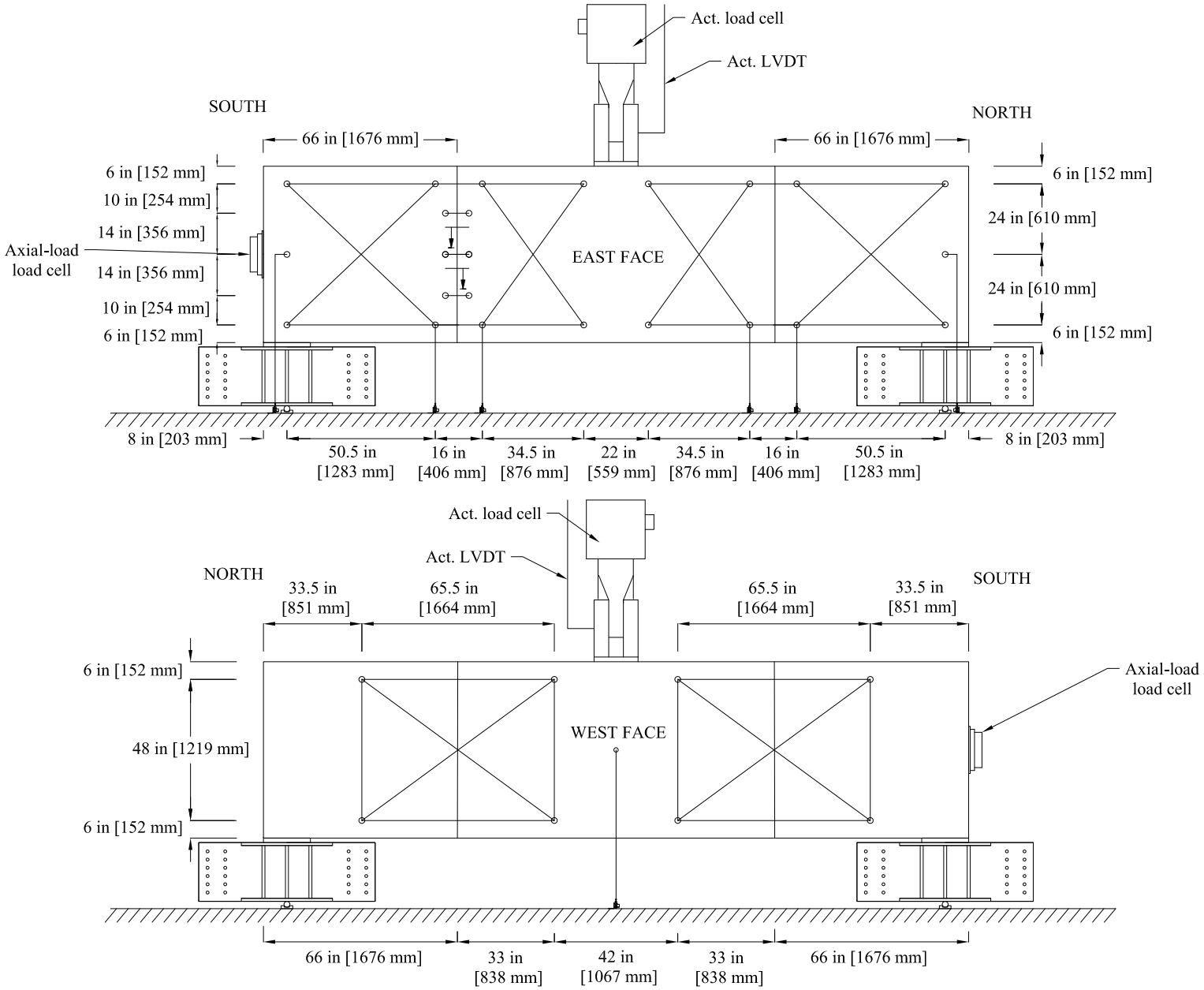

Figure 9 – Typical instrumentation layout for CLT wall specimens.

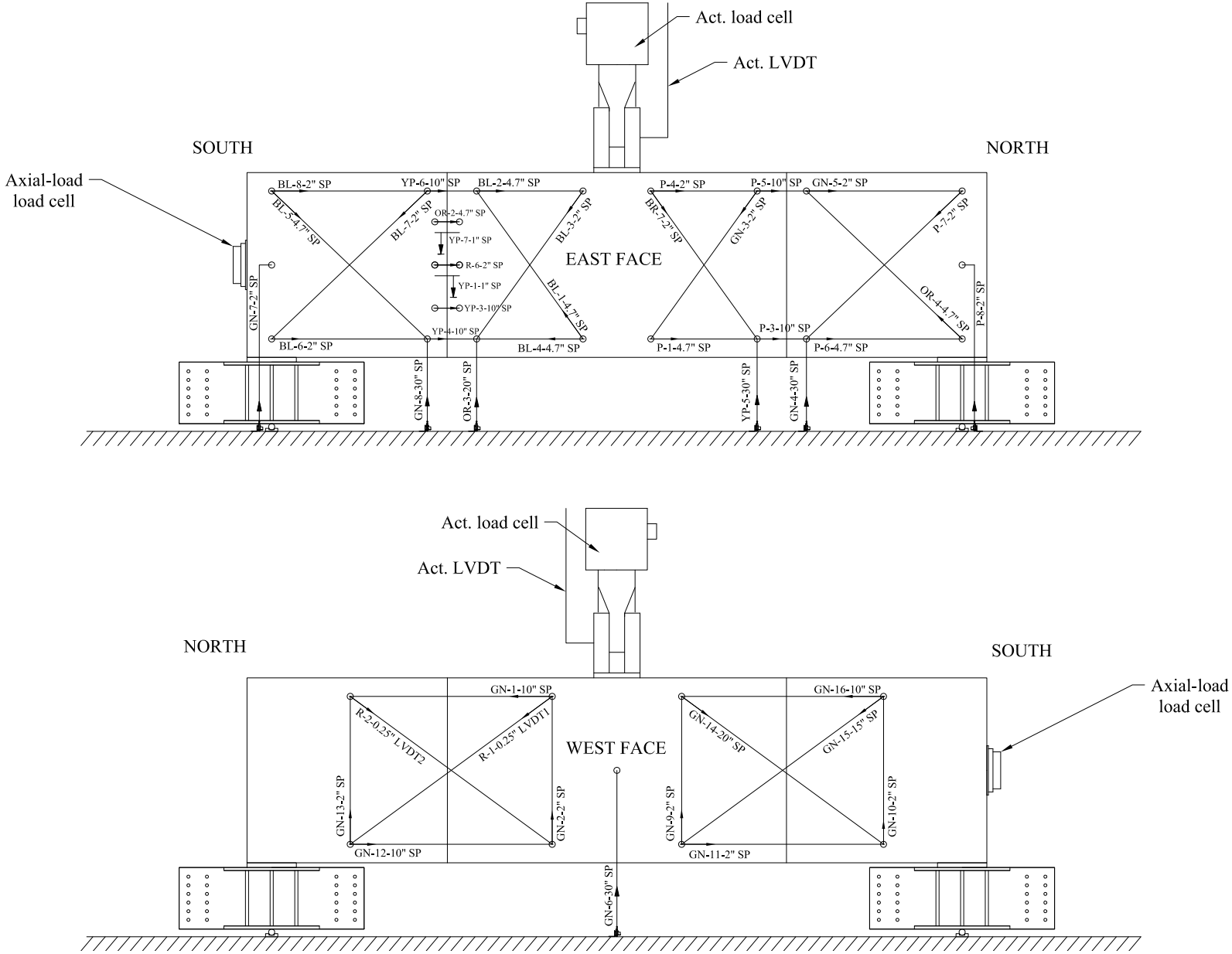

Figure 10 – Typical instrumentation labeling for CLT wall specimens.

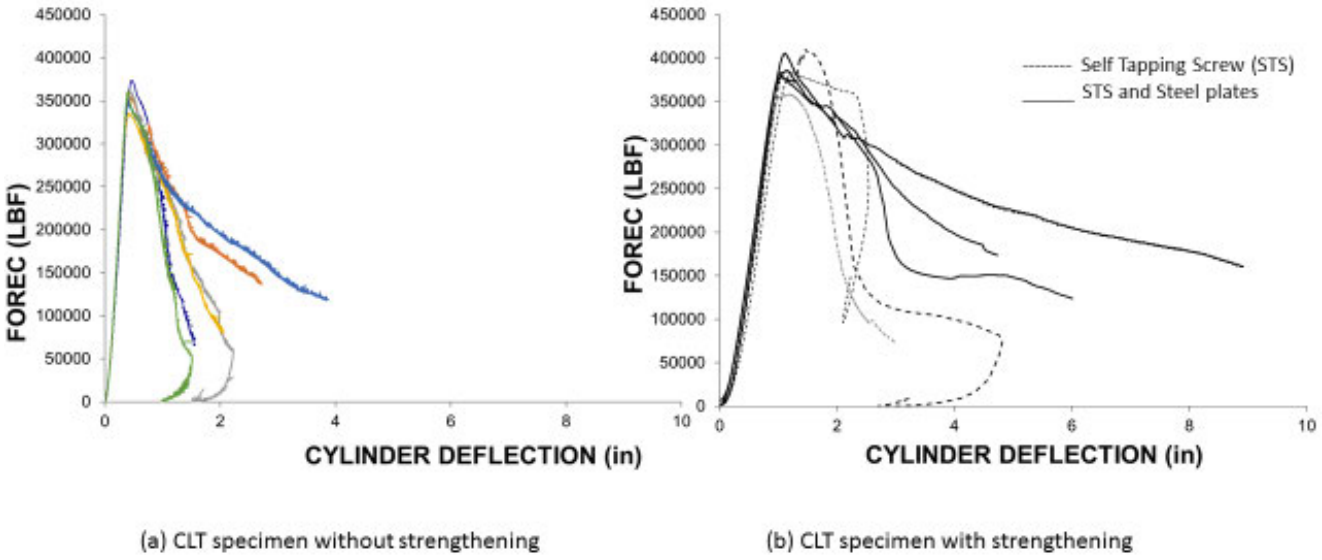

Figure 11 – Load deflection curves for all the specimens.

(a) Without strengthening test 4

(b) Without strengthening test 4

(c) With strengthening with STS

(d) With strengthening with STS and steel plate

(e) Opening up of the steel plate

Figure 12 – Different failure modes observed during CLT crushing test.

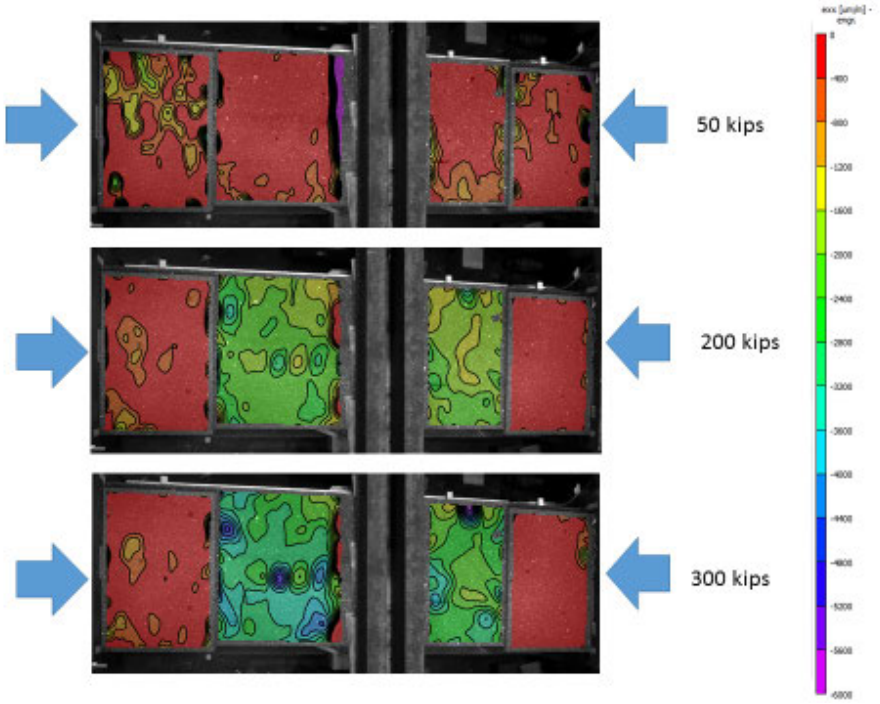

Figure 13 –Example of strain maps produced after analysis using digital image correlation.

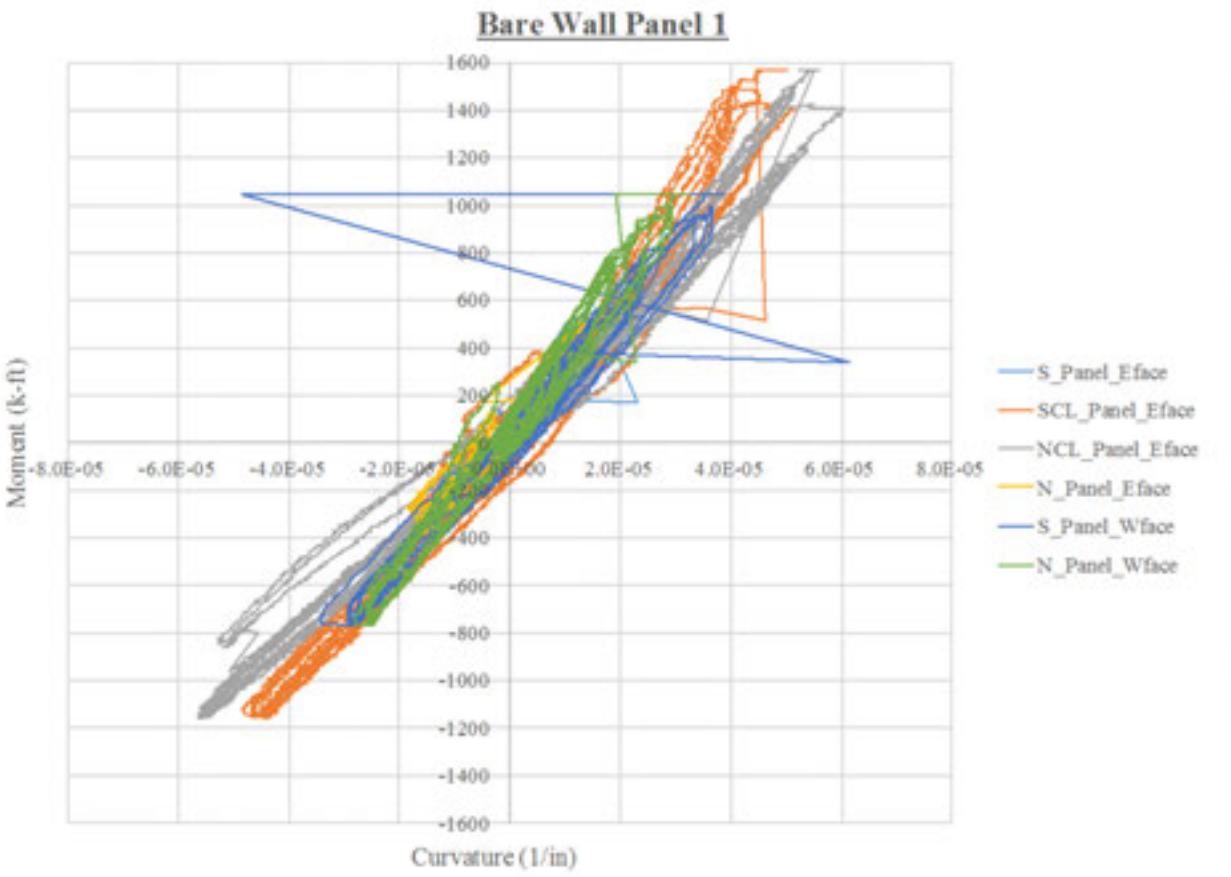

Figure 14 – Moment-curvature results at six locations of bare wall panel 1.

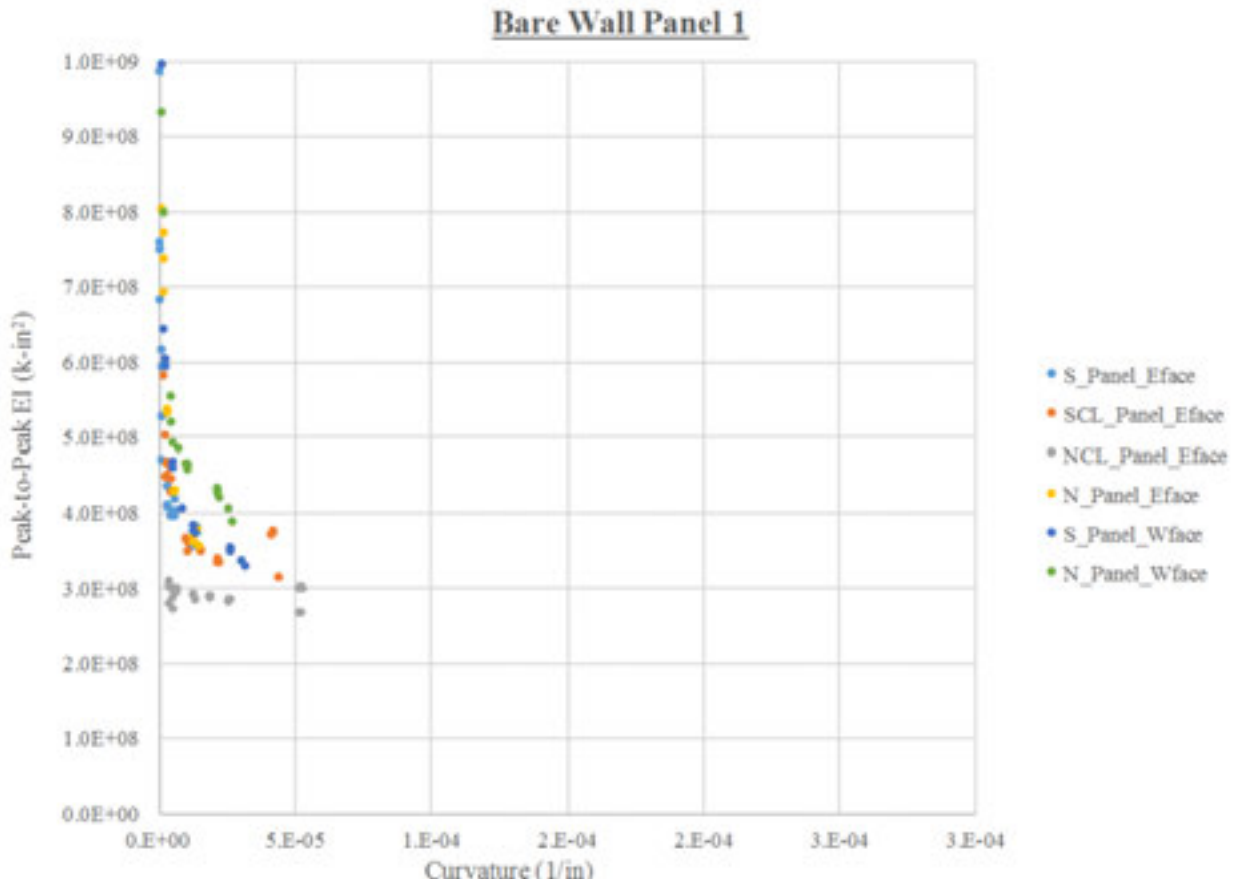

Figure 15 – Peak-to-peak flexural stiffness (EI) versus curvature results at six locations of bare wall panel 1.

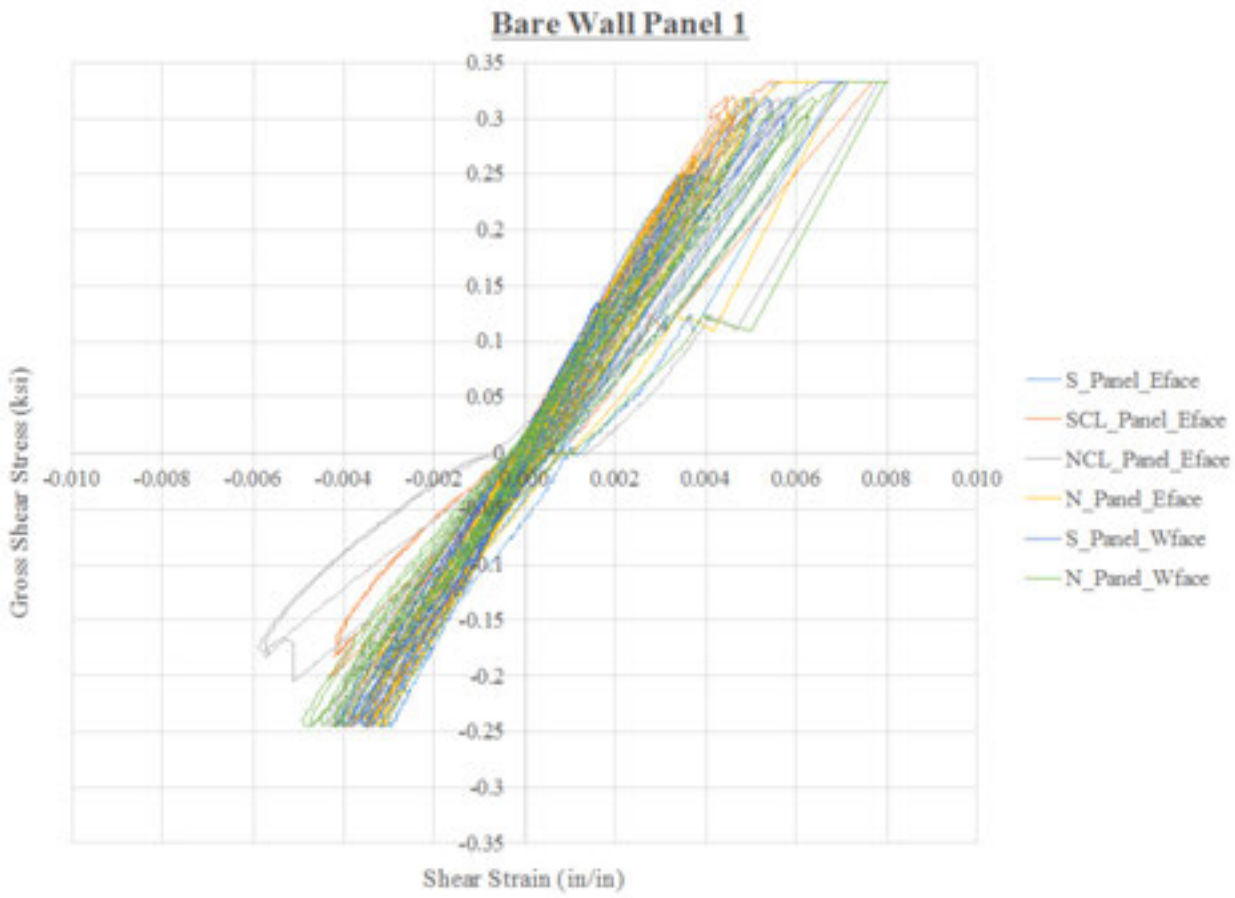

Figure 16 – Gross shear stress versus shear strains results at six locations of bare wall panel 1.

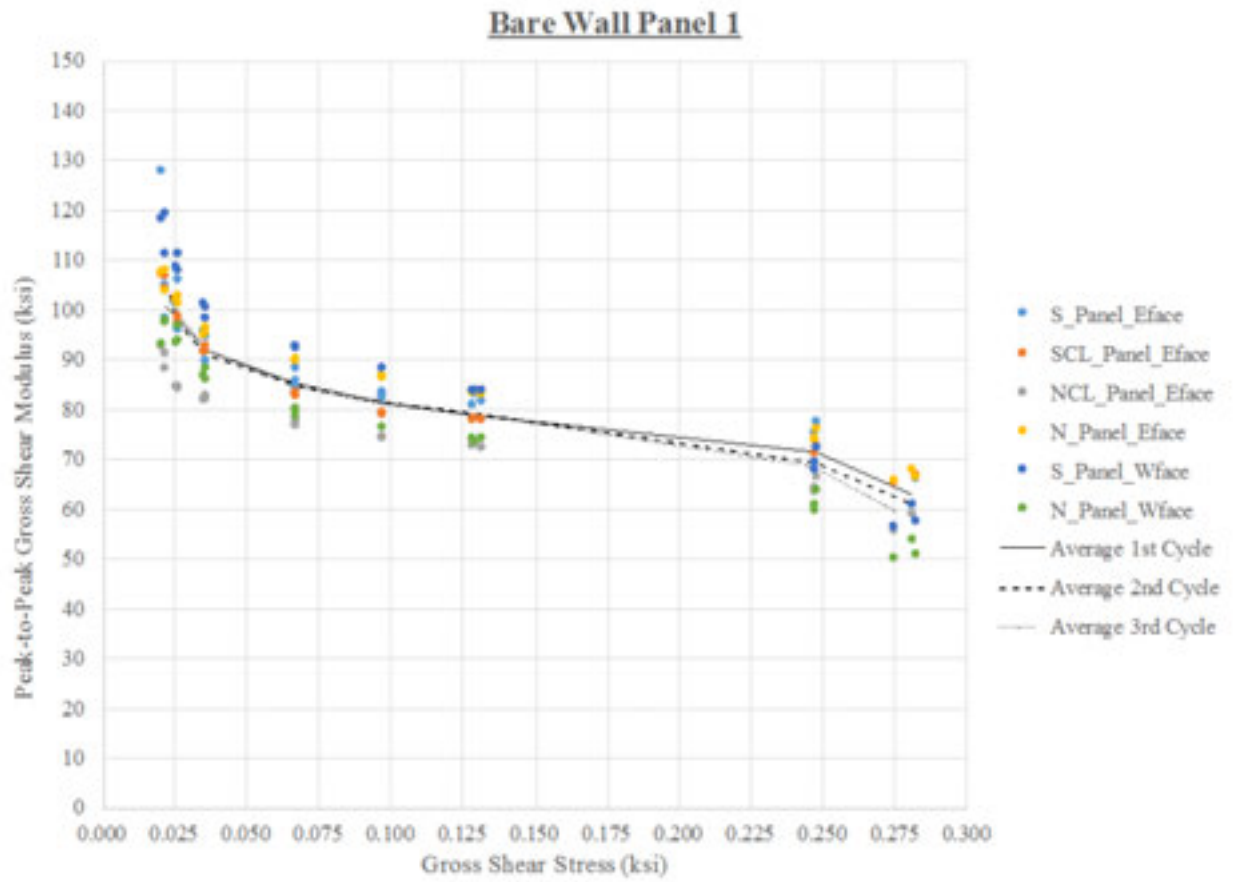

Figure 17 – Peak-to-peak gross shear modulus versus shear stress results at six locations of bare wall panel 1.

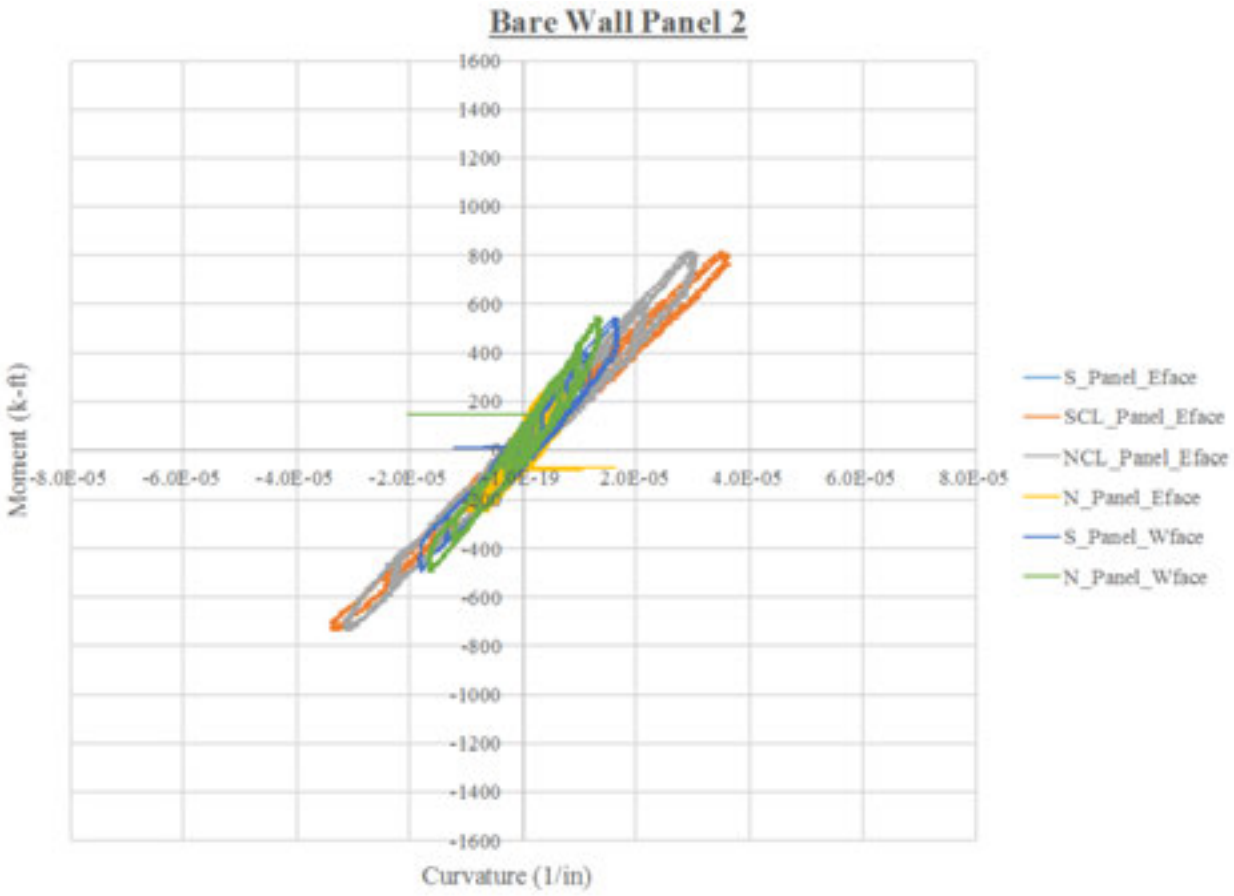

Figure 18 – Moment-curvature results at six locations of bare wall panel 2.

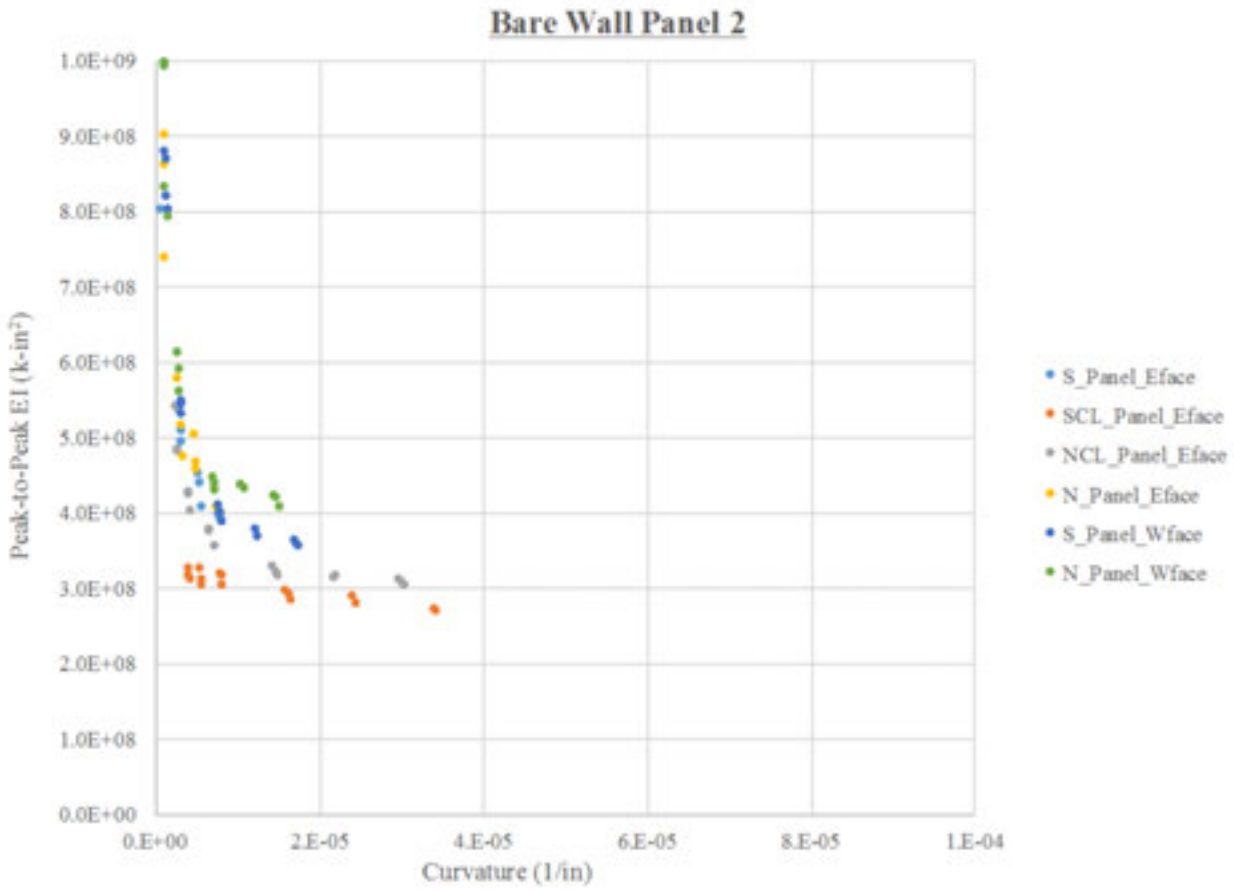

Figure 19 – Peak-to-peak flexural stiffness (EI) versus curvature results at six locations of bare wall panel 2.

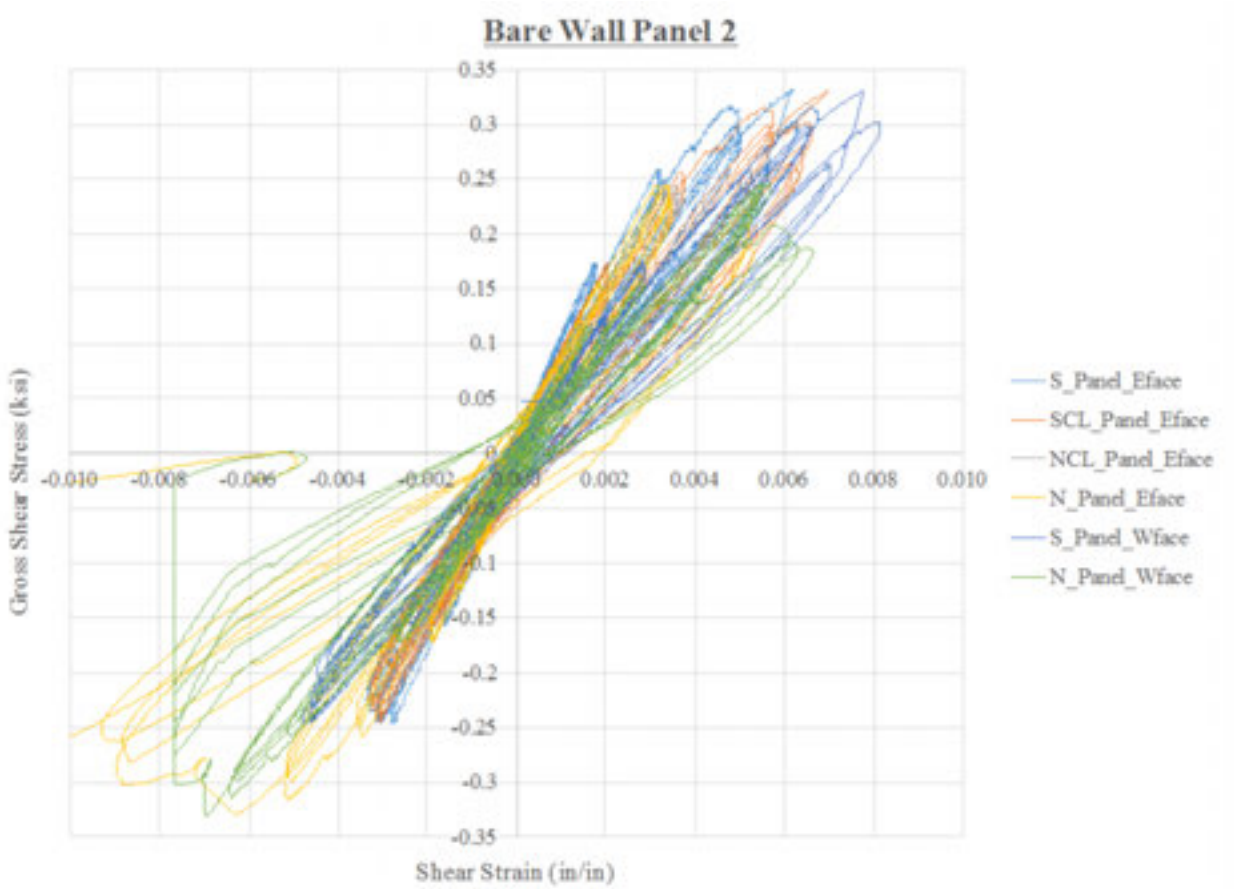

Figure 20 – Gross shear stress versus shear strains results at six locations of bare wall panel 2.

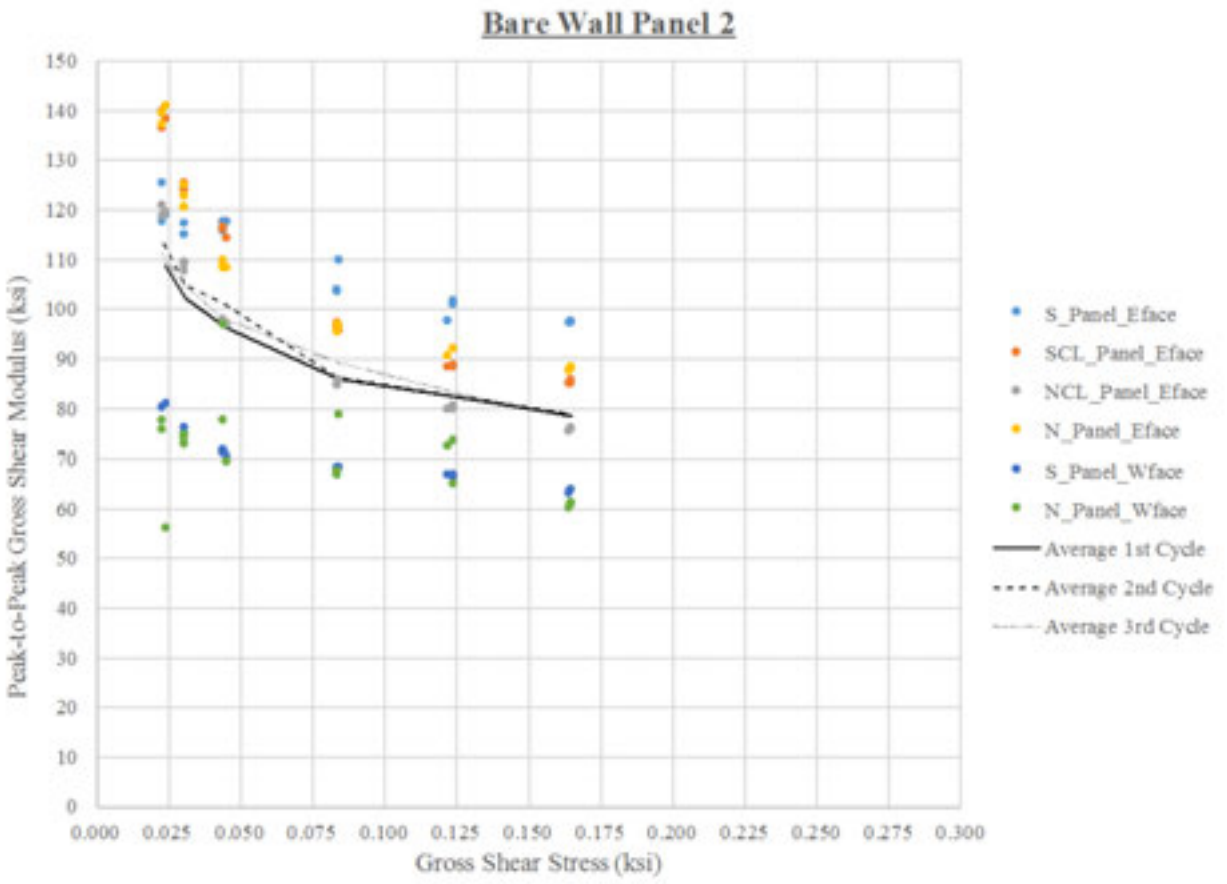

Figure 21 – Peak-to-peak gross shear modulus versus shear stress results at six locations of bare wall panel 2.

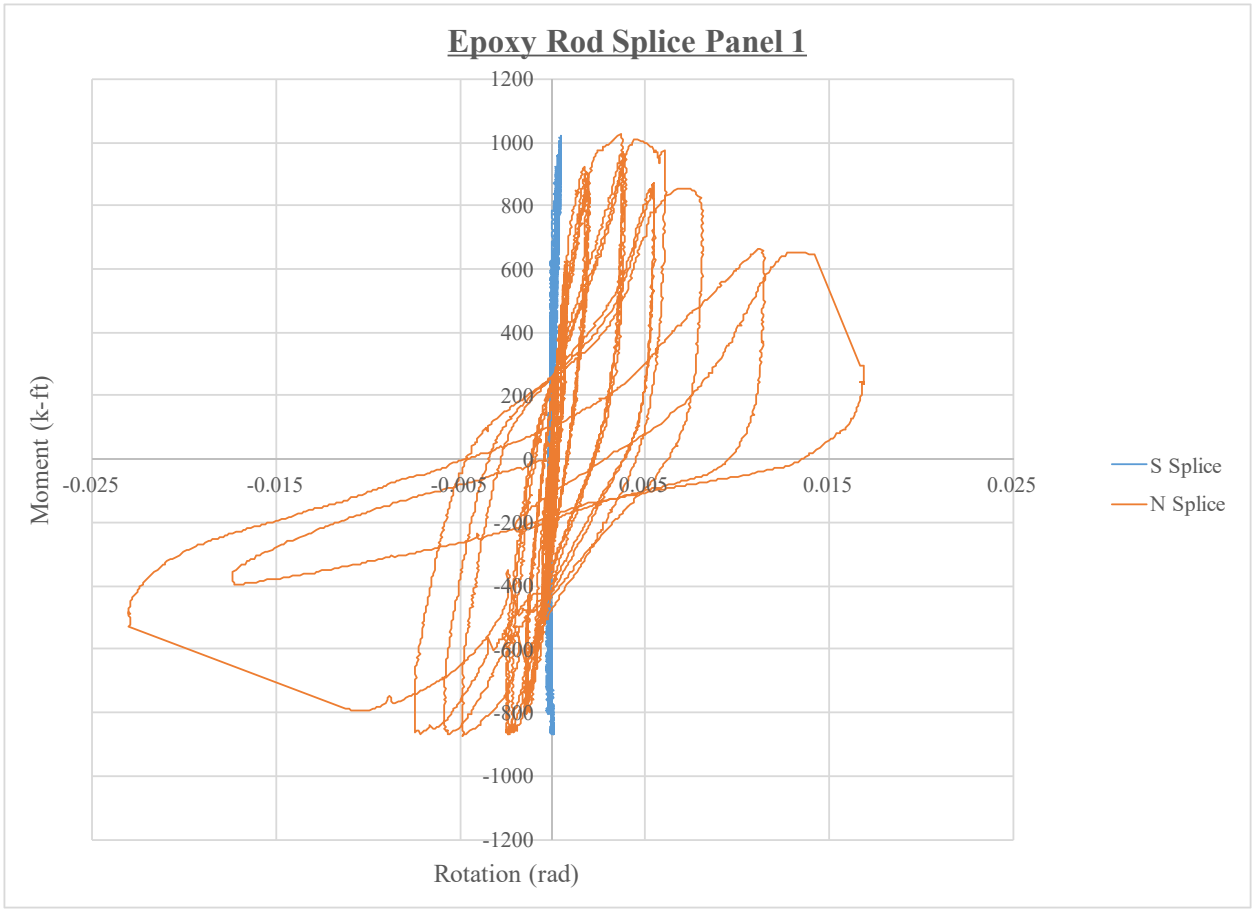

Figure 22 – Moment-rotation results at two splice locations of epoxy rod splice panel 1.

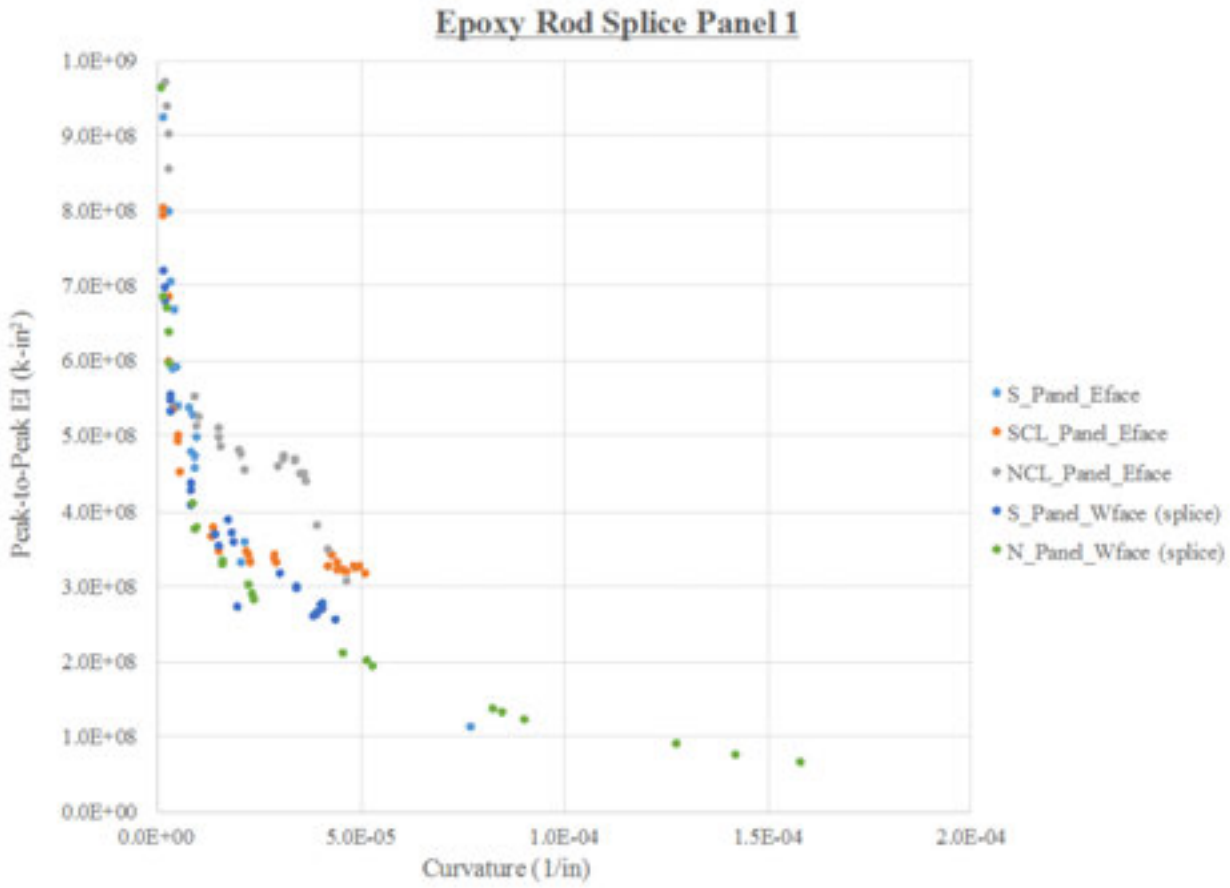

Figure 23 – Peak-to-peak flexural stiffness (EI) versus curvature results at 5 locations of the epoxy rod splice panel 1.

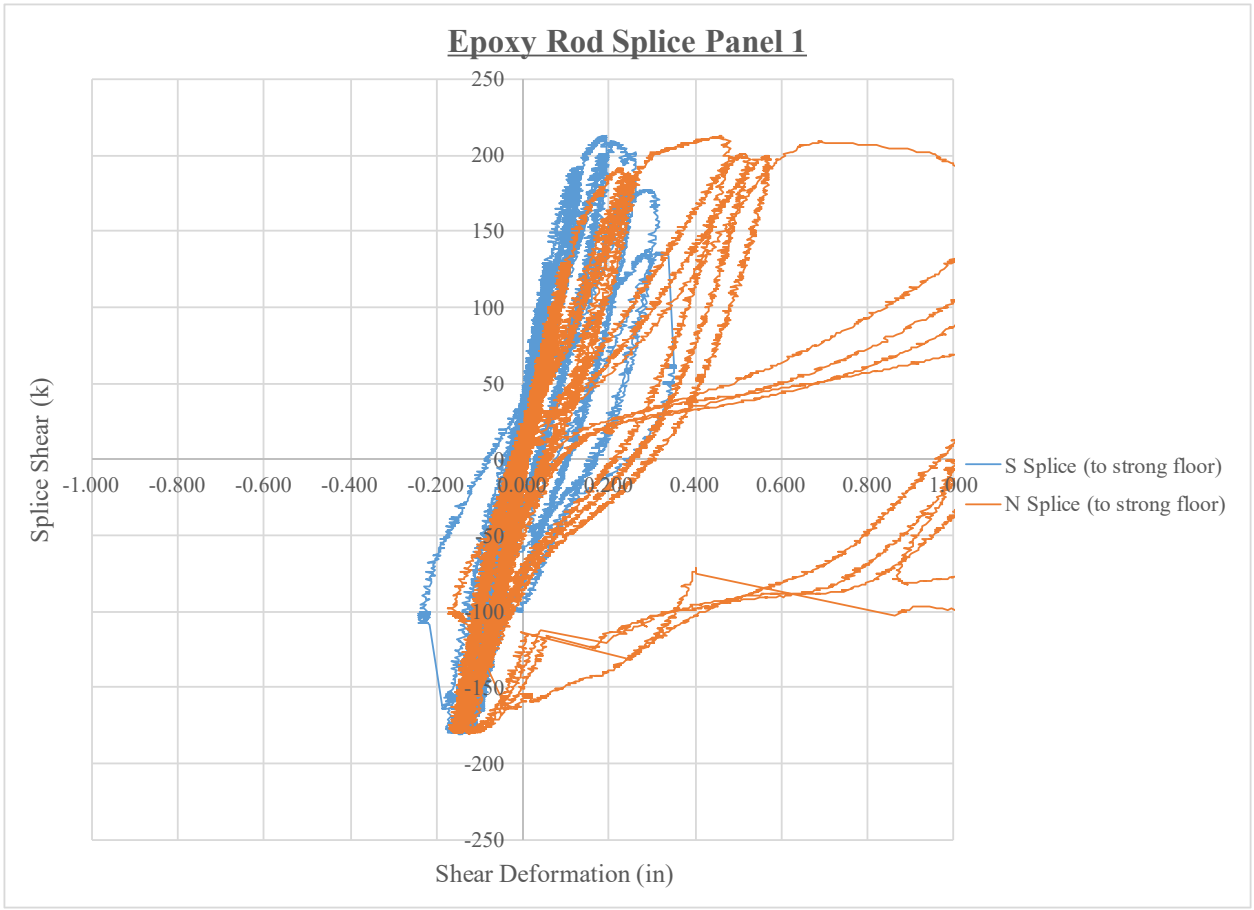

Figure 24 – Splice shear versus shear deformation results at two splice locations of the epoxy rod splice panel 1.

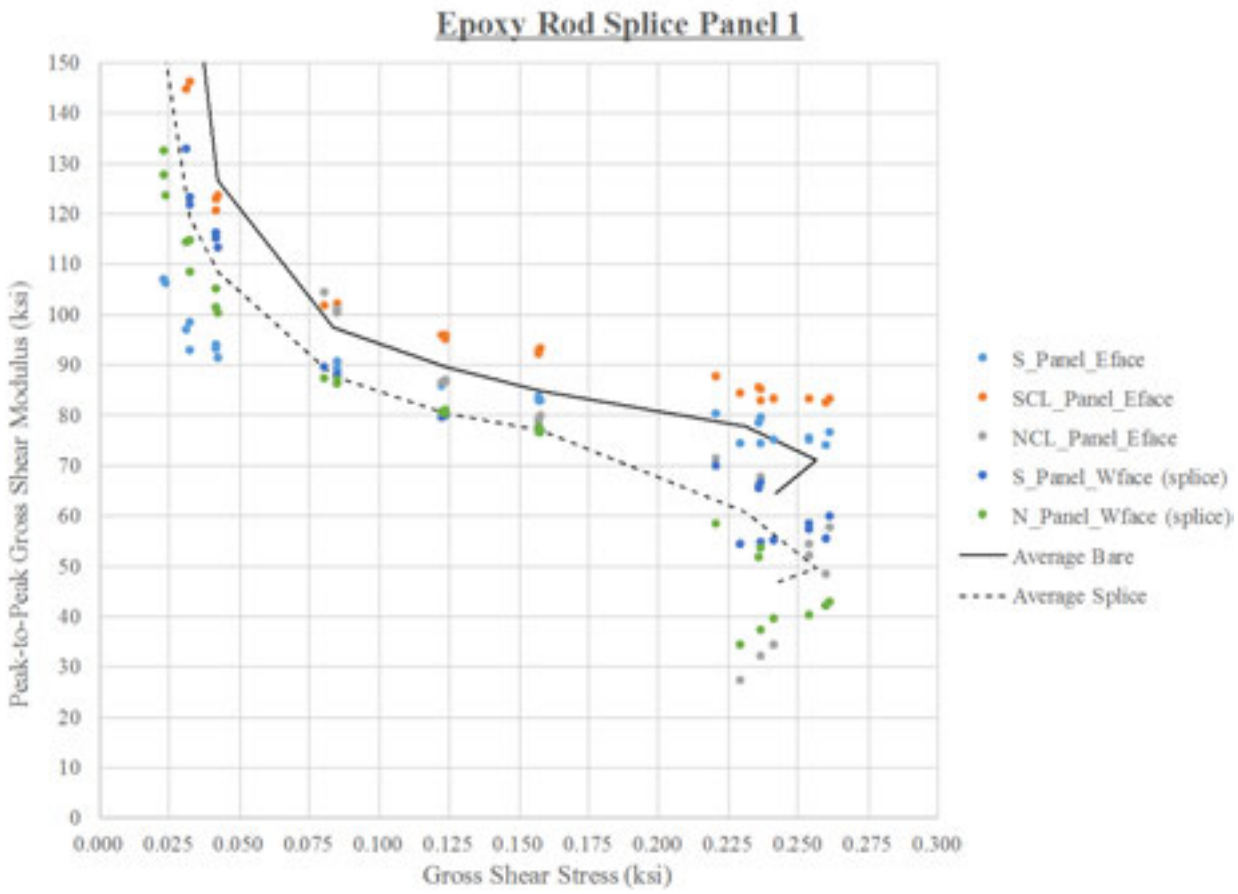

Figure 25 – Peak-to-peak gross shear modulus versus gross shear stress at 5 locations of the epoxy rod splice panel 1.

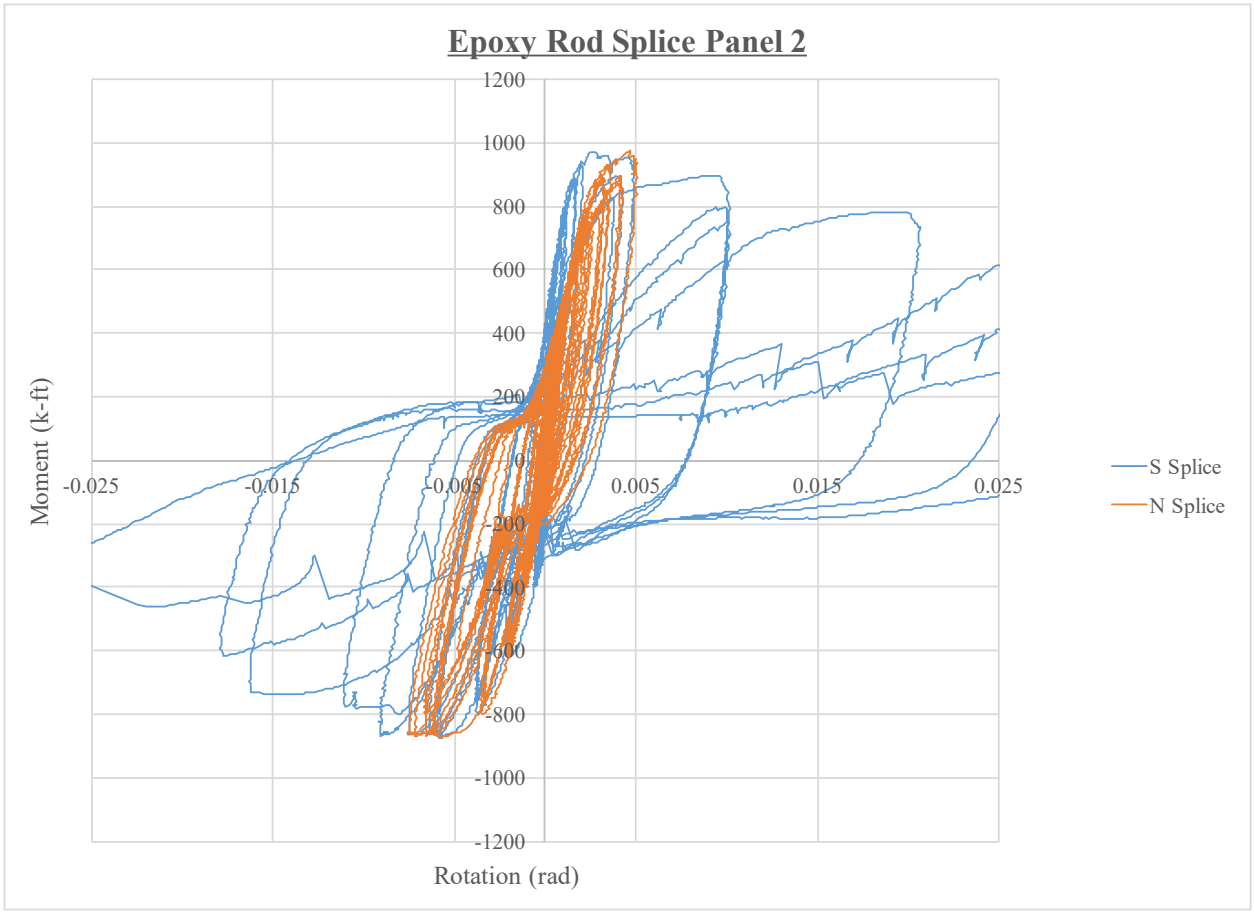

Figure 26 – Moment-rotation results at two splice locations of epoxy rod splice panel 2.

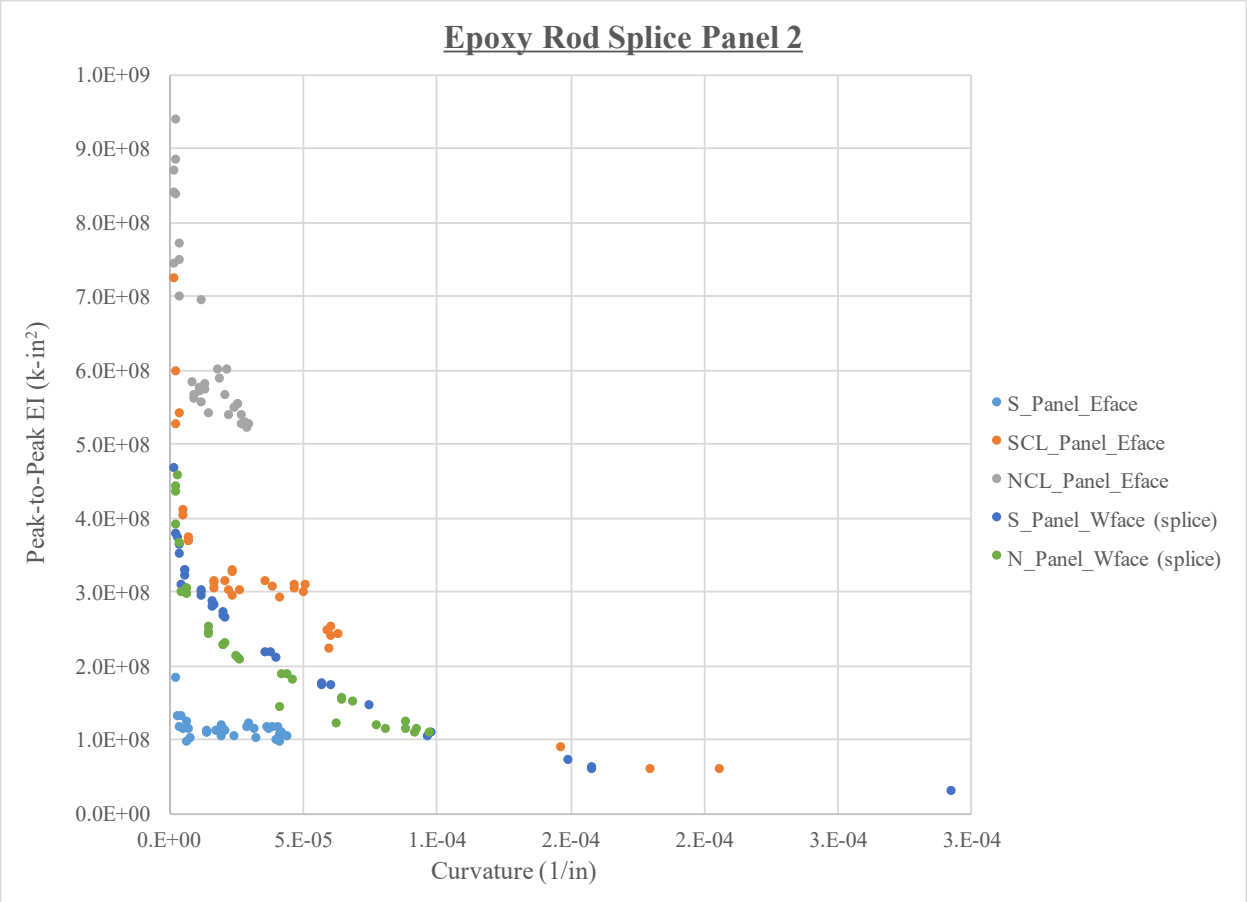

Figure 27 – Peak-to-peak flexural stiffness (EI) versus curvature results at 5 locations of the epoxy rod splice panel 2.

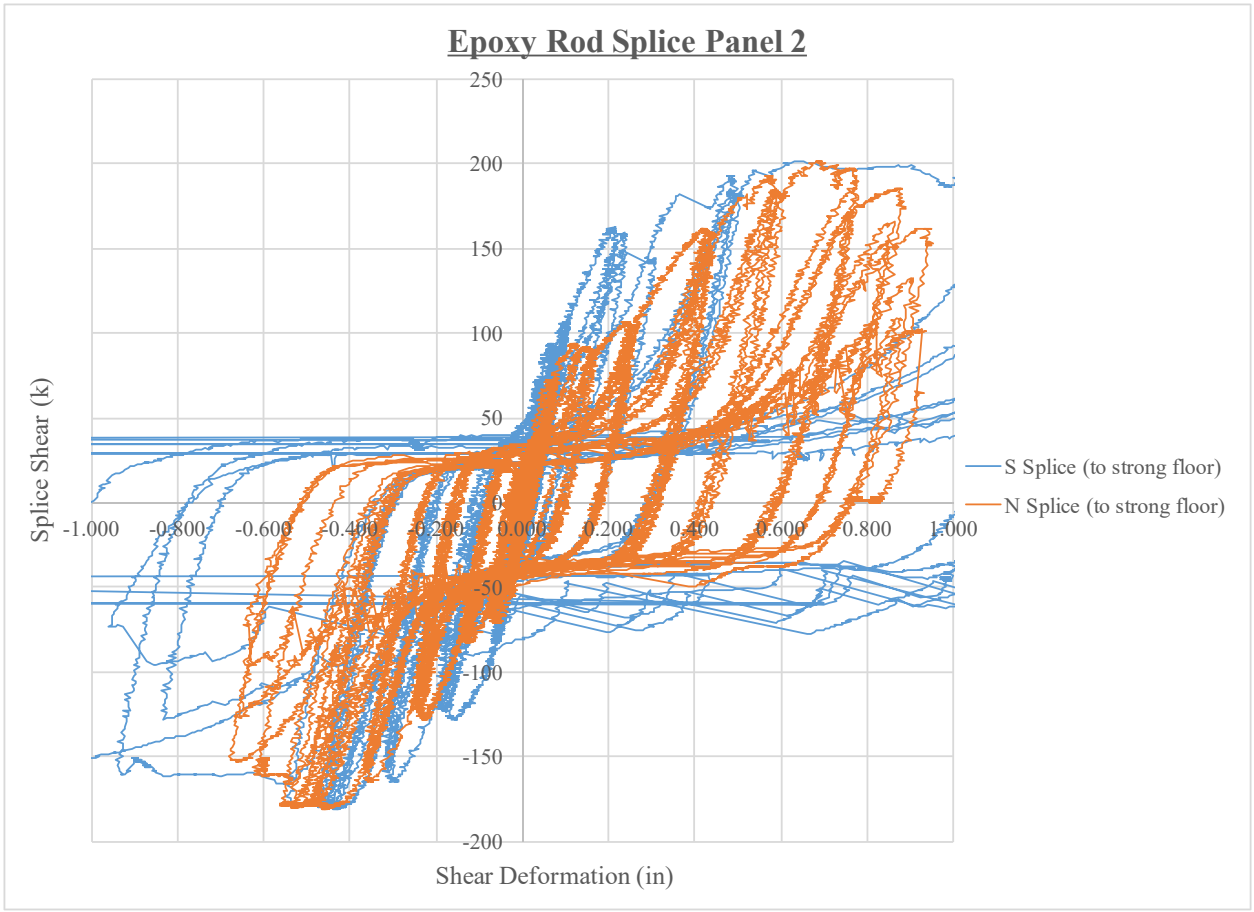

Figure 28 – Splice shear versus shear deformation results at two splice locations of the epoxy rod splice panel 2.

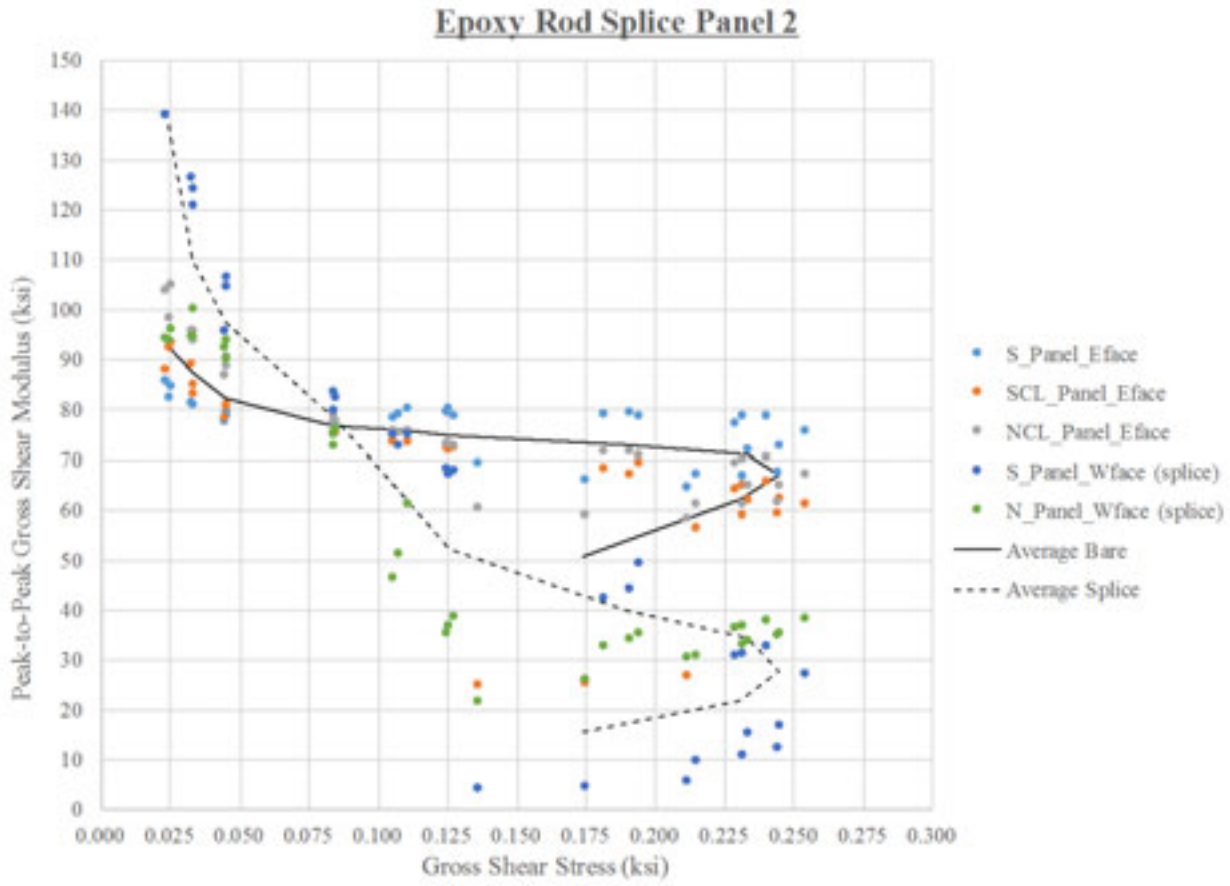

Figure 29 – Peak-to-peak gross shear modulus versus gross shear stress at 5 locations of the epoxy rod splice panel 2.

APPENDIX I – CLT Crushing Test Sketches

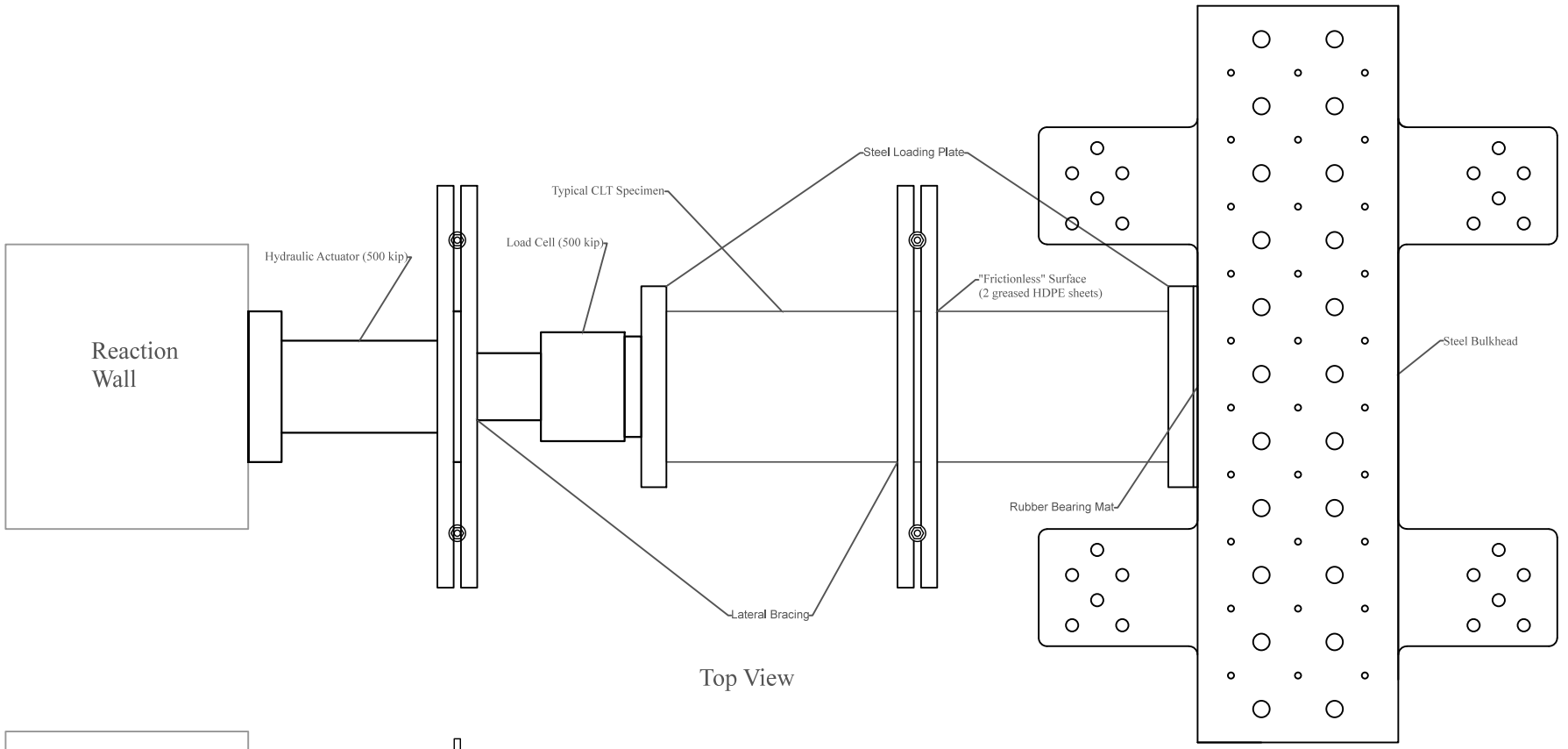

Top View

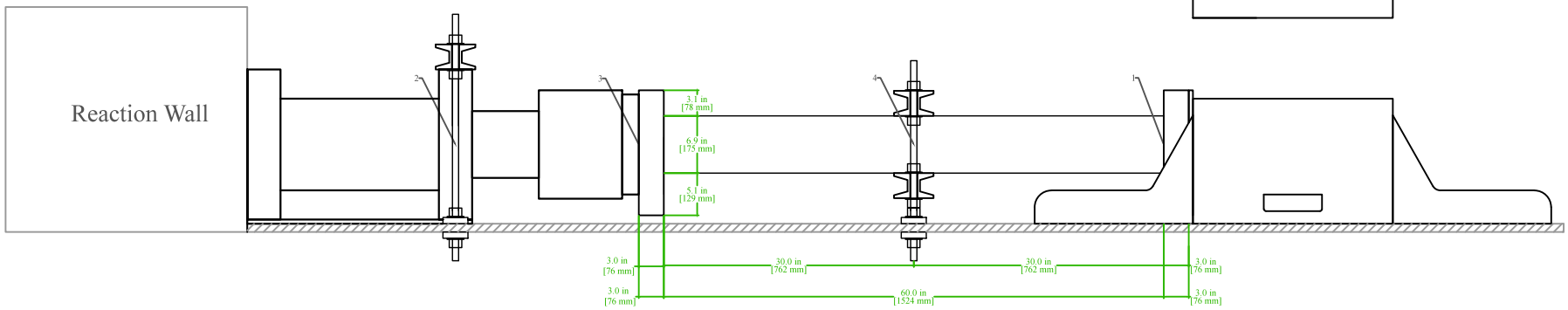

Elevation (East View)

Crushing CLT Specimens **Instrumentation East**	**E.1**
Arijit Sinha & Milo Clauson	8/2/2016
Oregon State University	541-737-6713
arijit.sinha@oregonstate.edu	Rev. 2

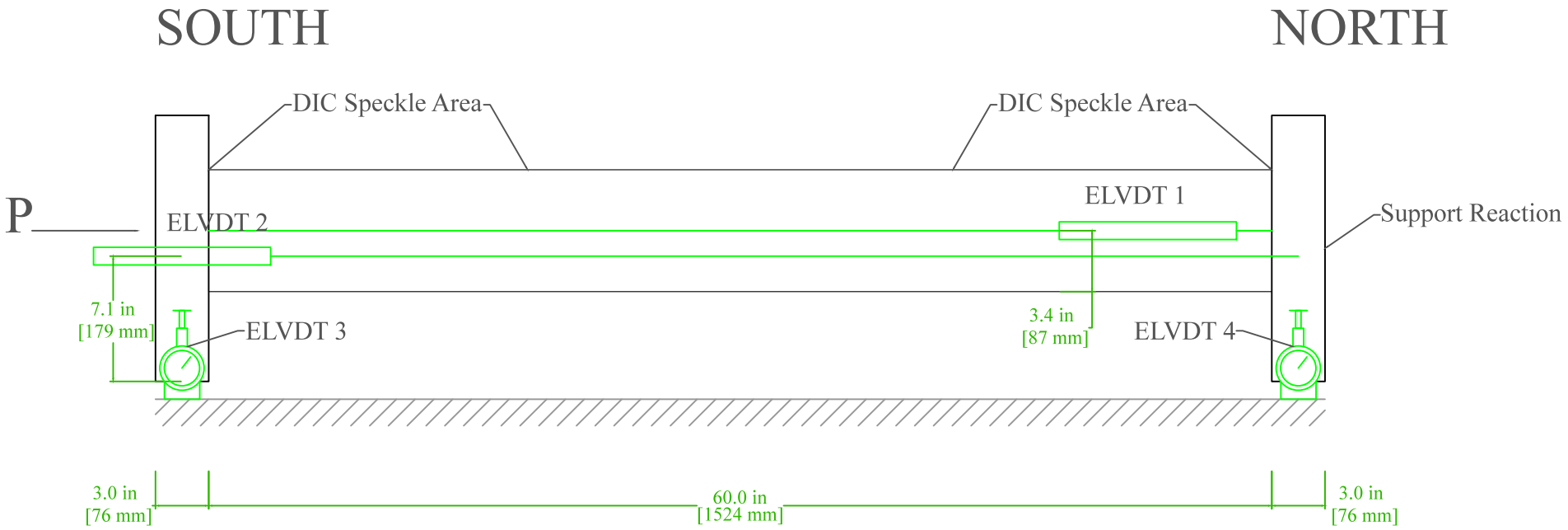

Elevation (East View)

Sensor Details :
Code for each sensor is (Side).(Sensor type). (Number)
For example W (West Side). LVDT (Sensor type). 1 (Number)

E.LVDT.1 - measures the compression of the entire panel along the panel's centerline. Will be used to determine a stress-strain relationship. Scale: +/- 2 in. Resolution: 0.0002 in

E.LVDT.2 - measures the relative displacement between the two steel bearing plates, measured from centerline to centerline. Scale: +/- 2 in. Resolution: 0.0002in

E.LVDT.2 and **E.LVDT.3** - measure the vertical displacement of the steel plates to ensure minimal slipping. Scale: +/- 0.5 in. Resolution: 0.0005

Crushing CLT Specimens **Instrumentation East**	**E.2**
Arijit Sinha & Milo Clauson	8/2/2016
Oregon State University	541-737-6713
arijit.sinha@oregonstate.edu	Rev. 2

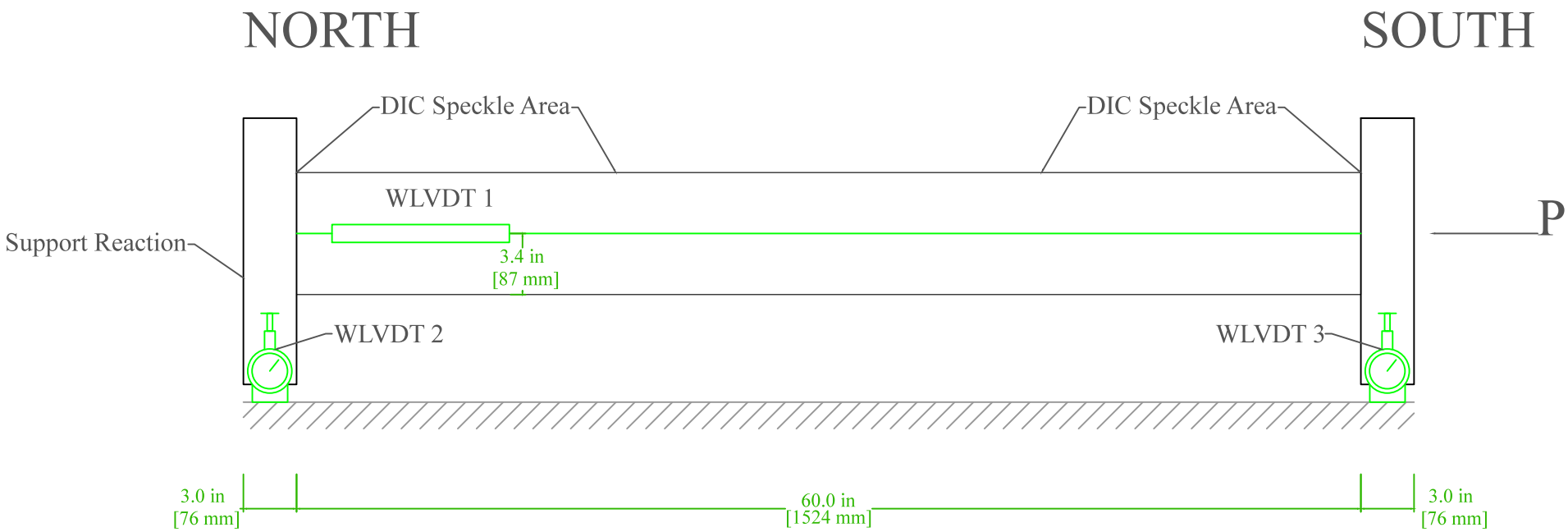

Elevation (West View)

Sensor Details:
Code for each sensor is (Side).(Sensor type). (Number)
For example W (West Side). LVDT (Sensor type). 1 (Number)

W.LVDT.1 - measures the compression of the entire panel along the panel's centerline. Will be used to determine a stress-strain relationship. Scale: +/- 2 in. Resolution: 0.0002 in

W.LVDT.2 and **W.LVDT.3** - measure the vertical displacement of the steel plates to ensure minimal slipping. Scale: +/- 0.5 in. Resolution: 0.0005

DIC AREA - Two cameras over specimen will record images throughout testing and will be analyzed for localized deformation in the ends with the zone being approximately 18 inches long on either side.

Crushing CLT Specimens **Instrumentation West**		**E.3**
Arijit Sinha & Milo Clauson	8/2/2016	
Oregon State University	541-737-6713	
arijit.sinha@oregonstate.edu	Rev. 2	

①

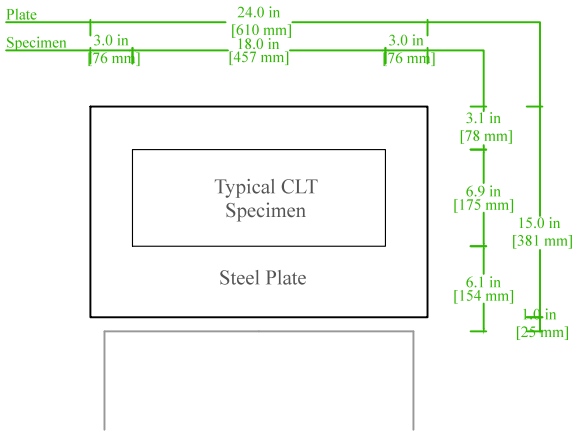

②

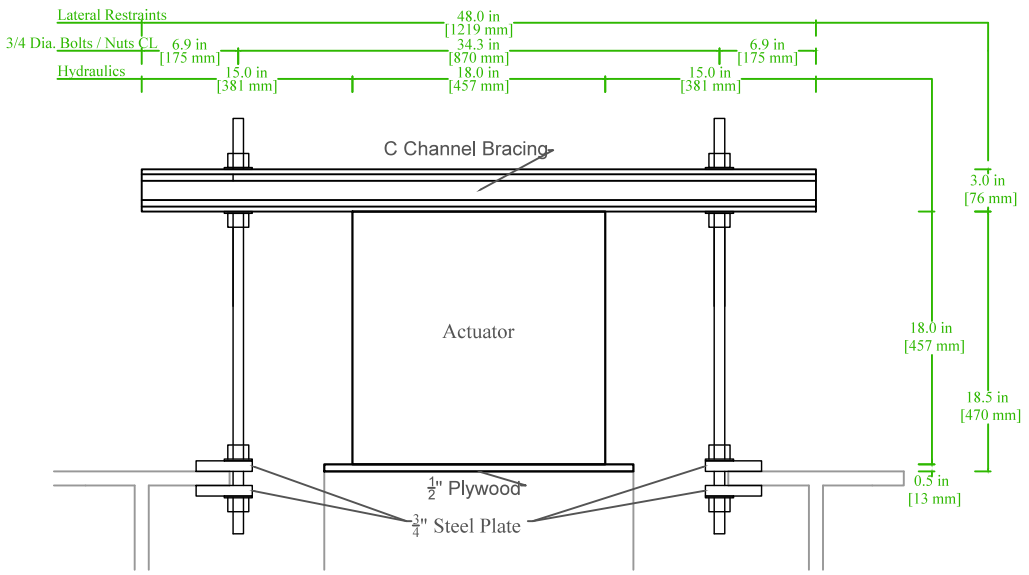

③

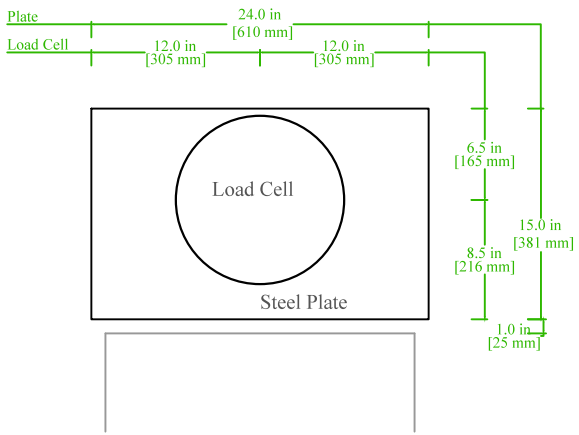

④

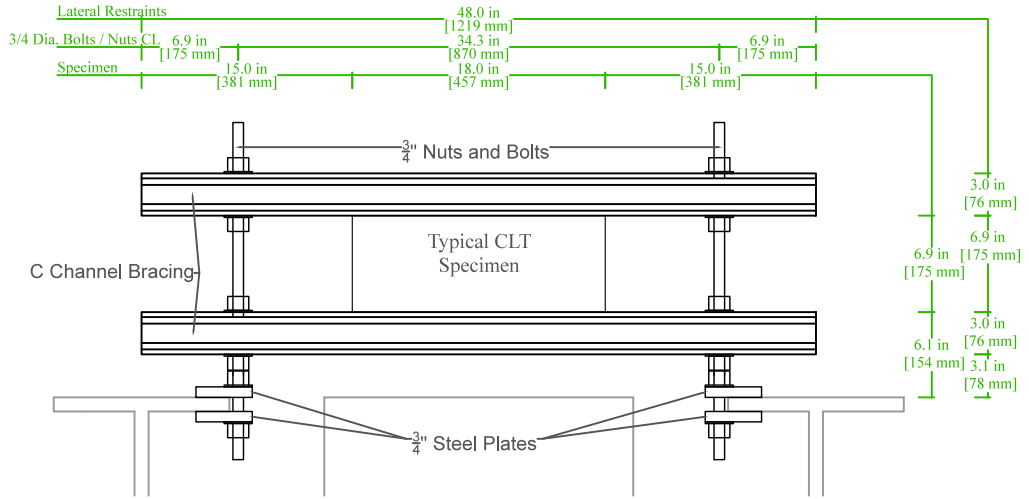

Crushing CLT Specimens **Details**	**E.4**
Arijit Sinha & Milo Clauson	8/2/2016
Oregon State University	541-737-6713
arijit.sinha@oregonstate.edu	Rev. 2

APPENDIX II – CLT Wall Test Sketches

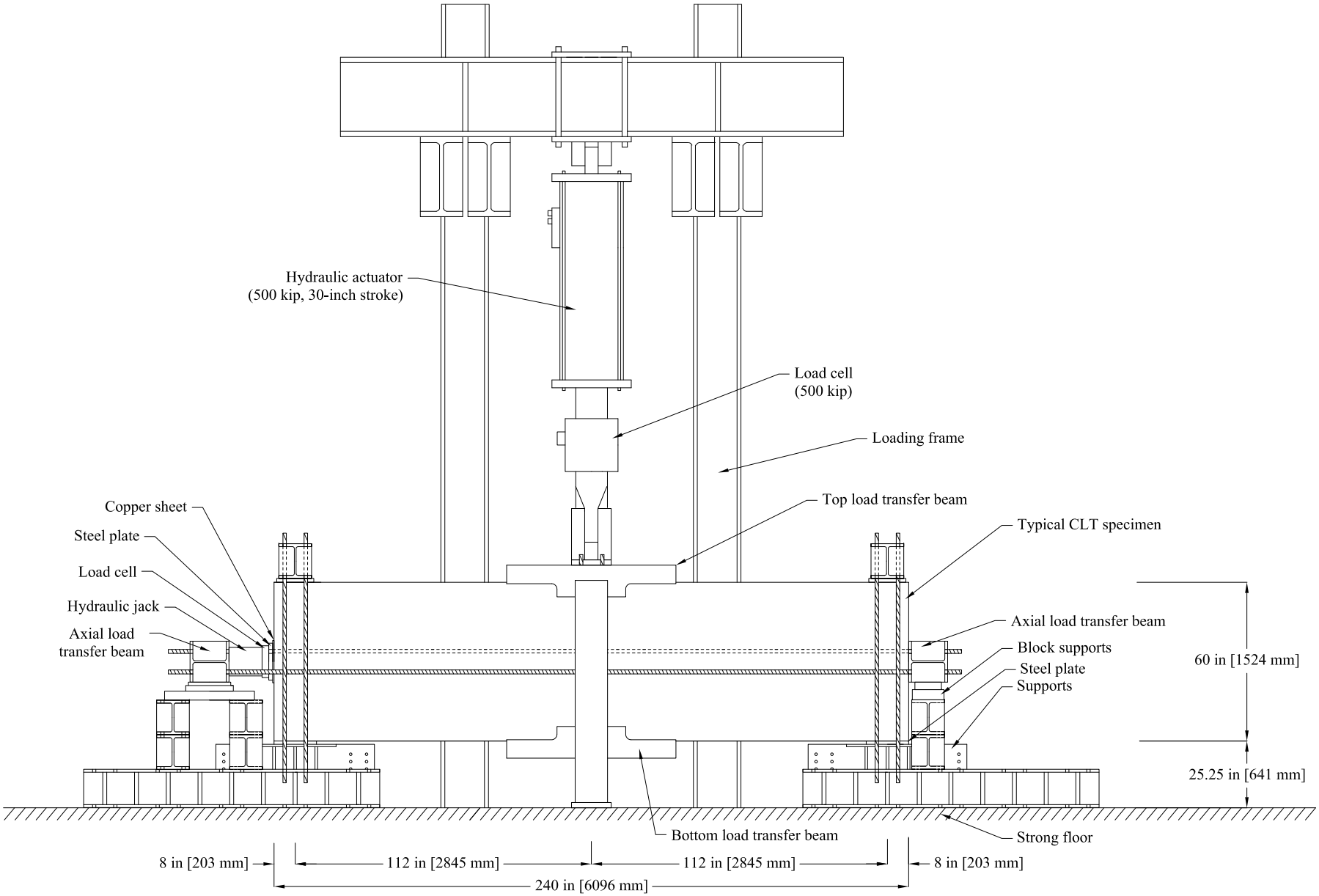

Shear Wall Specimens **Experimental Setup (typ.)**		**E.1**
Andre Barbosa & Chris Higgins	6/1/2017	
Oregon State University	541-737-7291	
barbosa@oregonstate.edu	Rev. 5	Drawn by: KAF Reviewed by: ARB

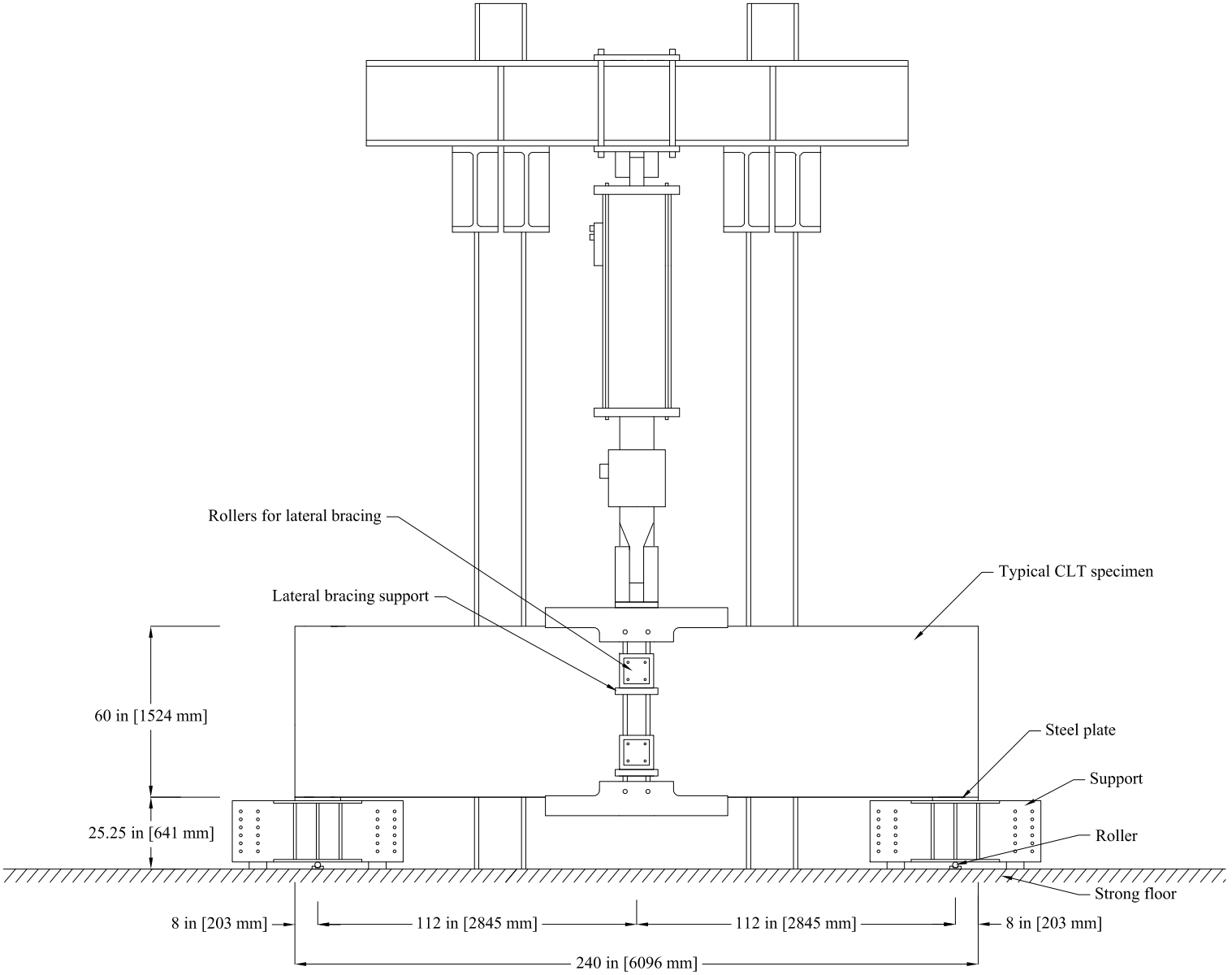

Shear Wall Specimens **CLT Specimen Supports (typ.)**		**E.2**
Andre Barbosa & Chris Higgins	6/1/2017	
Oregon State University	541-737-7291	
barbosa@oregonstate.edu	Rev. 5	Drawn by: KAF Reviewed by: ARB

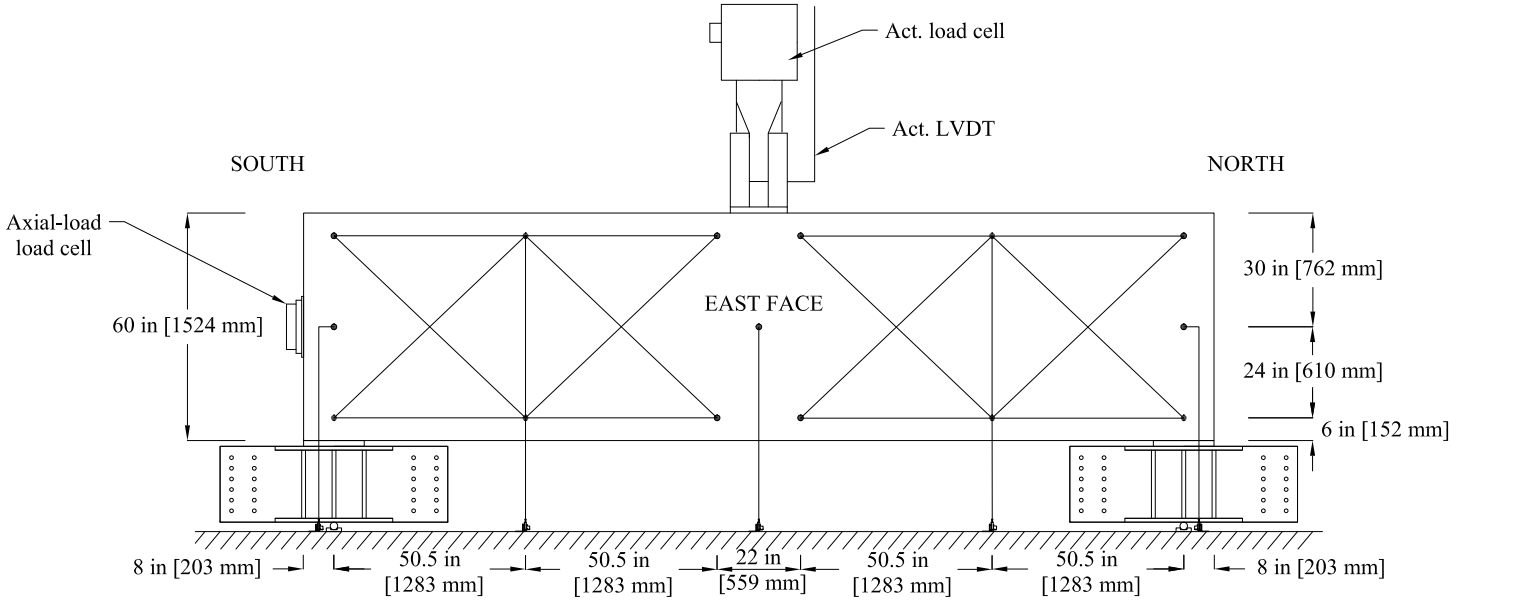

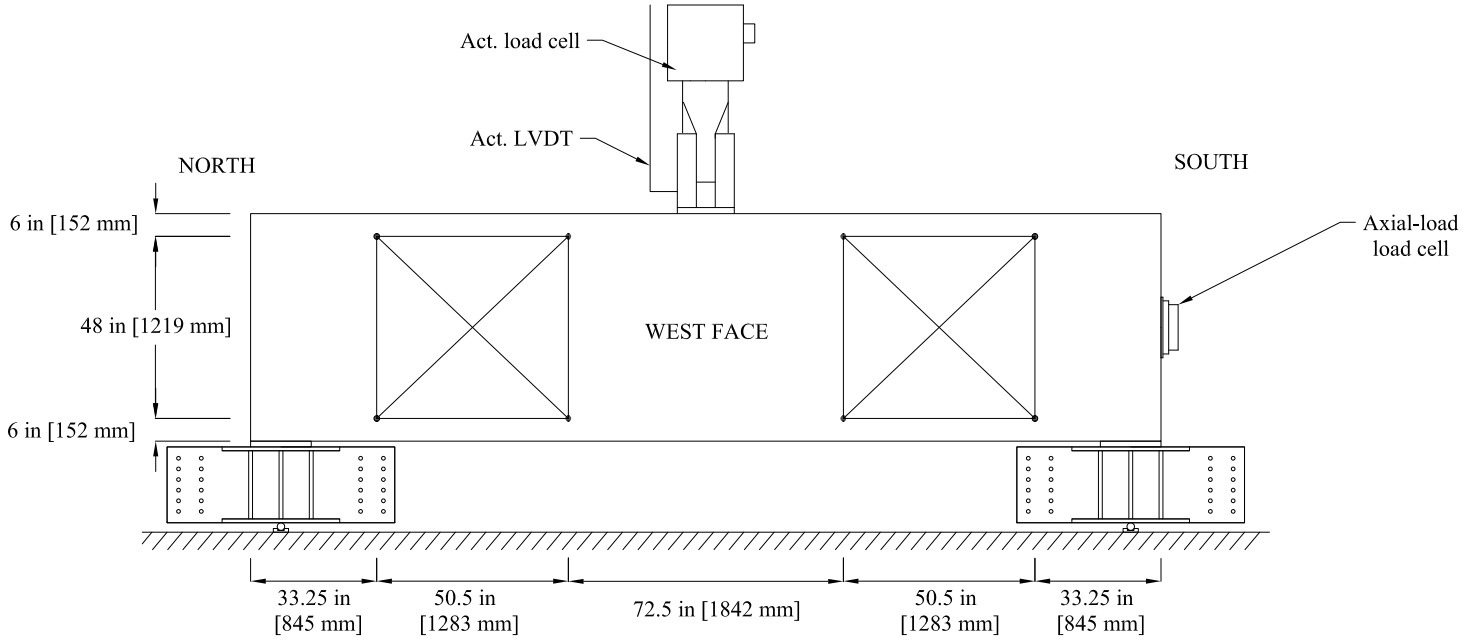

Continuous Shear Wall Specimen **Wall 1 and 2 Instrumentation Layout**		**E.3**
Andre Barbosa & Chris Higgins	6/1/2017	
Oregon State University	541-737-7291	
barbosa@oregonstate.edu	Rev. 5	Drawn by: KAF Reviewed by: ARB

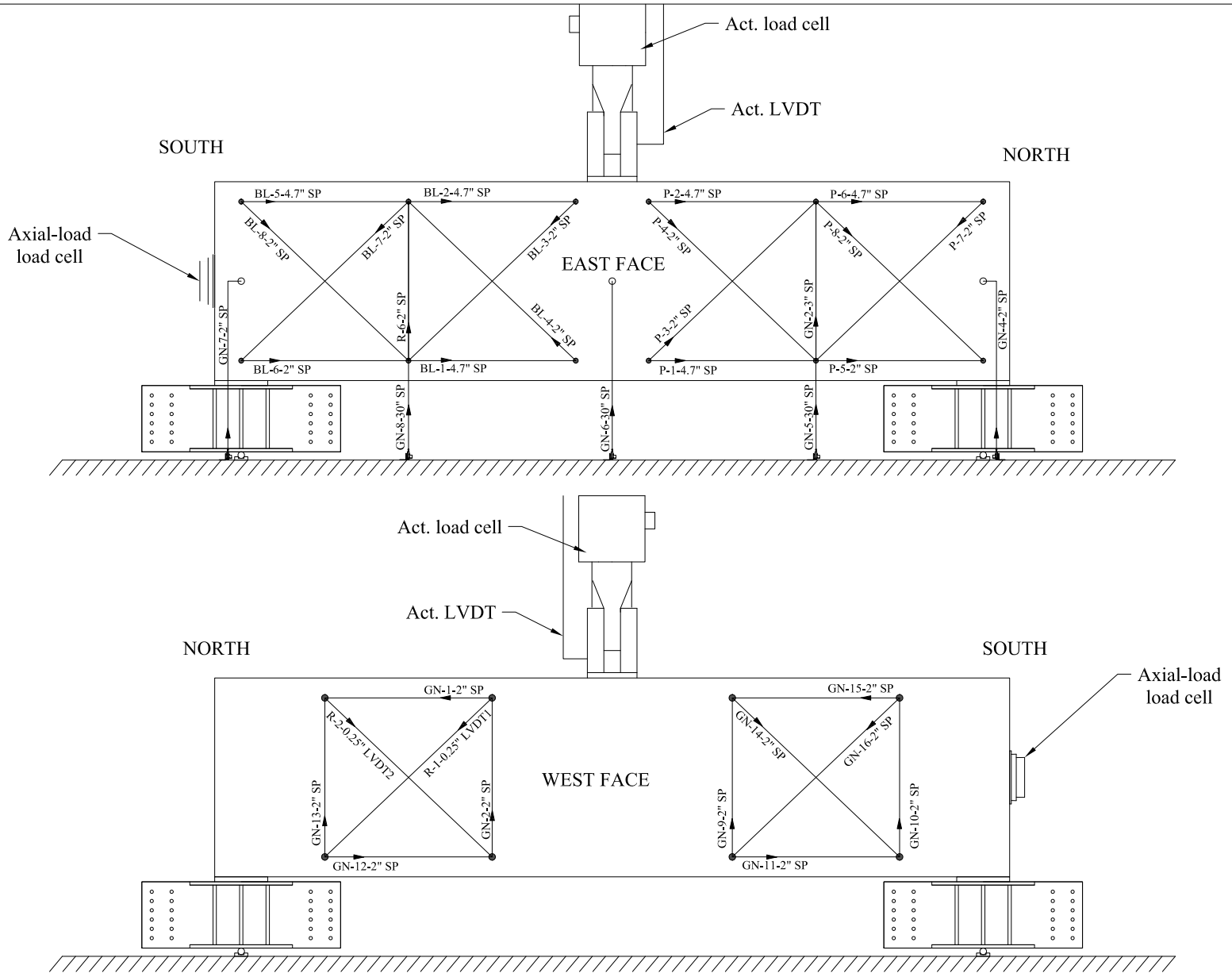

NOTES:		
Sensor labels:	"cable color - # - length- sensor type"	
Cable color:	GN - Green BL - Blue OR - Orange	P - Purple R - Red YP - Yellow purple
Sensor type:	SP - String potentiometer LVDT - Linear variable displacement transducer	

Continuous Shear Wall Specimen
Wall 1 and 2
Instrumentation Sensor Labels

E.4

Andre Barbosa & Chris Higgins

Oregon State University

barbosa@oregonstate.edu

6/1/2017

541-737-7291

Rev. 5

Drawn by: KAF

Reviewed by: ARB

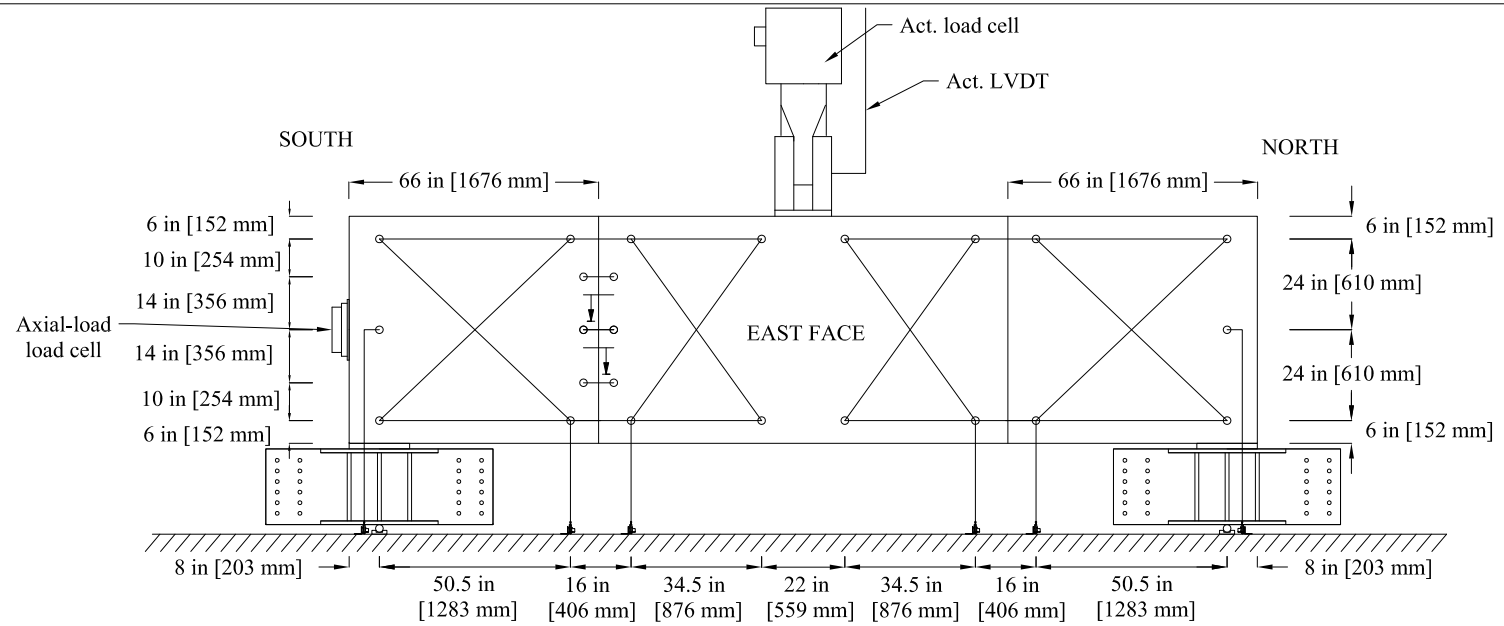

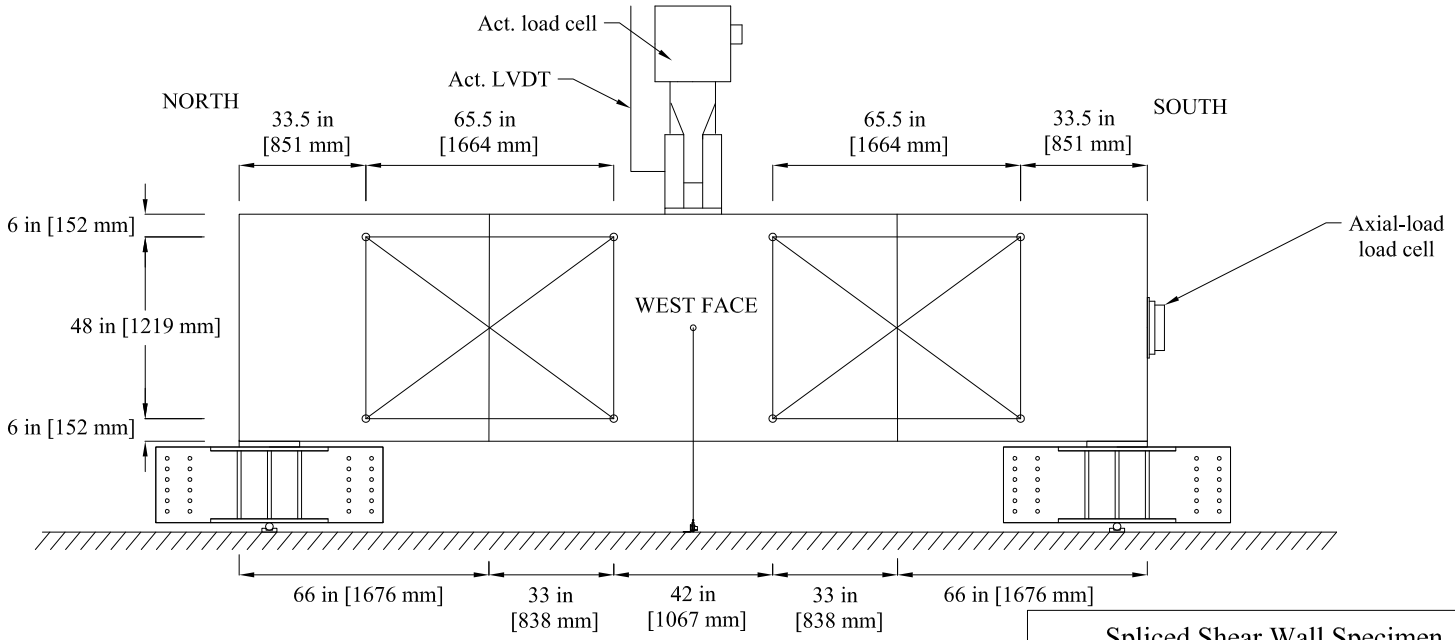

Spliced Shear Wall Specimen **Walls 3, 4, 5, and 6 Instrumentation Layout**		**E.5**
Andre Barbosa & Chris Higgins	6/1/2017	
Oregon State University	541-737-7291	
barbosa@oregonstate.edu	Rev. 5	Drawn by: KAF Reviewed by: ARB

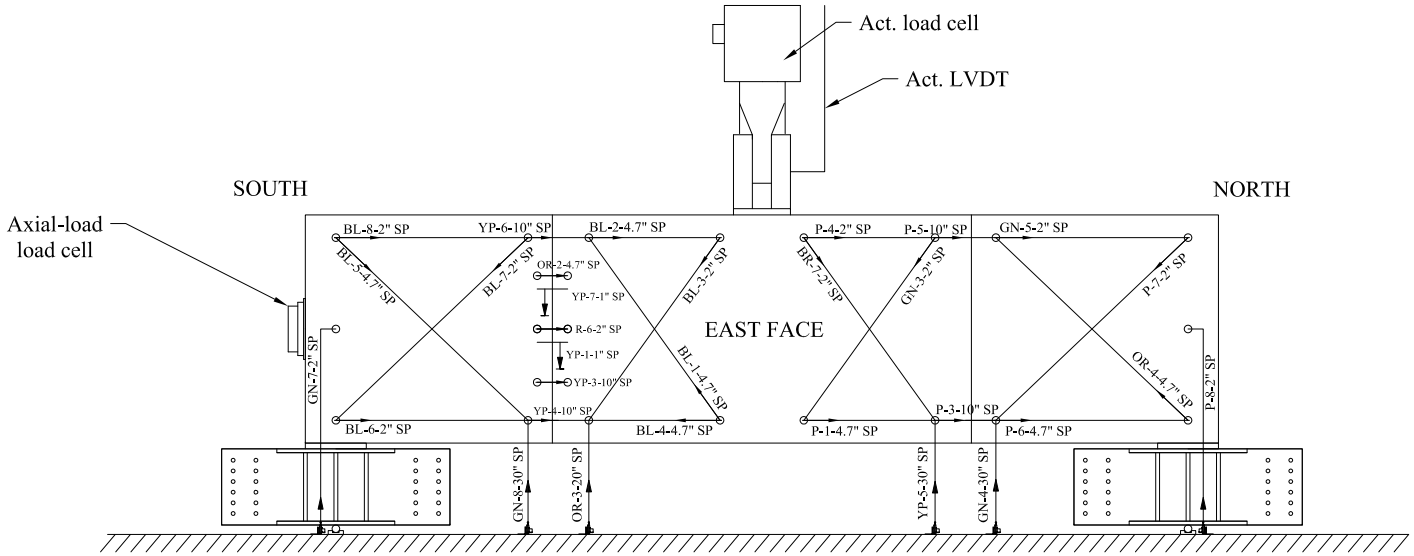

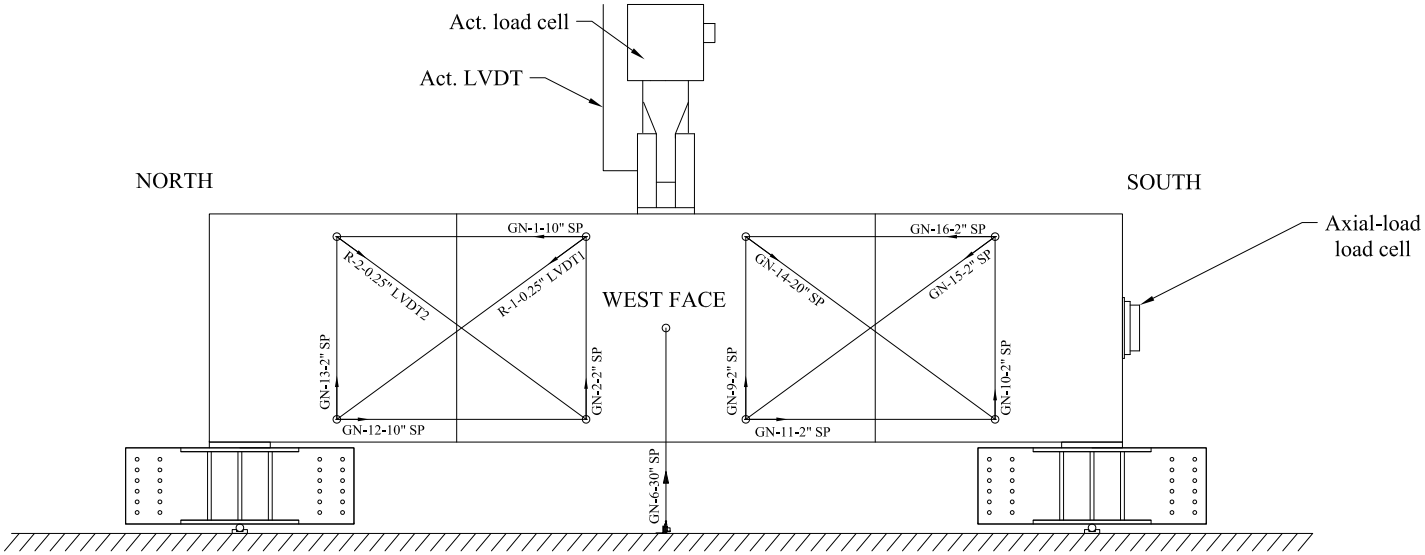

NOTES:		
Sensor labels:	"cable color - # - length- sensor type"	
Cable color:	GN - Green BL - Blue OR - Orange	P - Purple R - Red YP - Yellow purple
Sensor type:	SP - String potentiometer LVDT - Linear variable displacement transducer	

Spliced Shear Wall Specimen
Wall 4 Instrumentation Sensor Labels

E.6

Andre Barbosa & Chris Higgins

Oregon State University

barbosa@oregonstate.edu

6/1/2017

541-737-7291

Rev. 5

Drawn by: KAF

Reviewed by: ARB

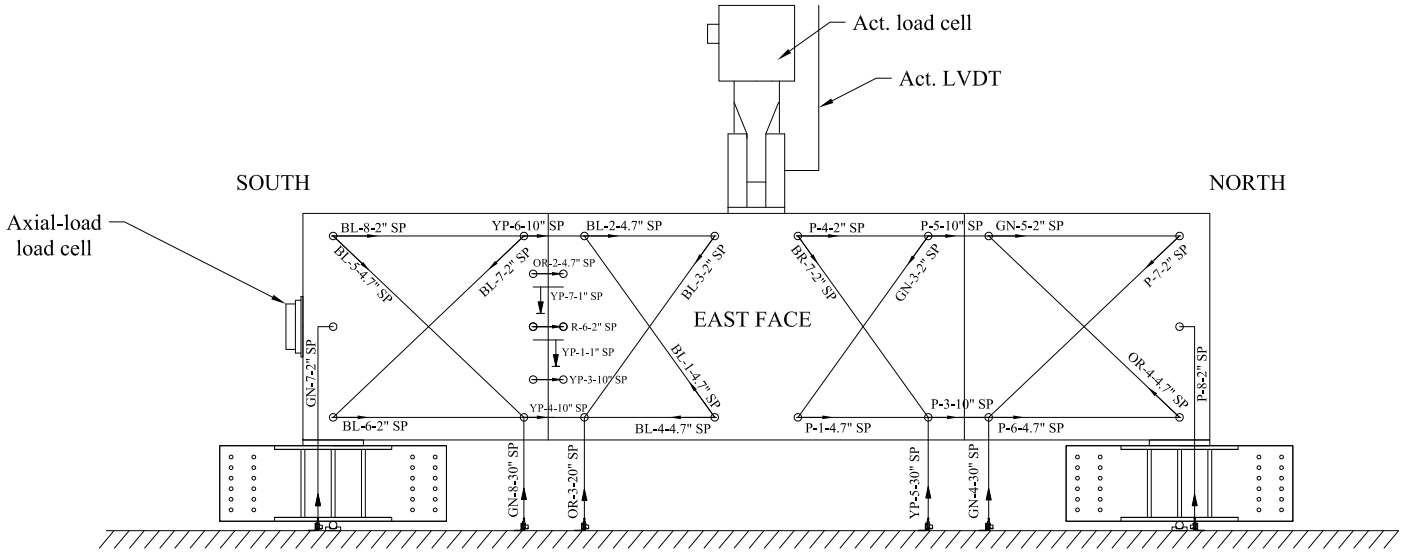

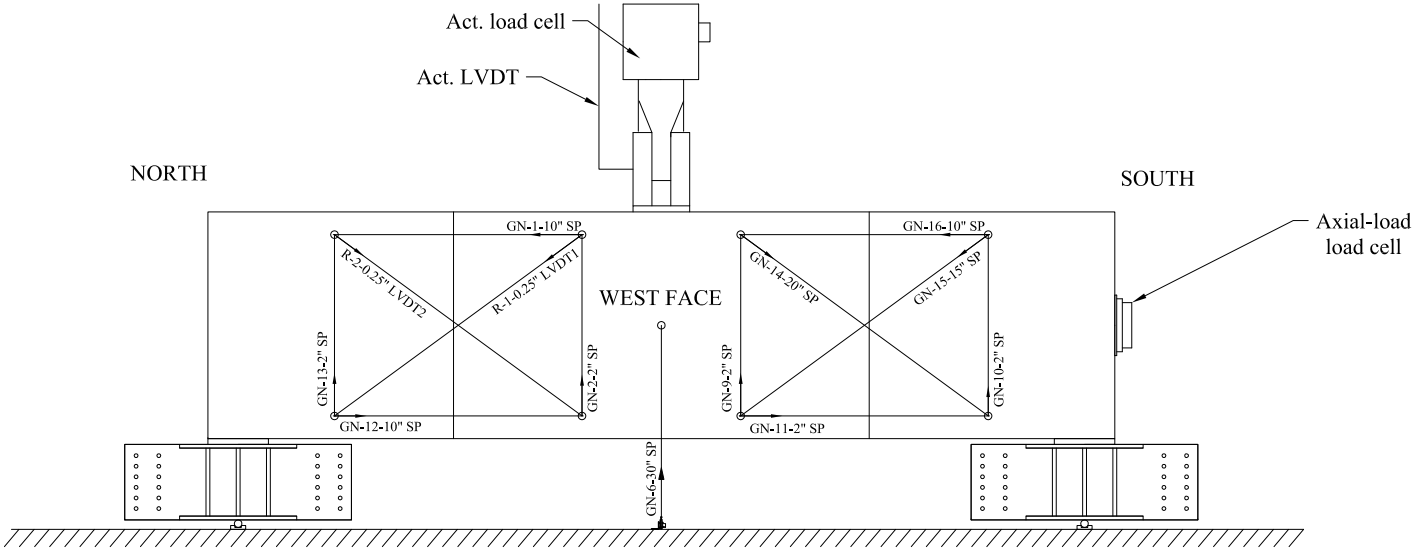

NOTES:		
Sensor labels:	"cable color - # - length- sensor type"	
Cable color:	GN - Green BL - Blue OR - Orange	P - Purple R - Red YP - Yellow purple
Sensor type:	SP - String potentiometer LVDT - Linear variable displacement transducer	

Spliced Shear Wall Specimen
Wall 5 Instrumentation Sensor Labels

E.7

Andre Barbosa & Chris Higgins
Oregon State University
barbosa@oregonstate.edu

6/1/2017

541-737-7291

Rev. 5

Drawn by: KAF

Reviewed by: ARB

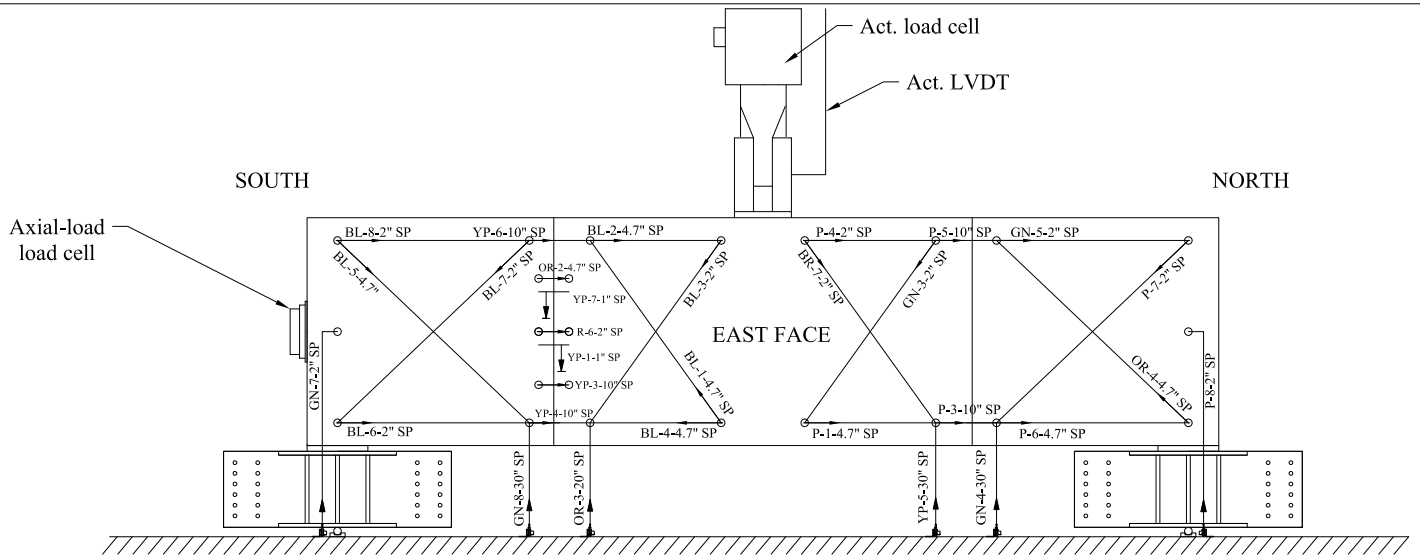

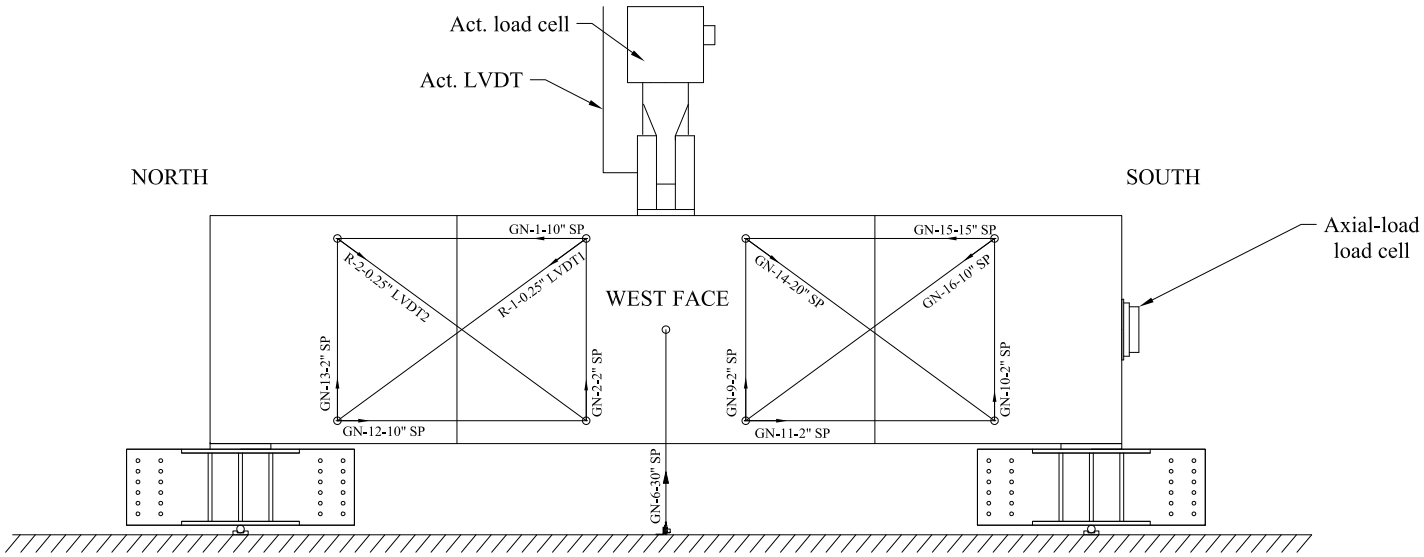

NOTES:		
Sensor labels:	"cable color - # - length- sensor type"	
Cable color:	GN - Green BL - Blue OR - Orange	P - Purple R - Red YP - Yellow purple
Sensor type:	SP - String potentiometer LVDT - Linear variable displacement transducer	

Spliced Shear Wall Specimen
Wall 6 Instrumentation Sensor Labels

E.8

Andre Barbosa & Chris Higgins
Oregon State University
barbosa@oregonstate.edu

6/1/2017

541-737-7291

Rev. 5

Drawn by: KAF

Reviewed by: ARB

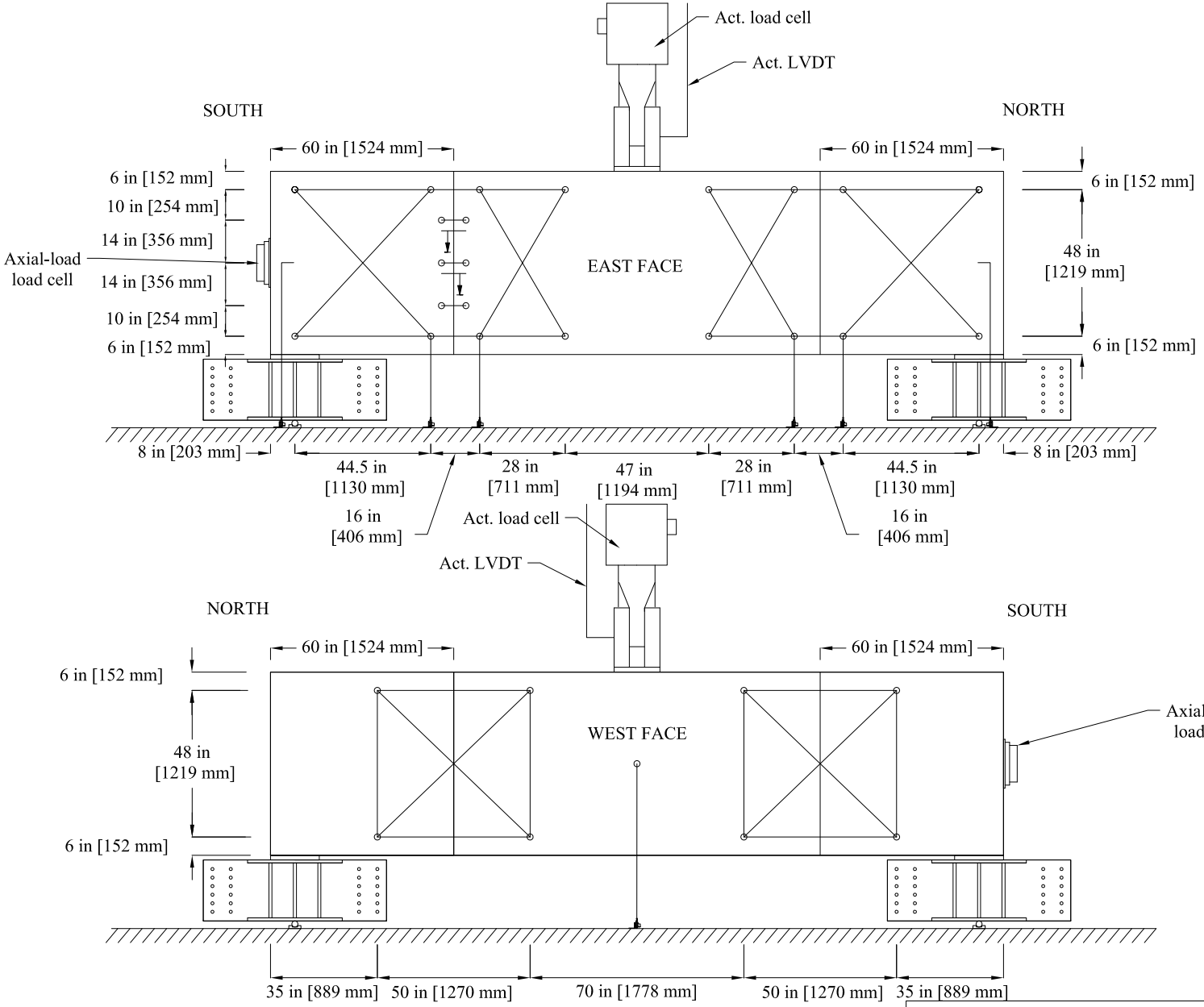

Spliced Shear Wall Specimen
Wall 7 Instrumentation Layout

E.9

Andre Barbosa & Chris Higgins

Oregon State University

barbosa@oregonstate.edu

6/1/2017

541-737-7291

Rev. 5

Drawn by: KAF

Reviewed by: ARB

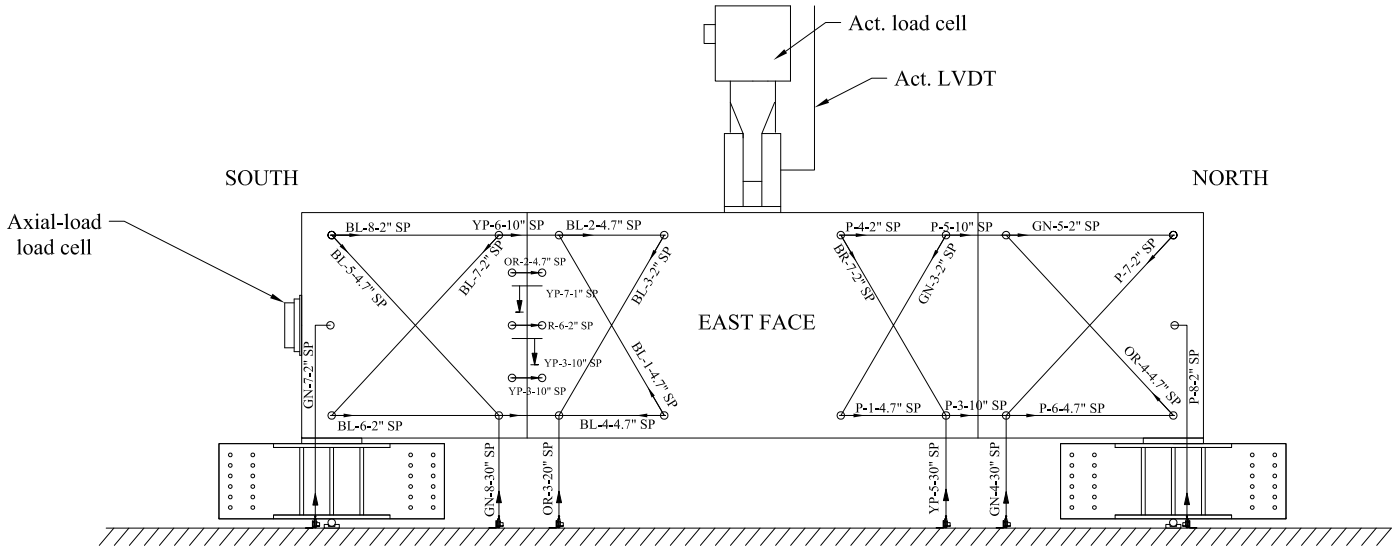

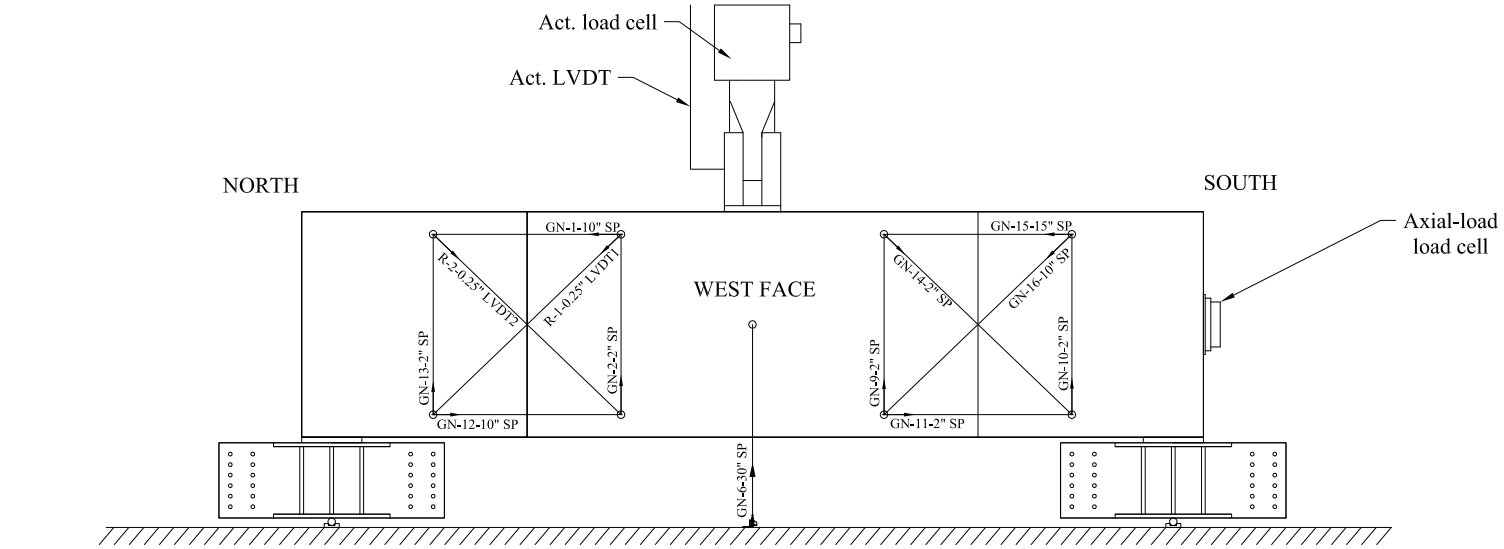

NOTES:		
Sensor labels:	"cable color - # - length- sensor type"	
Cable color:	GN - Green BL - Blue OR - Orange	P - Purple R - Red YP - Yellow purple
Sensor type:	SP - String potentiometer LVDT - Linear variable displacement transducer	

Spliced Shear Wall Specimen
Wall 7 Instrumentation Sensor Labels

E.10

Andre Barbosa & Chris Higgins

Oregon State University

barbosa@oregonstate.edu

6/1/2017

541-737-7291

Rev. 5

Drawn by: KAF

Reviewed by: ARB

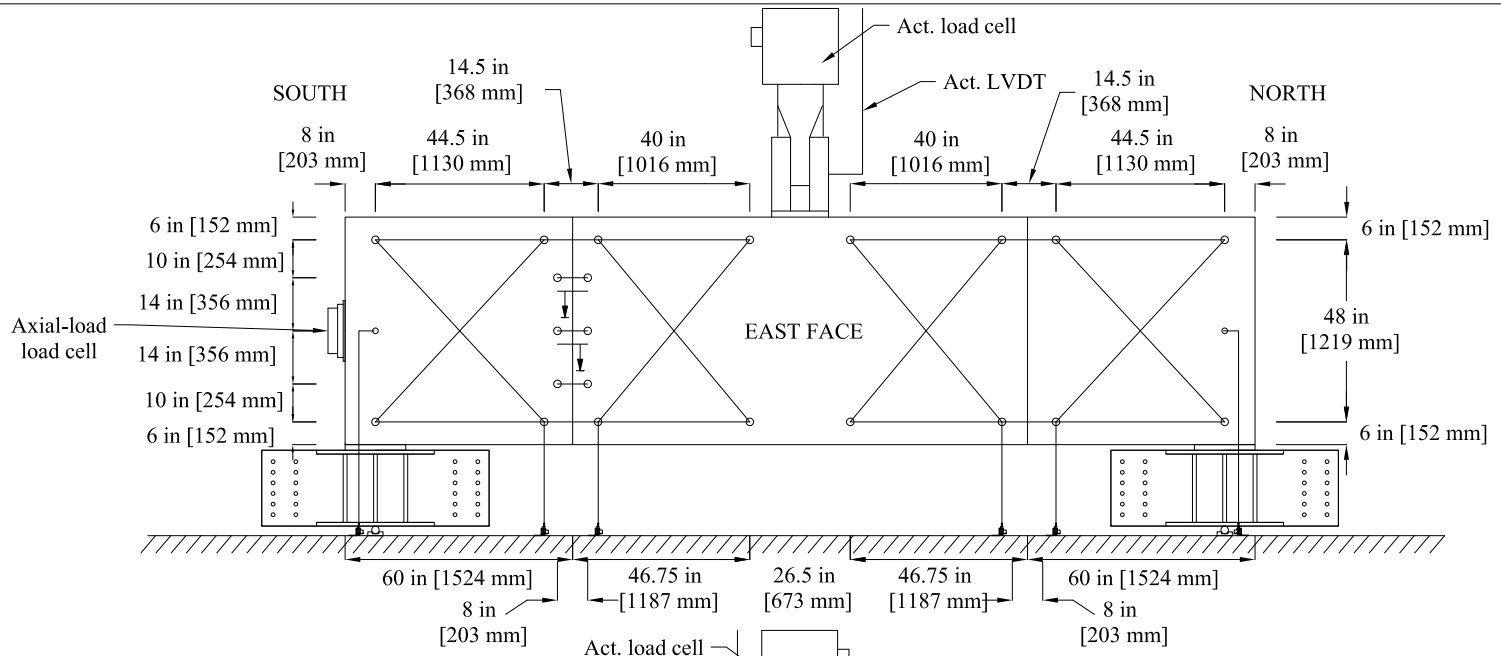

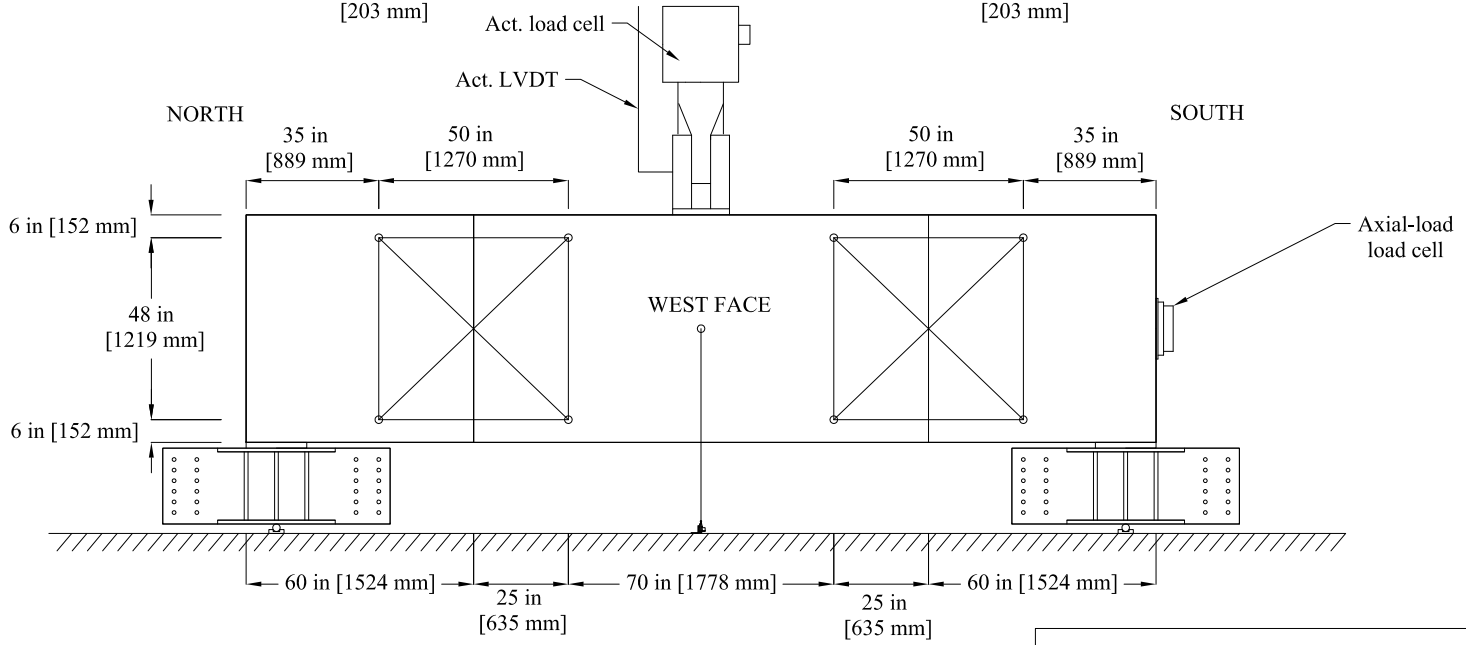

Spliced Shear Wall Specimen **Wall 8 Instrumentation Layout**		**E.11**
Andre Barbosa & Chris Higgins	6/1/2017	
Oregon State University	541-737-7291	
barbosa@oregonstate.edu	Rev. 5	Drawn by: KAF Reviewed by: ARB

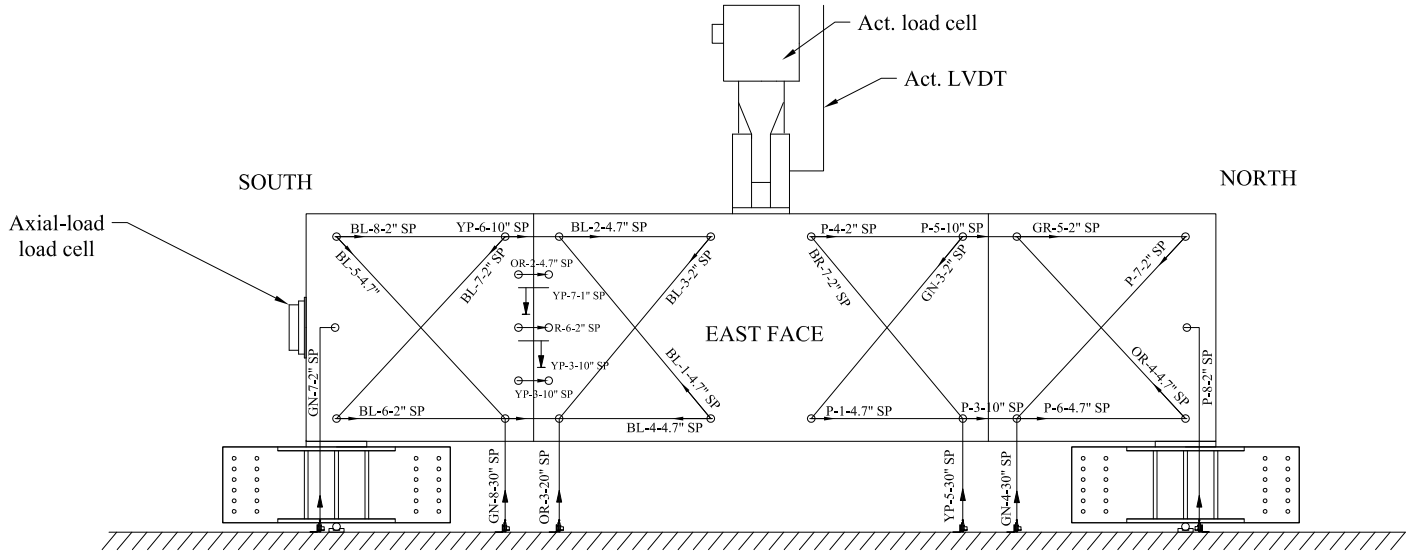

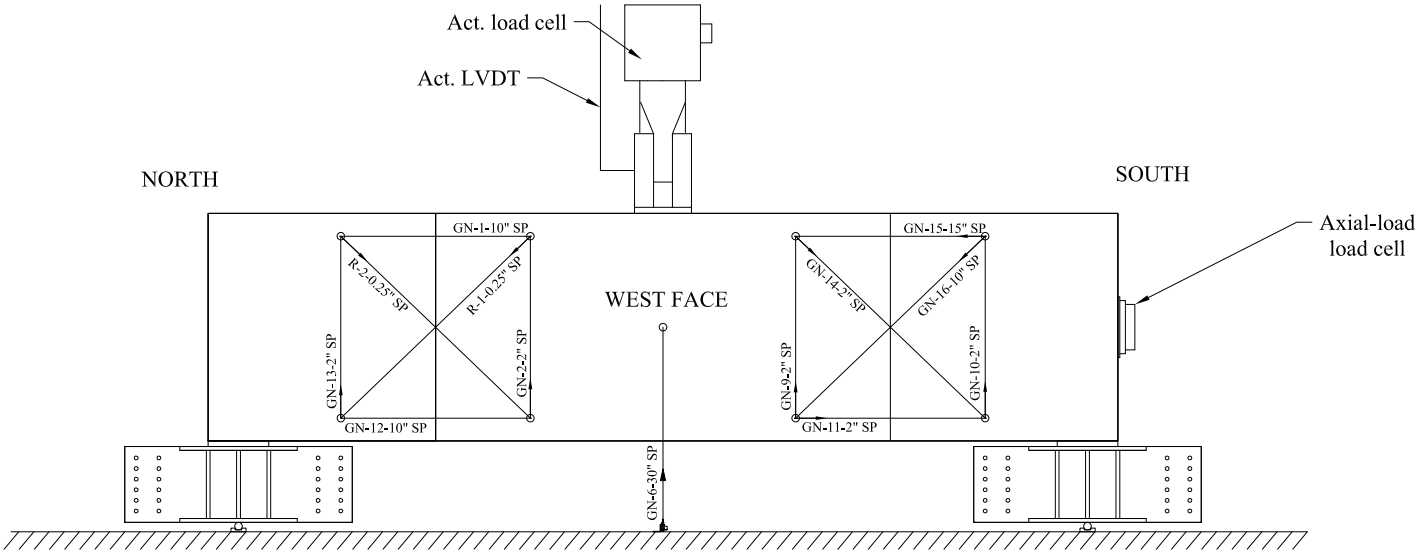

NOTES:		
Sensor labels:	"cable color - # - length- sensor type"	
Cable color:	GN - Green BL - Blue OR - Orange	P - Purple R - Red YP - Yellow purple
Sensor type:	SP - String potentiometer LVDT - Linear variable displacement transducer	

Spliced Shear Wall Specimen
Wall 8 Instrumentation Sensor Labels

E.12

Andre Barbosa & Chris Higgins
Oregon State University
barbosa@oregonstate.edu

6/1/2017

541-737-7291

Rev. 5

Drawn by: KAF

Reviewed by: ARB

REPORT DELIVERABLE 18-C:
Test 3: Glulam Beam-Column Connection Test Report

***infra*Structure Testing & Applied Research (*i*STAR) Laboratory**
Department of Civil & Environmental Engineering
Portland State University
P.O. Box 751, Portland, OR, 97207-0751

Portland State UNIVERSITY

Report prepared for The Framework Project, LLC

and submitted c/o KPFF Consulting Engineers

GLUE-LAMINATED TIMBER BEAM-TO-COLUMN CONNECTION TESTS FOR THE FRAMEWORK PROJECT

by

Tyler Williams, Graduate Research Assistant

Peter Dusicka, Ph.D., P.E., Associate Professor

Department of Civil and Environmental Engineering

Portland State University

P.O. Box 751, Portland, OR 97207

Email: dusicka@pdx.edu, Phone: (503) 725-9558

April 3, 2017

Contents

1.0 INTRODUCTION

1.1 Purpose

This report outlines project specific testing in support of the Framework Project in Portland, OR. The testing is based on "Section 4.0 GLT Beam to Column Connection Tests" of the "Experimental Testing Objectives" document written by KPFF Consulting Engineers dated April 7th, 2016 and was conducted at the infraStructure Testing and Applied Research (iSTAR) Laboratory at Portland State University (PSU), Portland, OR in October – November 2016.

The objective of the glulam timber beam to column (BTC) connection tests was to demonstrate that the proposed beam-to-column connection is capable of withstanding cyclic deformations up to the lateral drifts expected in the building at the risk-targeted maximum considered earthquake without loss of gravity-carrying capacity. This report summarizes three tests of a BTC connection designed by KPFF Consulting Engineers for potential use in an innovative mass timber building. The connection was designed as part of the Framework project, a proposed high-rise mass timber building in Portland, Oregon. Funding for this testing was made possible from the U.S Tall Wood Building Prize Competition, a partnership between the United States Department of Agriculture, Softwood Lumber Board, and the Binational Softwood Lumber Council. Figure 1, courtesy of Lever Architecture, is a rendering of a typical office story showing several bays of BTC connections visible along the perimeter of the building. Separate tests were conducted by others on the BTC column connection to validate a 2-hour fire resistance rating.

Figure 1 – Architectural rendering of typical office-use story with multiple BTC connections (image courtesy of Lever Architecture)

1.2 Connection Details

The connection details and associated terminology are illustrated in Figure 2. The BTC connection was designed to carry gravity loads and behave as a rotating pin with minimal moment transfer under lateral load conditions. This connection was not intended to be a resisting load element as part of the lateral force resisting system (LFRS), but was intended to accommodate the design lateral drifts associated with earthquake response of the building.

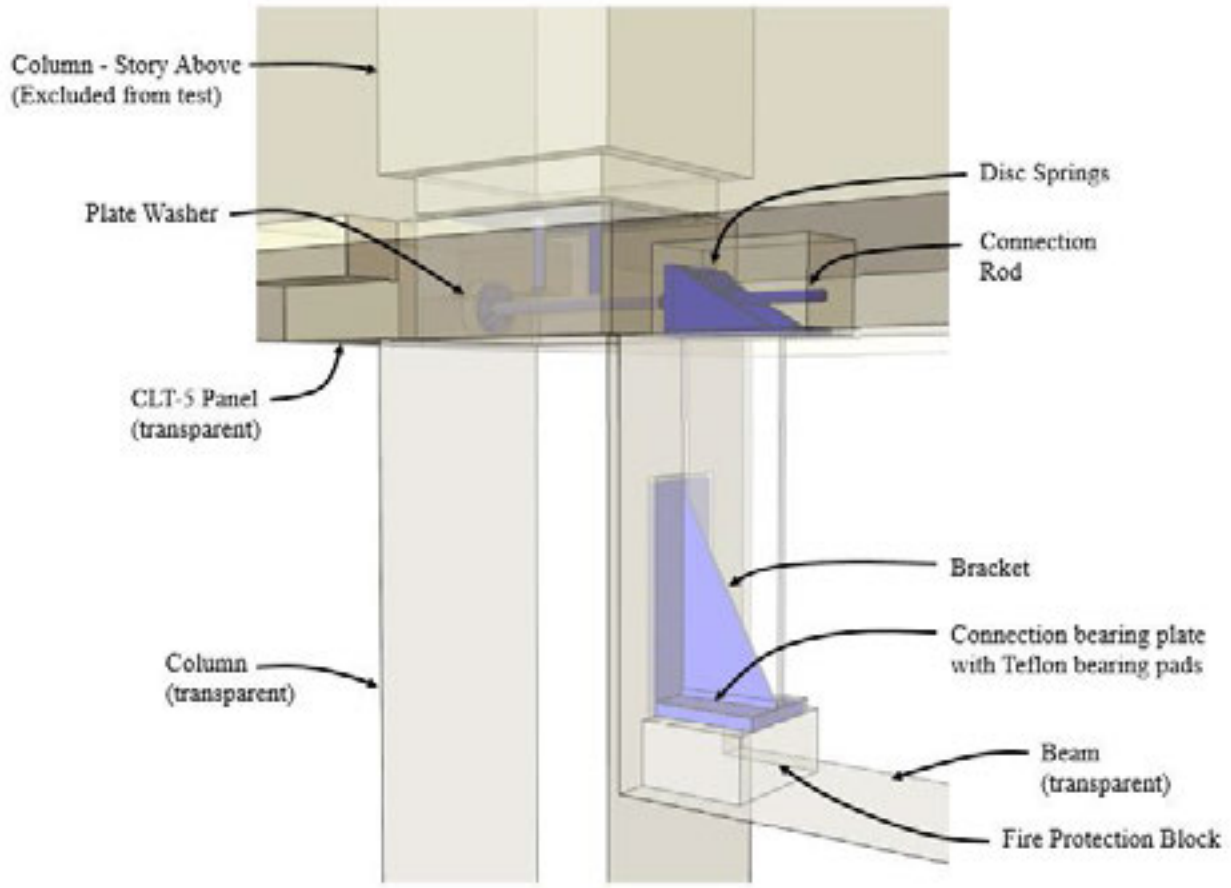

Figure 2 – Rendering of BTC connection with critical components labeled (courtesy StructureCraft)

The BTC connection consists of several components, a selected number of which were varied and altered throughout the course of testing. A stiffened steel bracket is screwed and nailed into the face of the column. The bearing plate on the bottom of this bracket holds the beam and transfers all gravity loads (connection shear) from the beam to the column. The bearing plate has a 1/8" Teflon pad on each side of the bracket stiffener to reduce friction between the beam and the bracket during lateral displacements.

The connection incorporates a mechanism intended to close gaps between the beam and the column that may open due to the imposed lateral displacements. This mechanism, installed at the top of the beam, utilizes a steel connection rod and disc springs (also called Belleville washers) to develop the clamping

force between the beam and the column. The connection rod is secured to the back side of the column using a nut and 3/8" circular plate washer. A 1" gap was provided between the CLT and glulam column at the front and rear of the connection in order to accommodate up to 4% drift.

The specimens were assembled and erected in accordance with methods prescribed by KPFF Consulting Engineers and the specimen fabricator, StructureCraft. The connection bracket and gap-closure bracket were installed by StructureCraft prior to delivery to iSTAR Laboratory. Each test followed the same assembly process. First, the column was erected, plumbed and braced in place. The beam was then lifted into place with care to minimize the initial gab between the beam and column. The gap-closure mechanism was installed and the nut on the connection rod was tightened to a pre-load of 400 pounds in each test to eliminate slack in the connection prior to displacement. The CLT was then placed on top of the beam and column and screwed into top of the beam.

2.0 TEST SETUP AND SPECIMEN DETAILS

2.1 Test Setup

The experiment used full-scale timber members and connections to investigate lateral displacement response from expected seismic excitation using a quasi-static displacement protocol. The test setup simulated half-length of one full-height bay of a typical story as illustrated in Figure 3. All beams and columns were glulam timber members, the beams conforming to 24F-V4 (DF-L) and the columns conforming to L2 (DF-L) standards. In each test, a full size 14-1/4"x16-1/2"x11'6-3/4" long column was connected to a beam with a full-sized 12-1/4"x24" cross section with an overall length of 14'0". This length corresponds to one-half of the 28'-0" bay span of the proposed Framework building design. The base of the column was supported using a zero-slack pin apparatus. A floor slab measuring 17'-0"x8'-0" of five-ply cross laminated timber (CLT-5) was installed on top of the beam to check displacement compatibility between the floor decking and top of columns.

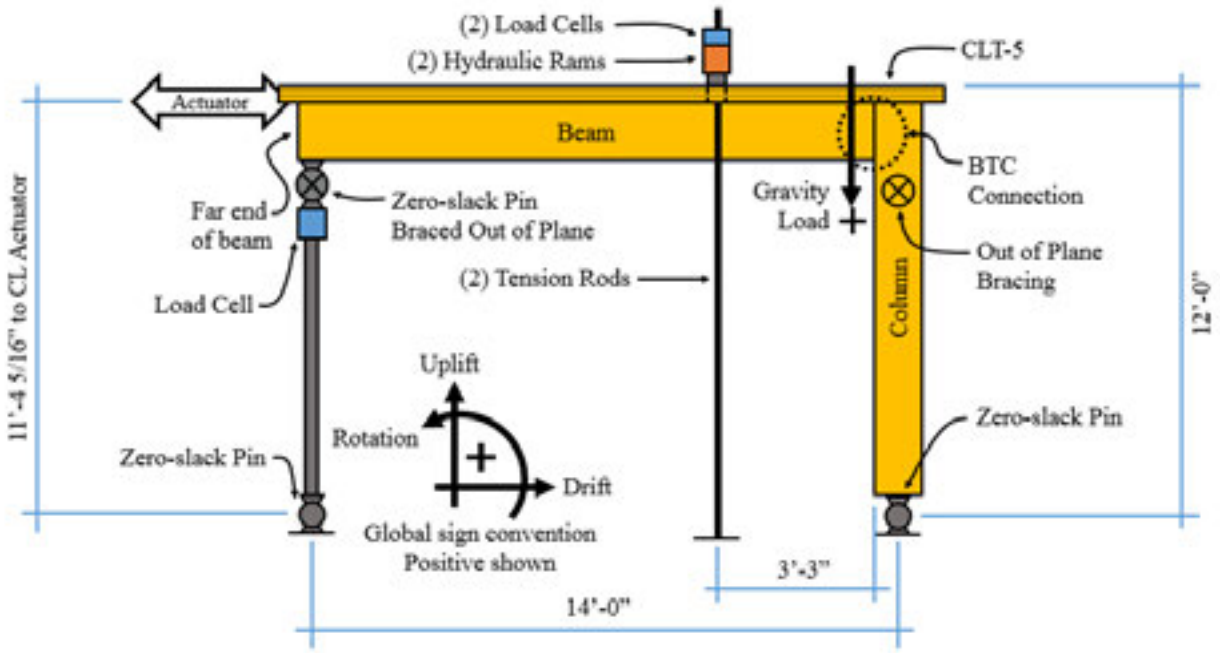

Figure 3 – Test Setup Overview

The test beams were supported on one end by the BTC connection and at the other (far) end by a zero-slack pin apparatus. This pin connection at the end of the half-length beam simulates the inflection point of the full-length beam. Supporting the beam at its inflection point assumes that in the real structure, equal and opposite displacement and rotational behaviors occur at each end of the beam. As such, overall beam and BTC connection performance is representative of the as built loading conditions.

Three individual tests were conducted with three nominally identical sets of beams and columns. The CLT floor slab was re-used for all of the tests. The beams and the columns were assigned individual names according to their corresponding test: B01 and C01 for Test 1, B02 and C02 for Test 2, and B03 and C03 for Test 3. This naming convention is used throughout this report to identify specimens from each individual test.

Gravity load in the beam was simulated using hydraulic cylinders attached to tension rods, which were in turn anchored into the laboratory strong floor. A slot was cut in the CLT-5 panel to allow the rams to apply load directly to the top of the beam. Had the load been directly applied to the CLT-5 panel on top of the beam, an unknown amount of load could have bypassed the BTC connection and entered the column through direct bearing between the CLT-5 and column. Bearing the rams directly on the beam ensured that the applied load had a direct path through the beam to the connection bracket, allowing the BTC connection's performance to be evaluated without unintended interference from the CLT-5 floor panel. At story drifts of 0.9% and greater, the rams were manually adjusted to ensure that the applied gravity load in the connection remained approximately constant at 24 kips. Unless otherwise noted, the connection shear remained within +/- 10% of the target load for the entire duration of each test.

Instrumentation was installed on each specimen as detailed in Appendix A, where individual instruments are uniquely identified. The rotation of the BTC connection was assessed by two sets of instruments:

LVDTs 1 and 2 were attached to the beam and reacted against an arm extending from the column, and LVDTs 15 and 16 were attached to the column and used to measure the rotational displacements of the column base relative to the floor beam. LVDT 3 measured any potential crushing at the BTC connection.

The gap between the beam and the column was monitored by LVDTs 4, 5 and 6, each attached to the side of the beam and reacting against the face of the column. LVDT 12 monitored the gap between the top of the column and the top of the CLT-5 floor panel.

The CLT floor panel was instrumented to monitor any potential movement relative to the beam and the column. LVDT 7 was affixed to the beam to measure longitudinal slip of the CLT floor panel relative to the beam. LVDTs 8, 9, 10, 11 and 13 were attached to the beam or column to monitor uplift of the CLT-5 floor panel. The overall lateral deformation of the specimen was monitored using a string pot displacement transducer LVDT 14, measuring the absolute displacement of the column relative to the laboratory strong floor. Longitudinal slip of the column support was monitored by LVDT 17.

Forces in the system were monitored using several load cells as depicted in Appendix A. Lateral load applied by the displacement actuator were monitored with an integrated load cell (LC1). Gravity loads imposed by the rams were monitored using a compression-only load cell installed on each tension rod shown as LC2. The load developed within the connection rod of the BCT connection was monitored using LC3. The reaction force at the far side of the beam was monitored with load cell LC4, which was incorporated within the support structure assembly.

Global coordinates for the test setup were assigned as shown in Figure 3. Positive drift is considered as displacement in the positive longitudinal direction. Likewise, negative drift refers to story displacement in the negative longitudinal direction. Positive drift cycles opened a gap at the top of the BTC connection and compressed the disc springs in the gap-closure mechanism, while negative drift cycles did not engage the gap-closure mechanism.

Actuator loads are shown as negative when in compression and positive when in tension. Connection shear in the direction of gravity is considered positive. The test setup was braced out-of-plane at the locations shown in Figure 3. Thus, all deformations remained in plane of the setup shown.

2.2 Loading Protocol

The lateral displacements were imposed using an actuator attached to the far end of the beam in line with the seam between the CLT panel and the beam itself. Cyclic displacements followed a modified version of the CUREE W-02 abbreviated displacement history. The target displacement, Δ, was set to 3% drift, which equals the expected inter-story drift under the Maximum Considered Earthquake (MCE_R). The Design Basis Earthquake (DBE) inter-story drift was 2%. The CUREE W-02 abbreviated displacement protocol was modified at the request of KPFF Consulting Engineers such that each primary cycle was followed by only two trailing cycles of the same amplitude as the primary cycle as depicted in Table 1.

Table 1 – Modified CUREE W-02 abbreviated displacement protocol. Δ = 3% (4.32 in).

Cycles	Amplitude (Δ)	Displacement [in]	% Drift
1-3	0.05	0.216	0.15%
3-5	0.075	0.324	0.23%
6-8	0.1	0.432	0.30%
9-11	0.2	0.864	0.60%
12-14	0.3	1.296	0.90%
15-17	0.4	1.728	1.2%
18-20	0.7	3.024	2.1%
21-23	1	4.32	3.0%
24-26	1.5	6.48	4.5%
27-29	1	4.32	3.0%
30-32	0.4	1.728	1.2%
33-35	2	8.64	6.0%

2.3 Test-Specific Variables

Although the specimens and connections were nominally the same for each of the three tests, selected variations were implemented as summarized in Table 2. The variations were chosen based on observations made from the preceding test in an effort to further refine performance of the connection.

Table 2 – Variable conditions for each of the three BTC connection tests

Variable	Test 1	Test 2	Test 3
Specimens	B01 & C01	B02 & C02	B03 & C03
Beam Moisture Content	9.4%	7.7%	8.0%
Col. Moisture Content	8.8%	7.7%	7.8%
Teflon Bearing Pads	Unglued	Glued	Glued
Column to CLT Gap	None	1/16”	1/16”
Number of Disc Springs	8	8	12
Disc Spring Thickness	2.5 mm	2.5 mm	3.0 mm
Disc Spring Height	5.7 mm	5.7 mm	6.0 mm
Connection Rod	5/8” all-thread	5/8” smooth rod with long threaded ends	5/8” smooth rod with short threaded ends

3.0 DATA PROCESSING

3.1 Story Displacement and Drift

The story drift was monitored using a string pot displacement transducer as illustrated in Figure 4. The free end of the string pot was attached to the column in each test at height, H, above the column’s support pin. Rigid body movement was assumed and overall story displacement was calculated using similar triangles as shown in Equation (1), where Δ_s is the displacement at the top of the story, Δ is the measured displacement at the height of the string pot displacement transducer, H is the height of the string pot above the center of rotation, and H_s is the overall story height.

$$\Delta_s = \left(\frac{\Delta}{H}\right) * H_s \tag{1}$$

Story drift, δ_s, is expressed as a percentage of the overall story height in this report. Story drift values were calculated as shown in Equation (2).

$$\delta_s = \frac{\Delta_s}{H_s} * 100\% = \left(\frac{\Delta}{H}\right) * 100\% \tag{2}$$

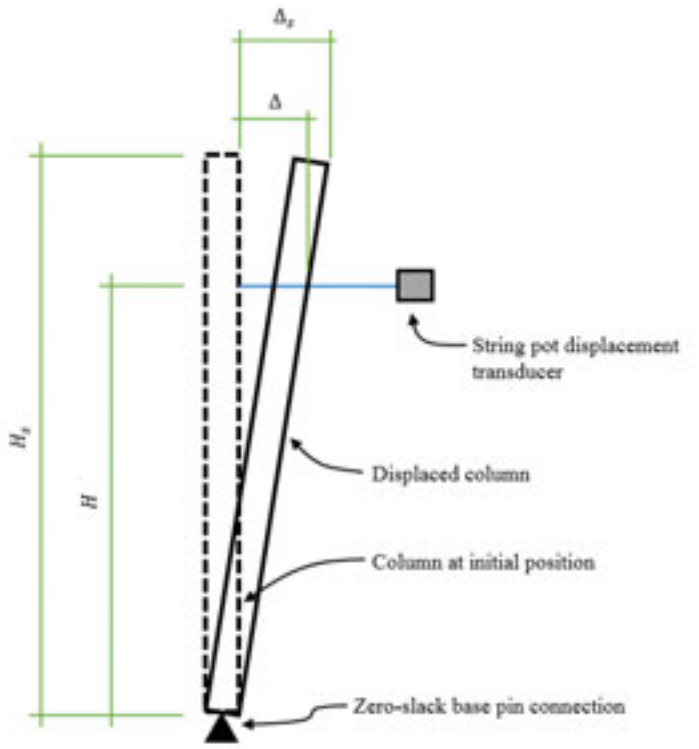

Figure 4 – Calculation of story drift

3.2 Connection Rotation

Beam to column rotation was independently monitored in two separate ways: Method 1 used LVDTs 1 and 2 mounted on the beam that reacted on short member connected to the column, while Method 2 used LVDTs 15 and 16 mounted to the base of the column. Both methods calculated rotations using trigonometric relationships described below and yielded similar rotation values for each test. The similarity in rotations calculated via each method indicated rigid-body movement of the column and provided independent rotation measurements in the event of instrumentation problems. In this report, connection rotation values shown were calculated using Method 1 except for displacement cycles starting at 4.5% drift during Test 2. At these high displacements in Test 2, LVDT 1 stroked out and effectively stopped recording additional rotation data via Method 1. As such, Method 2 was used to calculate connection rotations for cycles 24-35 in Test 2.

Figure 5 illustrates the geometric relationships measured by LVDTs 1 and 2. These measurements were used in Method 1 to determine connection rotation as shown in Equation (3), where θ is the connection rotation, H_1 is the displacement measured by LVDT 1, H_2 is the displacement measured by LVDT 2, and L_1 is the distance between the instruments.

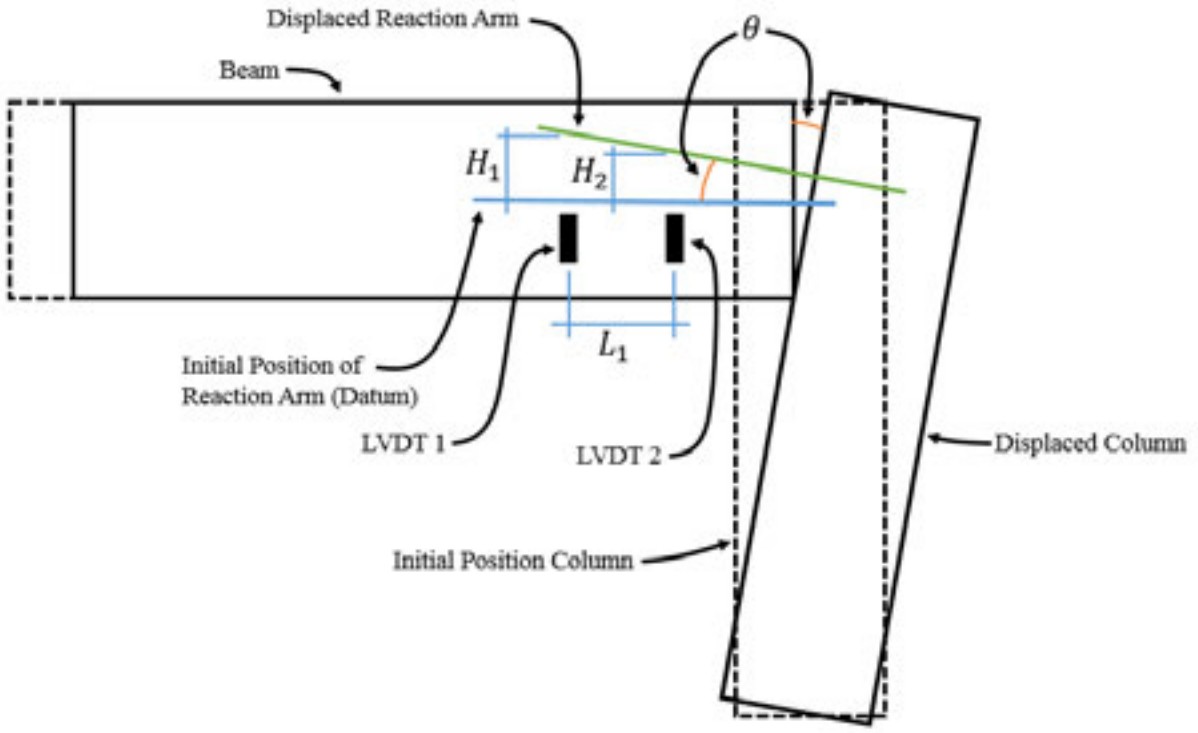

Figure 5 – Method 1 – Connection Rotation Calculation

$$\theta = atan\left(\frac{H_1 - H_2}{L_1}\right) \tag{3}$$

Figure 6 illustrates the geometric relationships measured by LVDTs 15 and 16. Data gathered with these instruments were used to calculate rotation values via Method 2 as shown in Equation (4) where α is the column rotation, H_s is the displacement measured by LVDT 15, H_n is the displacement measured by LVDT 16, and L is the distance between the instruments. The close relationship between θ and α allows for this method to be used to determine rotations at displacements of 4.5% and greater, where LVDT 1 stroked out.

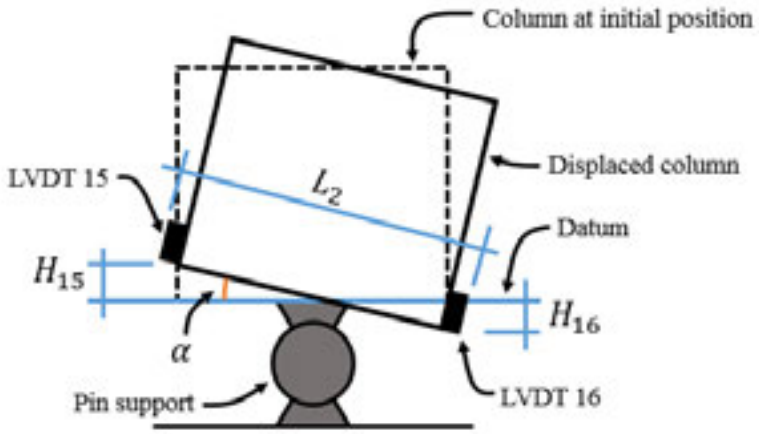

Figure 6 – Method 2 – Connection Rotation Calculation

$$\alpha = atan\left(\frac{H_{15} + H_{16}}{L_2}\right) \tag{4}$$

3.3 Connection Shear

Shear in the BTC connection was monitored indirectly in accordance with the principles of engineering mechanics. Figure 7 below shows a free body diagram of the beam during testing. LC3 was initially zeroed before the beam and CLT were installed for each test. The self-weights of the beam, CLT and actuator were monitored and recorded as each of these were installed on the test setup. The recorded values were compared to known weights of these items to confirm accurate measurements. The gravity load imposed by the rams was monitored using a load cell on each tension rod, as was the support reaction at the far end of the beam. Using statics, the total load in the BTC connection was calculated and monitored in real-time during testing as shown in Equation (5), where V_c is the connection shear, R is the measured reaction at the far end of the beam, F_a is the self-weight of supporting the actuator, F_r is the applied load from the hydraulic rams, and W_s is the self-weight of the beam and CLT-5 panel. In this experiment, the total length of the beam, L, was 14'-0" and the distance from the BTC connection to the hydraulic rams, L_r, was 3'-3".

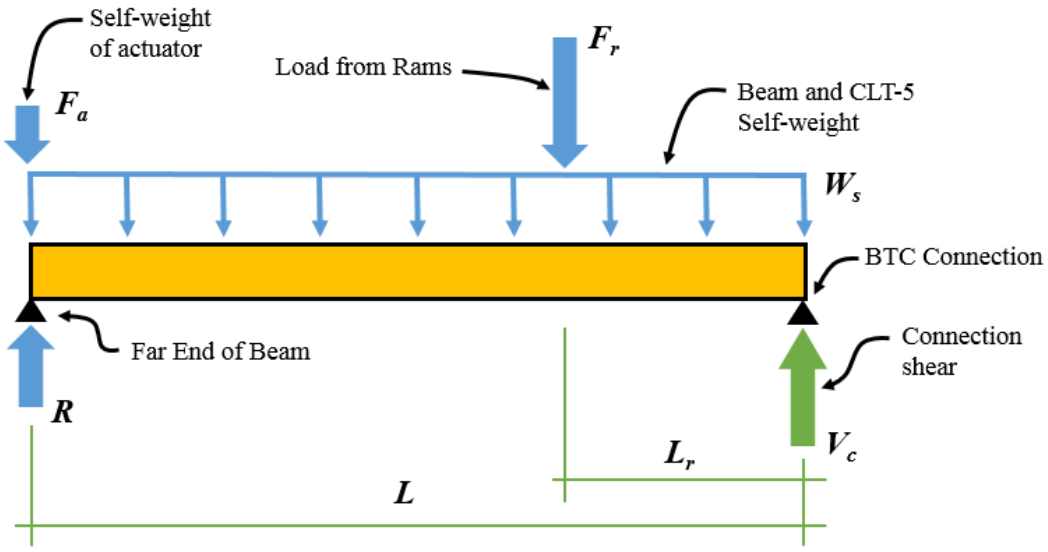

Figure 7 – Free body diagram of beam during experimental testing

$$V_c = F_a + F_r + W_s L - R \tag{5}$$

3.4 Connection Moment

Moment in the BTC Connection itself was calculated using the principles of engineering mechanics. The support at the far side of the beam was assumed to be a roller support only capable of reaction in the vertical direction. As such, all horizontal load from the actuator was resisted by the pin support at the base of the column. Figure 8 shows the idealized structure and a free body diagram of the column itself, with a section cut through the BTC connection. The horizontal reaction at the pin support was calculated according Equation (6). Moment in the connection was then calculated using Equation (7)

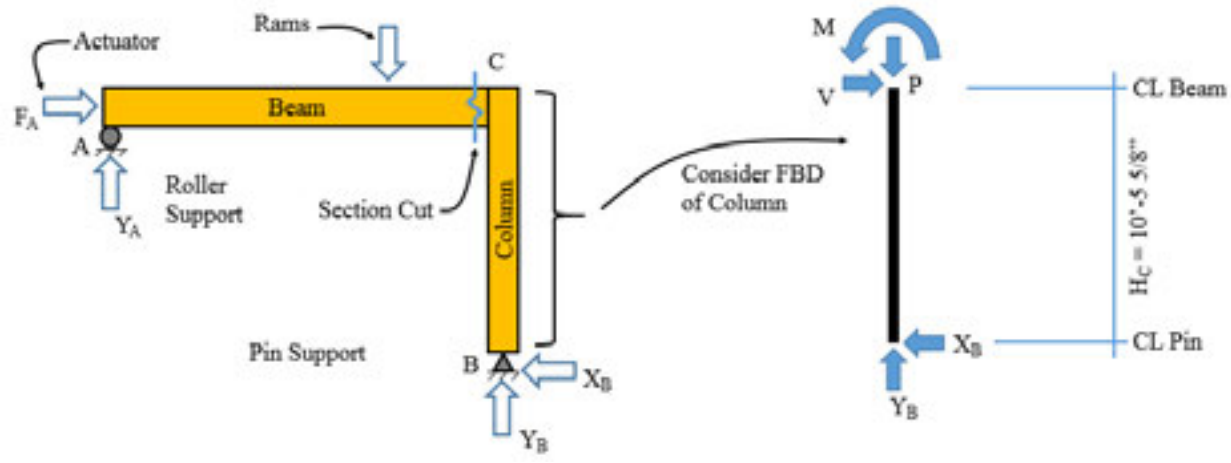

Figure 8 – Calculation of moment in BTC connection during experimental testing

$$\Sigma F_x = F_A - X_B = 0 \tag{6}$$

$$\Sigma M_{@c} = M - X_B * H_c = 0 \tag{7}$$

3.5 Displacement at Connection Rod

Displacement of the connection rod, and, by association, deformation of the disc springs, was calculated using LVDTs that monitored relative displacements between the beam and column. Figure 9 shows the positon of (3) LVDTs that measured displacement of the beam from the face of the column. Distance between these instruments and the connection rod (L_B, L_M, and L_T) were measured during instrumentation installation for each test. The gap distances recorded by each LVDT (G_b, G_m, and G_t) were recorded during testing and used to compute the slope of the beam relative to the column per Equation (8). The displacement of the connection rod, Δ_r, was calculated using this slope as shown in Equation (9).

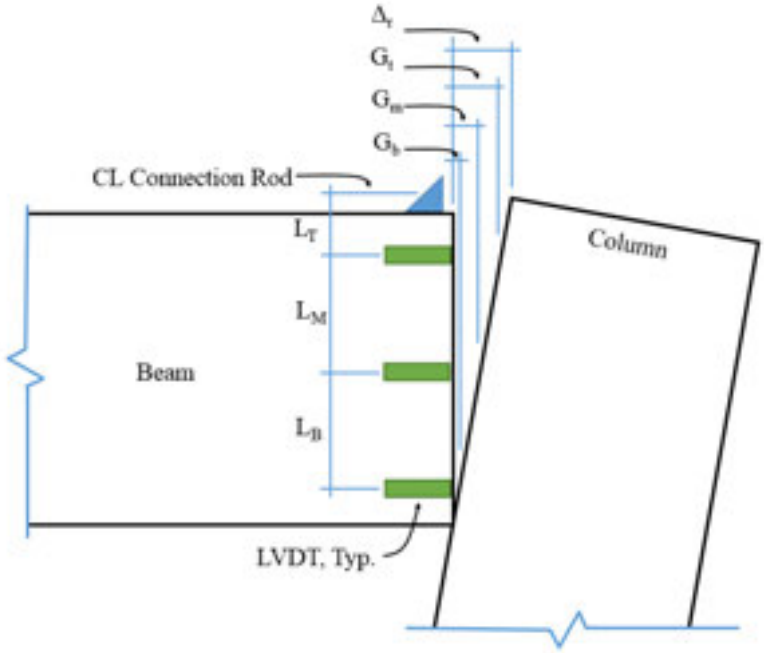

Figure 9 – Calculation of connection rod displacement

$$S = L_M/(G_t - G_m) \tag{8}$$

$$\Delta_r = G_t + (L_T/S) \tag{9}$$

3.6 Sample Rates and Plotting

Experimental data was collected at a rate of 100 Hz. Data was resampled down to a rate of 20 Hz for analysis purposes. Plots were generated using the resampled data with a moving average filter applied to reduce data noise.

4.0 TEST RESULTS

4.1 Test 1 – B01 and C01

Experimental test results for global behavior in Test 1 involving B01 and C01 are summarized in Figure 10, Figure 11, Figure 12 and Figure 13 on the following pages.

The following relevant observations were noted during Test 1:

- As the rams applied the simulated gravity load to B01-S-1 prior to beginning the displacement protocol, a compressive (negative) load was recorded in the actuator. This horizontal load was attributed to the eccentricity created by the vertical reaction on the bearing plate from the beam in the BTC connection, relative to the centerline of the column. This eccentricity produced a constant moment in the column that was resolved by a horizontal reaction at the column base. This horizontal reaction was in turn brought to static equilibrium with an equal and opposite force at the actuator. The eccentricity-induced compressive beam load was also observed in subsequent Tests 2 and Test 3.
- Starting on positive displacement cycles of 0.9% drift and above, non-linear behavior was observed in the disc springs as shown in Figure 13. A distinctive "S-shaped" pattern developed between the load in the connection rod and the gap between the top of B01 and the face of C01. This relationship indicated between 500-1000 pounds of load could develop in the connection rod before the bottom gap between B01 and C01 fully closed. The entire beam would then slide along the Teflon pad with little increase in load until the bottom gap closed. After bottom gap closure, the connection rod load increased as expected. Similar behavior was observed in Tests 2 and Test 3. Non-linear behavior was constrained to the disc springs and no other significant damage was observed in the system until displacements of approximately 4.5% drift. Above 4.5% drift, the disc springs were fully compressed and force in the connection rod rapidly increased with additional displacement.
- Audible cracking sounds were occasionally observed starting at displacement cycles of 3% drift. However, no visible cracks were observed on the outside face of B01 during Test 1. Repetitive cracking sounds were heard on positive displacement cycles starting at 4.5% drift.
- The CLT-5 panel was in contact with the top of C01 prior to the start of testing and was observed to rub on the top of C01 during all displacement cycles of Test 1. This resulted in localized splintering along the edge of the CLT-5 panel nearest the BTC connection as depicted in Figure 17.
- Positive drift cycles of 6% produced a rapid increase in compressive actuator load. This load developed as a result of fully compressing the disc springs in the connection, thereby engaging the stiffness of the connection rod, beam and column.
- Figure 14, Figure 15 and Figure 16 show the connection at its static state, positive 3% drift and negative 3% drift.

After the testing protocol was completed, the following relevant observations were noted:

- The first four rows of screws anchoring the CLT to the beam closest to the column showed signs of pull-through crushing at the screw heads.
- The disc springs showed inelastic deformation that resulted in slack in the gap-closure mechanism. This slack is illustrated in Figure 13, where the force-displacement curves for displacement cycles of 1.2% and larger have positive connection rod displacement with zero load. Thus, the slack in the connection at any given cycle is shown in Figure 13 as the flat region of the force-displacement curve where connection displacement increases with zero connection load. This slack can be largely attributed to the inelastic deformation of the disc springs after displacements of 1.2% drift and greater.
- The flat washer on the nut-side of the connection rod load cell had bent due to the applied loads. This washer was used to transfer the load into the load cell and is not part of the KPFF Consulting Engineers' design of the BTC connection. A thicker 1/2" plate washer was fabricated and used on Tests 2 and 3 to prevent this washer bending contribution to the slack created in the gap closure mechanism.
- The BTC connection bearing plate showed evidence of metal-to-metal rubbing, likely caused by the compression-reinforcing screws. The compression reinforcing screws on B01 were installed proud to the bearing surface. The Teflon bearing pads were not glued to the BTC connection bearing plate for Test 1. The Teflon bearing pad on the east side of the connection appeared to have shifted during beam installation or testing and was largely undamaged. The west-side Teflon bearing pad had been punctured and crushed by the beam's compression screws.
- A visible area of crushing was observed on the face of C01 where the bottom of B01 bared against the column during positive 6% drift displacement cycles, though this was not observed at drift cycles of 4.5% and under. Photograph is included in Figure 18. Crushing was relatively minor with a maximum depth of approximately 1/16".

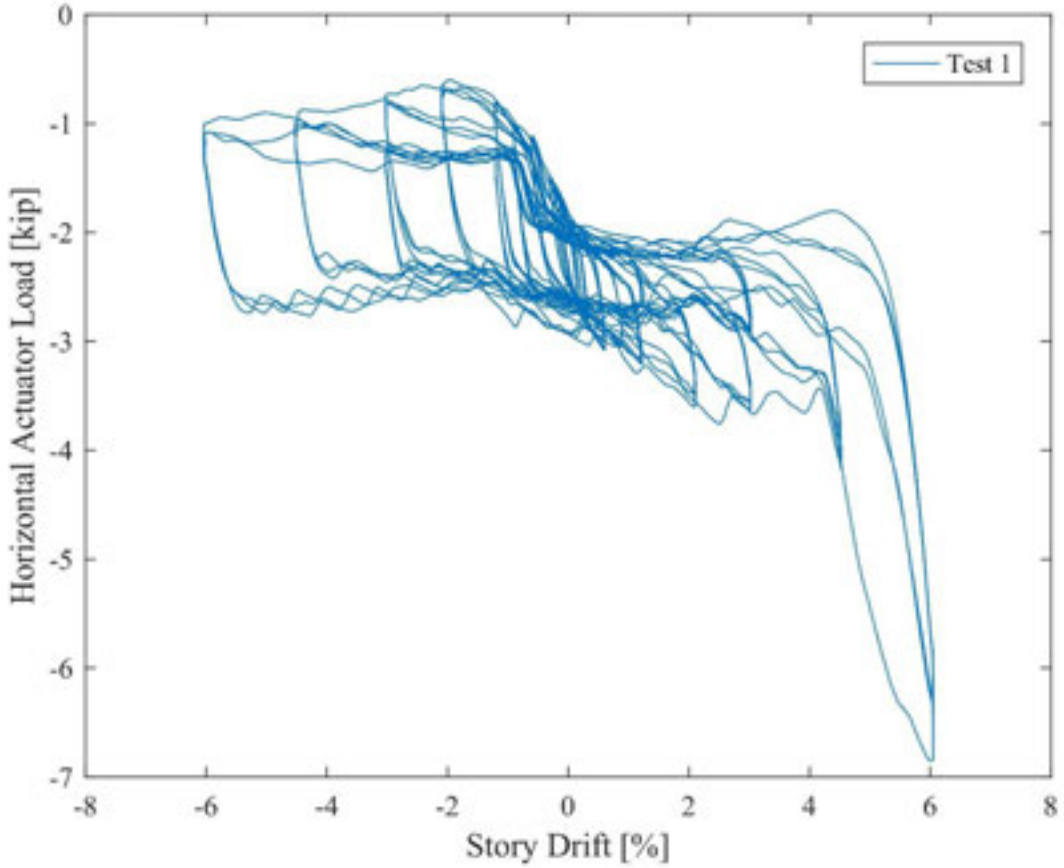

Figure 10 – Test 1 –Horizontal tip load vs. story drift

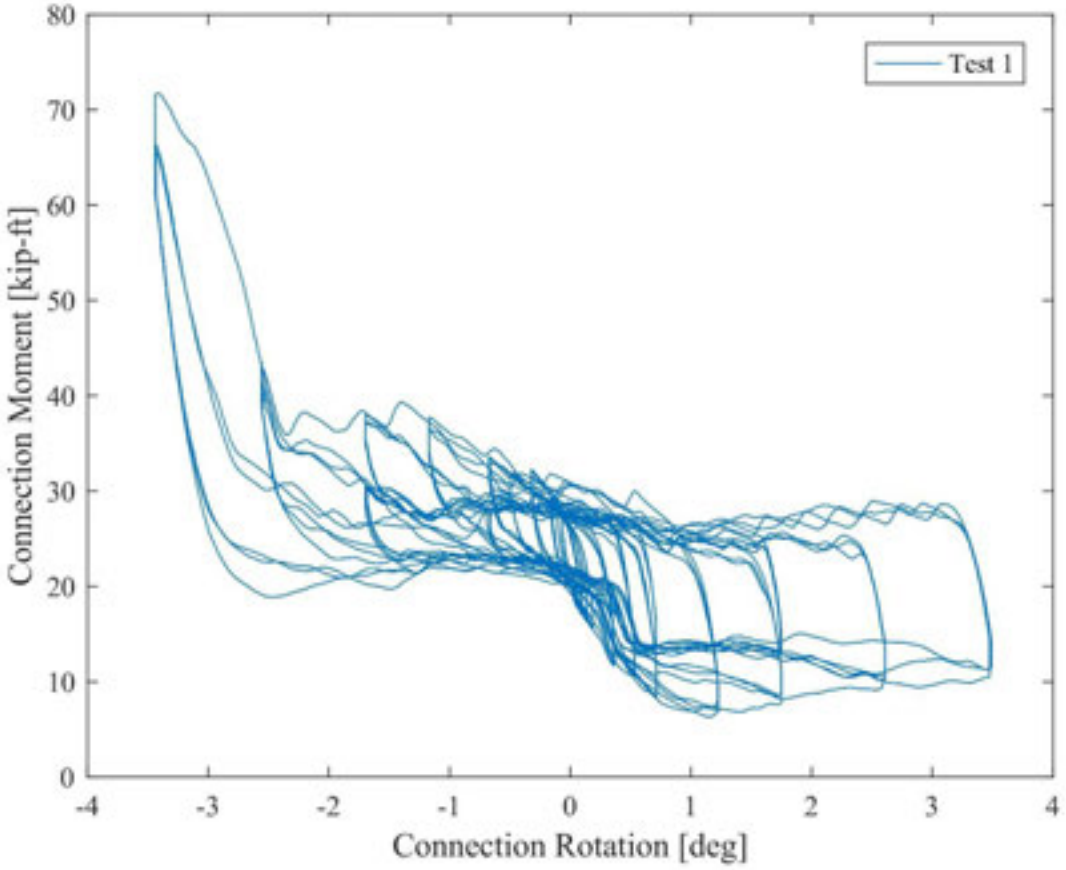

Figure 11 – Test 1 – Connection moment vs. connection rotation

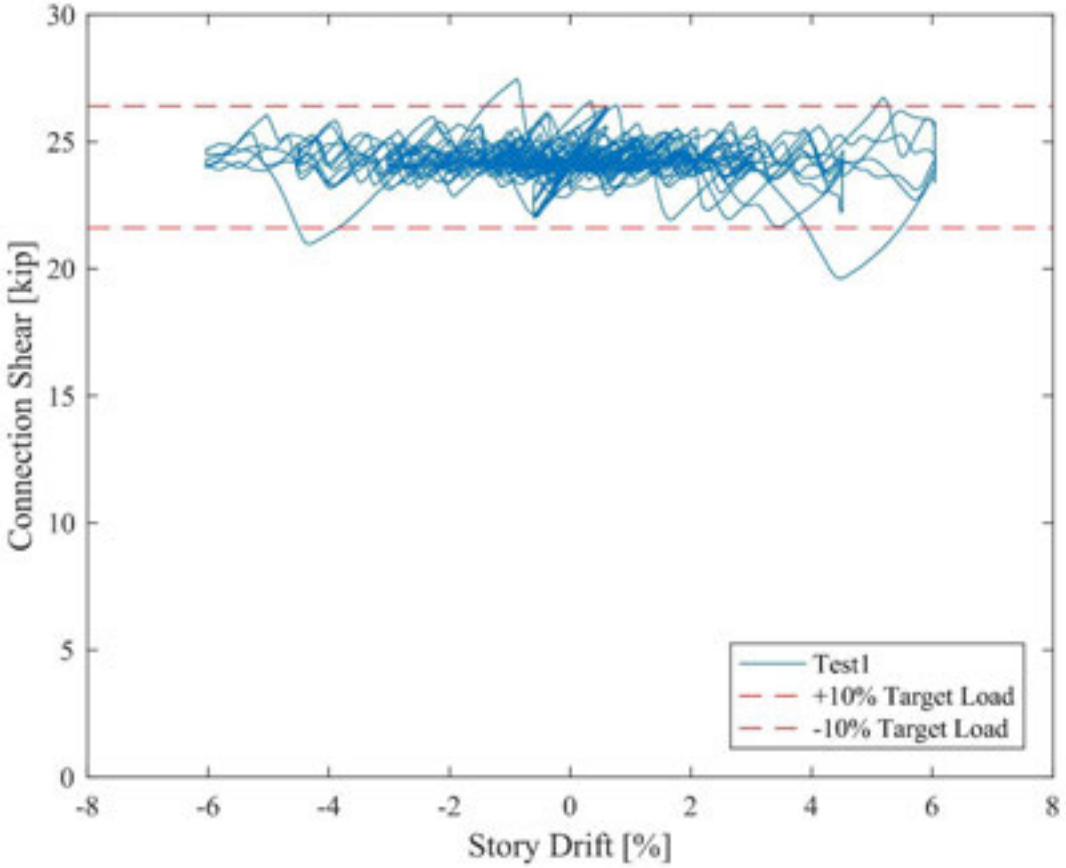

Figure 12 – Test 1 – Connection shear vs. story drift

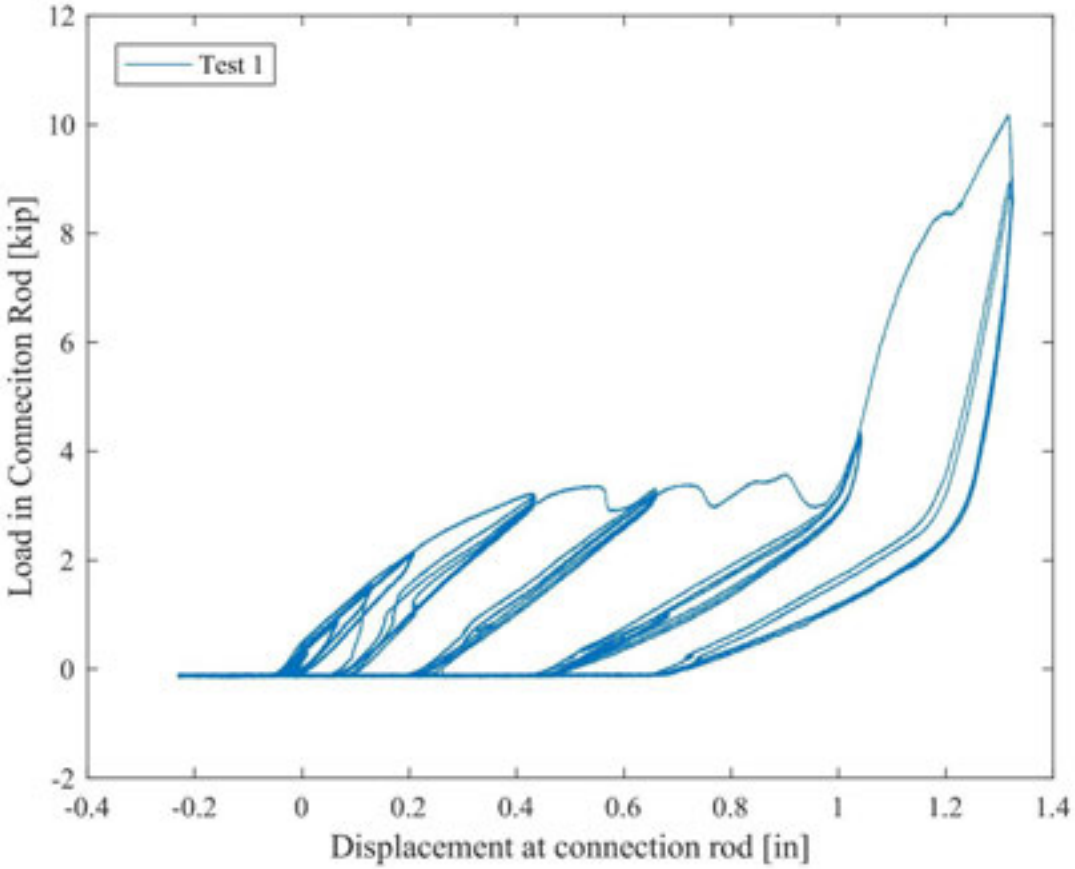

Figure 13 – Test 1 –Load in connection rod vs. displacement at connection rod

Figure 14 - Connection at Static State

Figure 15 – Connection at 3% positive drift

Figure 16 - Connection at 3% negative drift

Figure 17 – Splintering on edge of CLT-5 Panel post-Test 1

Figure 18 – Crushing on face of C01 post-Test 1

4.2 Test 2 – B02 and C02

Test 2 was nominally similar to Test 1, with minor changes made to the member specimens and connection components. The top of C02 was cut down to ensure a 1/16" gap existed between the top of the column and the CLT-5 floor panel when at zero displacement. The Teflon bearing pads were glued to the connection bearing plate to prevent slippage during testing. Experimental test results for global behavior in Test 2 involving B02 and C02are summarized in Figure 19, Figure 20, Figure 21 and Figure 22 on the following pages.

The following relevant observations were noted during Test 2:

- As with the previous test, nonlinearity was observed in the relationship between connection rod load and the top gap between B02 and C02 on positive displacement cycles of 1.2% drift and above. As with Test 1, this non-linear behavior is largely attributed to inelastic deformation of the disc springs.
- The S-shaped behavior was less pronounced in lower-displacement cycles for Test 2. However, all three 6% drift cycles showed jagged S-shaped slipping behavior during positive displacement.
- A gap was present between the CLT-5 and top of C02 for all displacement cycles up to and including 3% drift. The CLT-5 panel was observed to rub along the top of C02 in the 4.5% and

6% displacement cycles. This rubbing caused some crushing on the top of the column, as well as some localized splintering of the CLT-5.

- A loud cracking sound was heard on the first positive 6% displacement cycle. No visible cracks were seen on B02 and C02 during the test.
- Figure 24 shows the disc springs in the connection at its static state prior to large deformations. Figure 25 shows the disc springs fully compressed during a positive 6% drift displacement cycle. Finally, Figure 26 shows the disc springs again at the static state, but after large displacement cycles and illustrates the slack in the connection resulting from inelastic deformations of the disc springs.

After the testing protocol was completed, the following relevant observations were noted:

- Crushing and partial tear-out was observed on the four rows of CLT-5 screws nearest the column. The disc-springs showed similar permanent inelastic deformation to that observed in Test 1. On C02, back side of the column displayed approximately 1/8" of crushing around the round plate washer anchoring the connection rod to the column.
- The Teflon bearing pads used in Test 2 were physically glued to the BTC connection bearing plate and remained adhered to it for the duration of the test. The pads were punctured and showed evidence of tearing, likely due to the beam compression screws. After testing, all four of the beam compression screws on B02were observed to be proud to the wood bearing surface.
- Similar to Test 1, a crushing region was observed on the beam-side of C02 where B02 bared against the column during positive displacements as shown in Figure 23. This crushing did not appear to have caused any major structural damage to B02 and C02 and maximum crushing depth was limited to approximately 1/16".

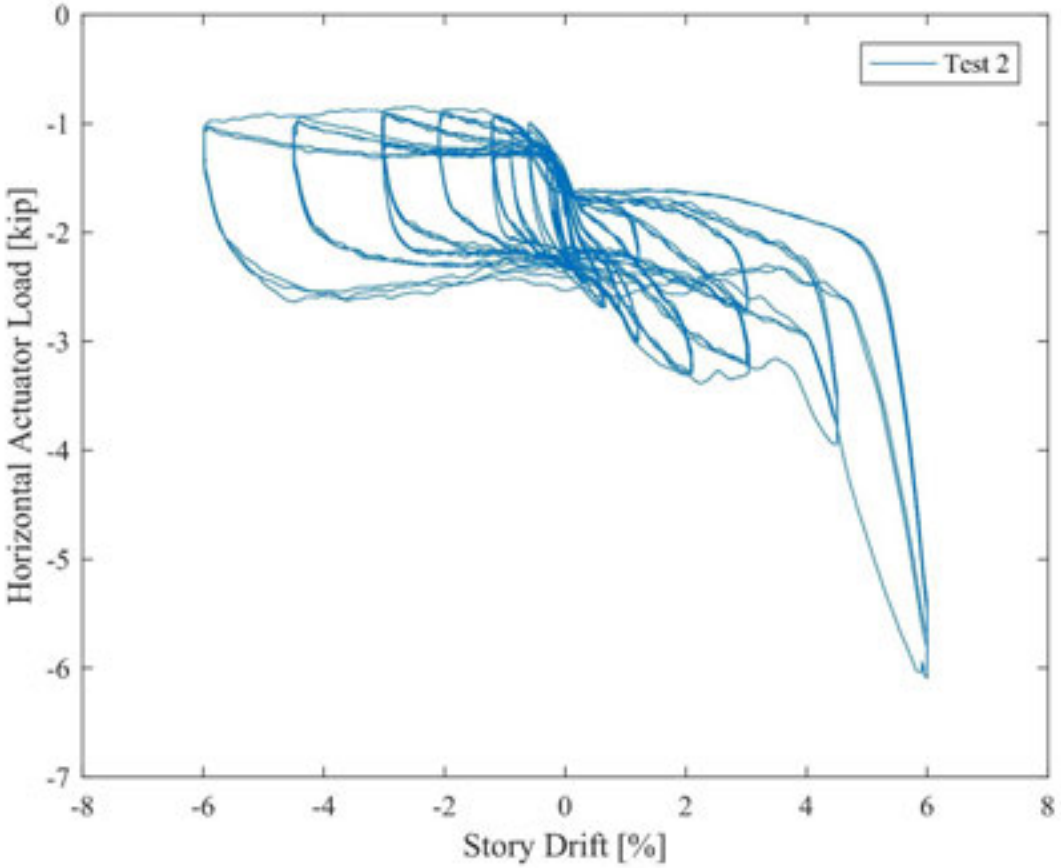

Figure 19 – Test 2 – Horizontal tip load vs. story drift

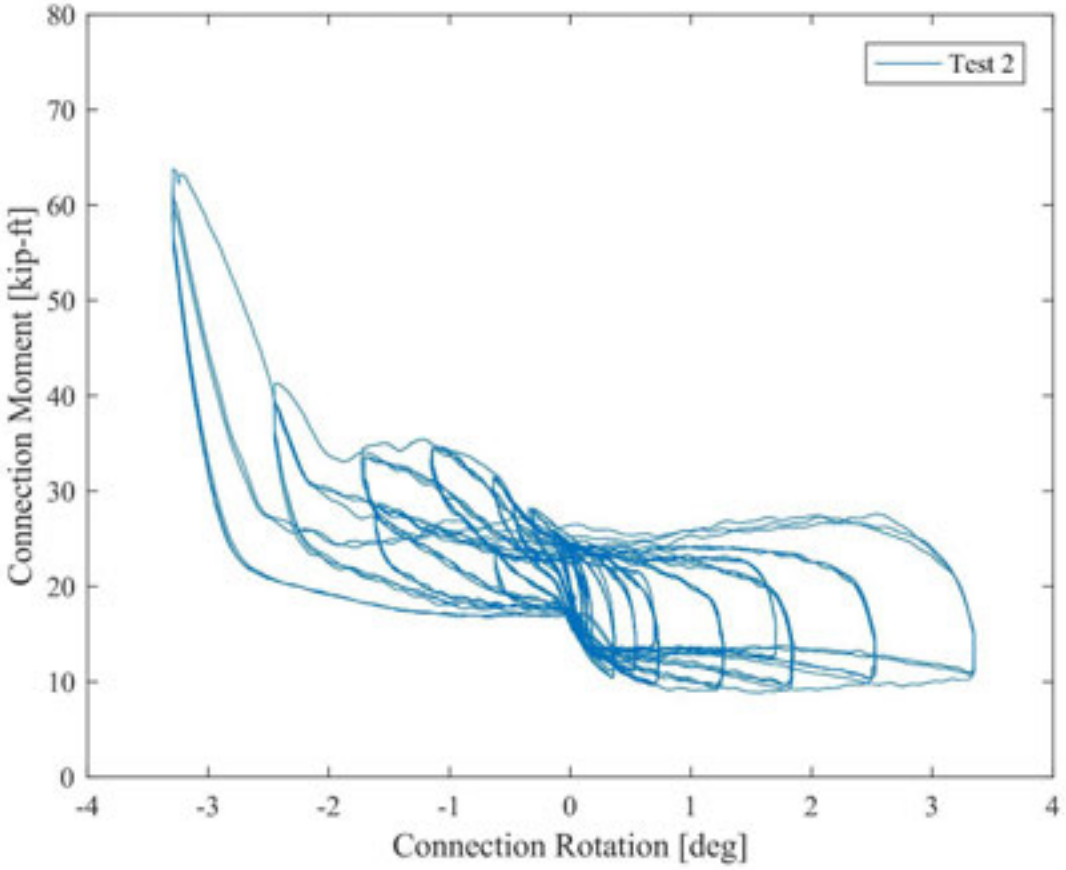

Figure 20 – Test 2 –Connection moment vs. connection rotation

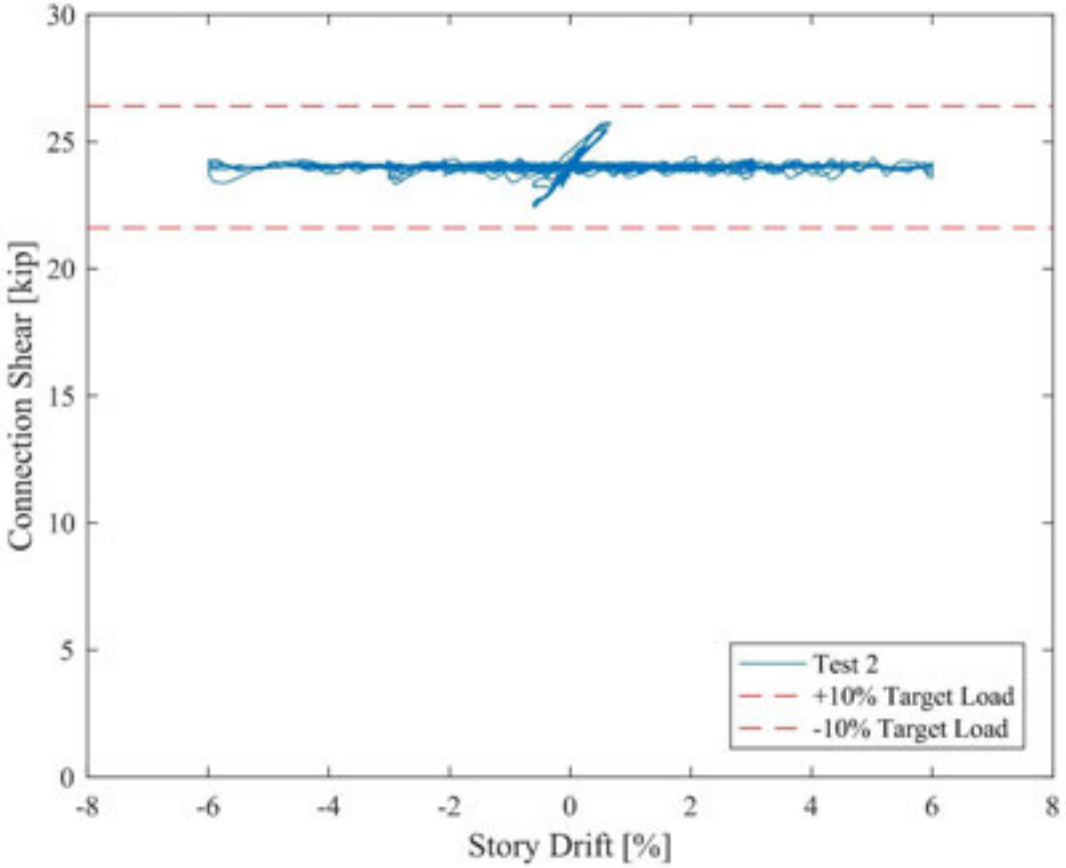

Figure 21 – Test 2 – Connection shear vs. story drift

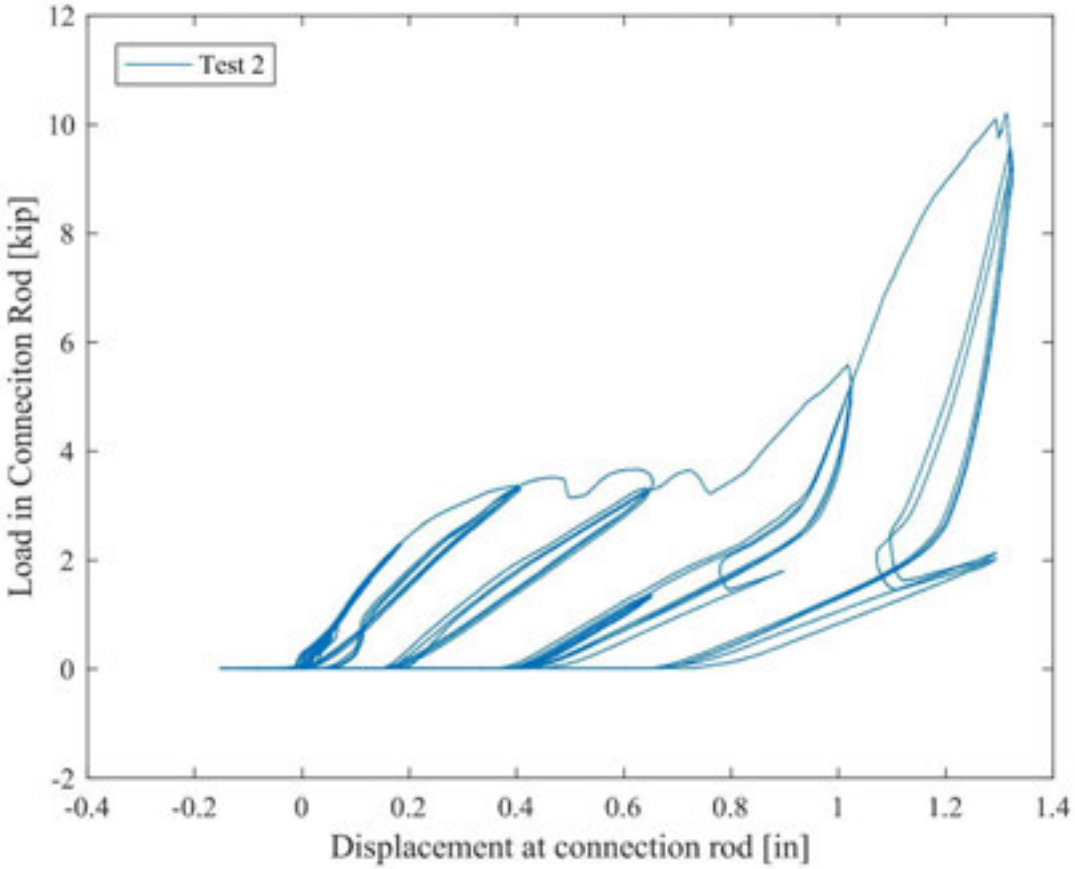

Figure 22 – Test 2 –Load in connection rod vs. displacement at connection rod

Figure 23 – Localized crushing of face C02 after 6% drift cycles

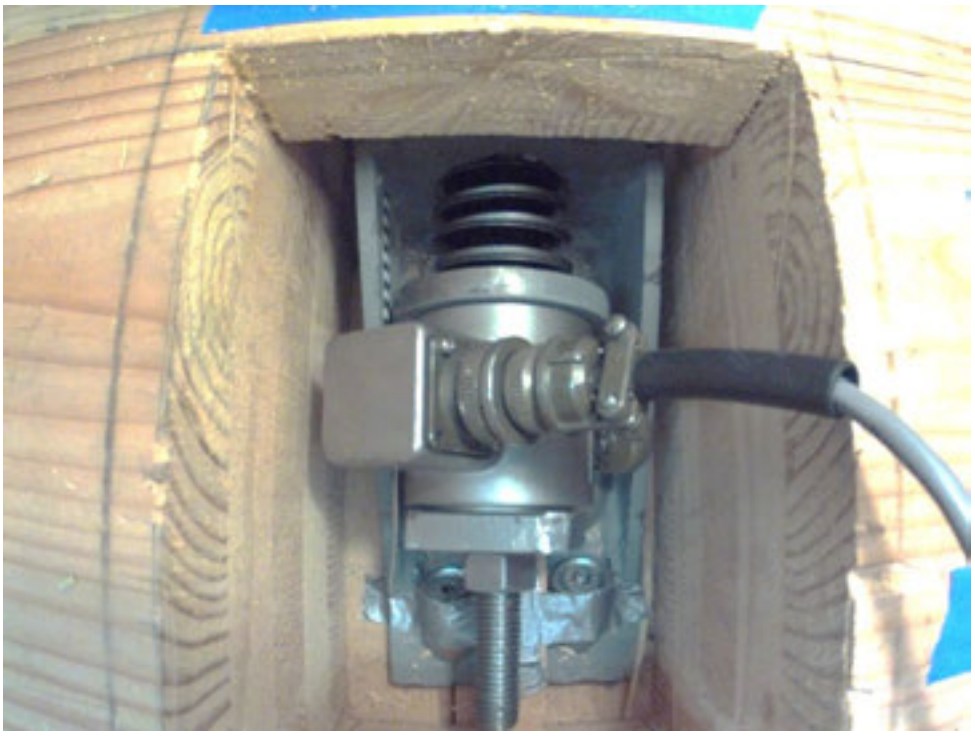

Figure 24 – Disc springs in connection at static state prior to displacement cycles

Figure 25 – Disc springs in connection fully compressed (at 6% drift)

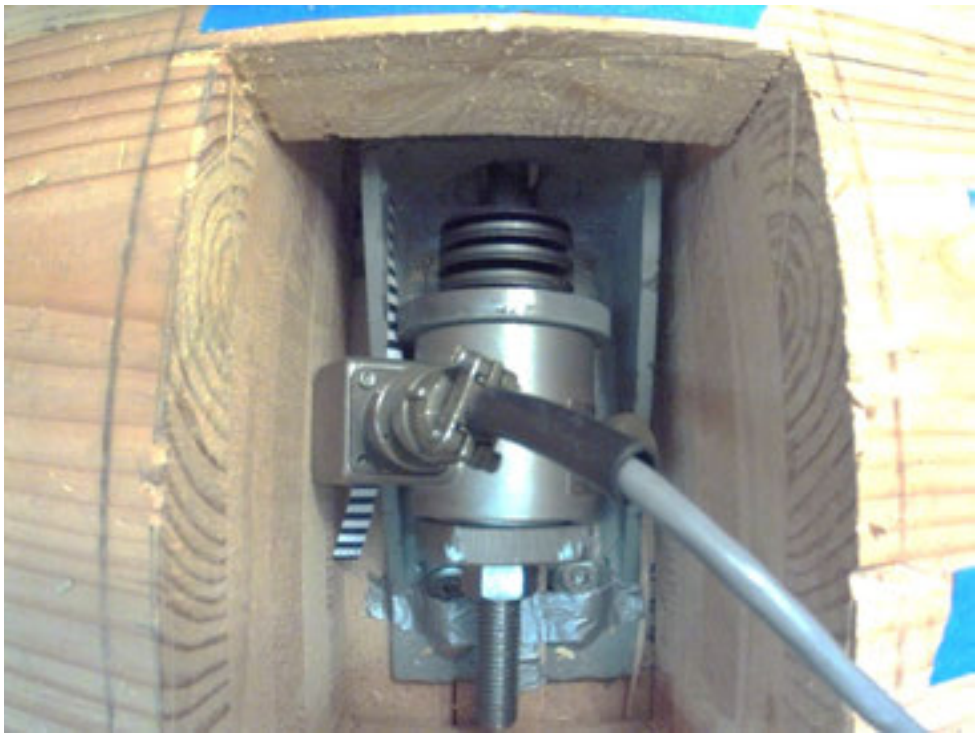

Figure 26 – Disc springs in connection at static state after 6% displacement cycles

4.3 Test 3 – B03 and C03

Test 3 altered the gap-closure mechanism by using thicker, taller disc springs and increased the total to 12 disc springs. As with Test 2, the top of C03 was cut down to ensure a 1/16" gap existed between the top of the column and the CLT-5 floor panel at zero displacement. The Teflon bearing pads were again glued to the connection bearing plate and the compression reinforcing screws were installed deeper into the beam to be flush with the bearing surface. Experimental test results for global behavior in Test 3 involving B03 and C03 are summarized in Figure 27, Figure 28, Figure 29 and Figure 30 on the following pages.

The following relevant observations were noted during Test 3:

- Significant nonlinearity in the force-displacement relationship of the connection rod and disc springs was observed on positive displacement cycles of 2.1% drift and above. Increasing the number of disc springs effectively increased the displacement capacity of the gap-closure mechanism and the test results show the system more drift capacity at lower loads before the connection was "stroked out." The modified disc springs used in Test 3 also extended the drift range of linear force-displacement behavior in the connection beyond that of previous tests.
- The CLT-5 was observed to rub against the top of C03 starting at displacements of 1.2% drift. A repeated rubbing/thumping sound was audible on negative displacement cycles starting at 2.1% drift.

- During all positive displacement cycles of 4.5% and 6% drifts, C03 began to rotate along its longitudinal axis. This appeared to be caused in part by uneven contact between the CLT-5 on the top of C03. As such, the gap between the end of B03 and the face of C03 was not consistent across the beam's cross section for high displacement cycles.
- Loud cracking and popping were heard at 6% drift cycles. No visible cracks were observed in either B03 or C03 during the test protocol.

After the testing protocol was completed, the following relevant observations were noted:

- Similar to Tests 1 and 2, crushing and partial tear-out was observed on the four rows of CLT-5 screws nearest the column.
- The disc-springs showed permanent inelastic deformation from displacements cycles of 2.1% drift and above. As such, the elastic displacement range for the modified disc spring configuration used in Test 3 extended beyond the elastic range from Tests 1 and 2.
- As with Test 2, the back side of C03 showed evidence of crushing around the round plate washer anchoring the connection rod to the column. The drift corresponding to this crushing cannot be directly confirmed from instrumentation, though this most likely occurred only during the 6% drift cycles when the disc springs were fully stroked-out and connection rod loads spiked upward.
- Similar to Tests 1 and 2, a crushing region was observed on the beam-side of C03 where B03 bared against the column during positive displacements. This crushing did not appear to have caused any major structural damage to the beam or column.

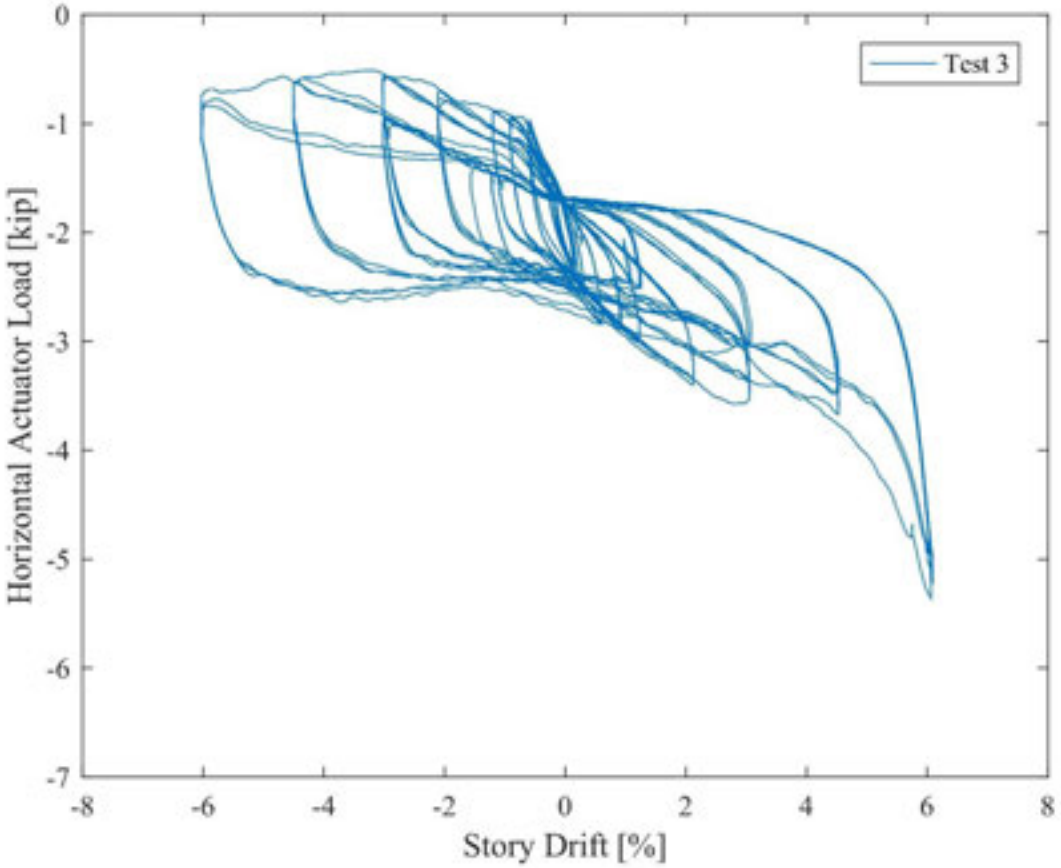

Figure 27 – Test 3 – Horizontal tip load vs. story drift

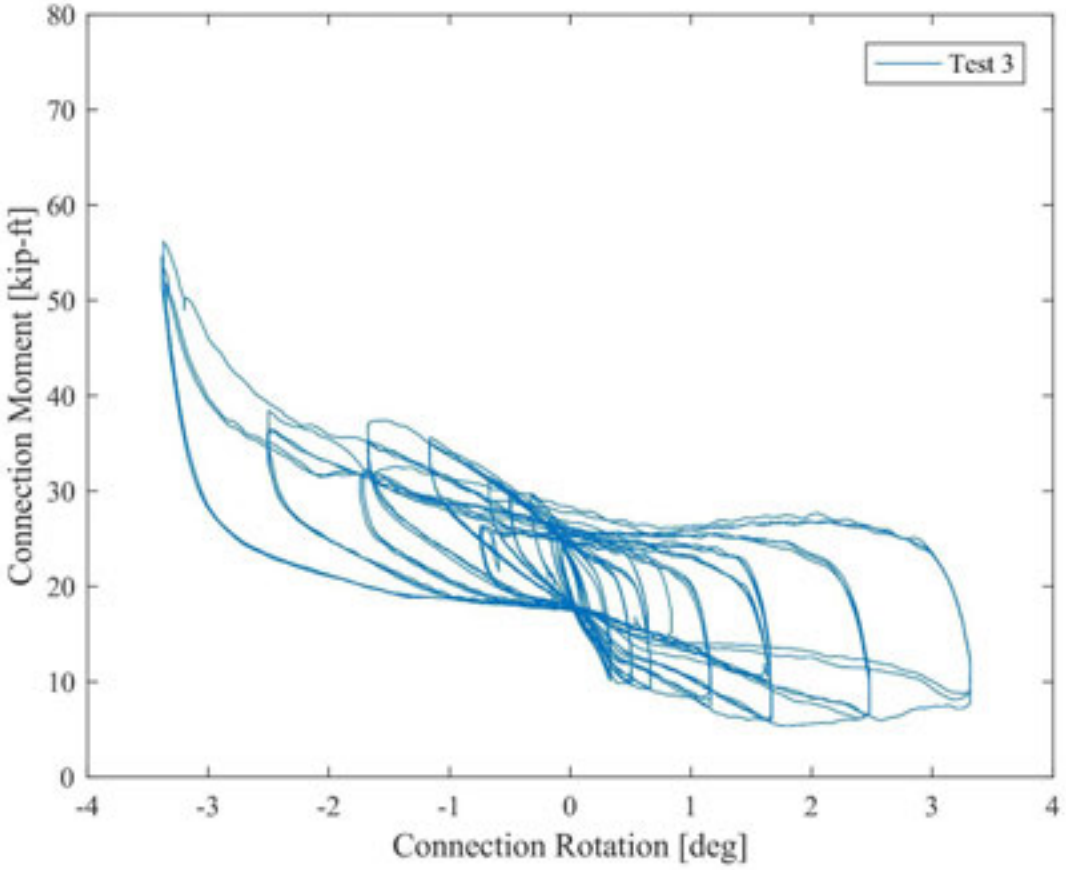

Figure 28 – Test 3 – Connection moment vs. connection rotation

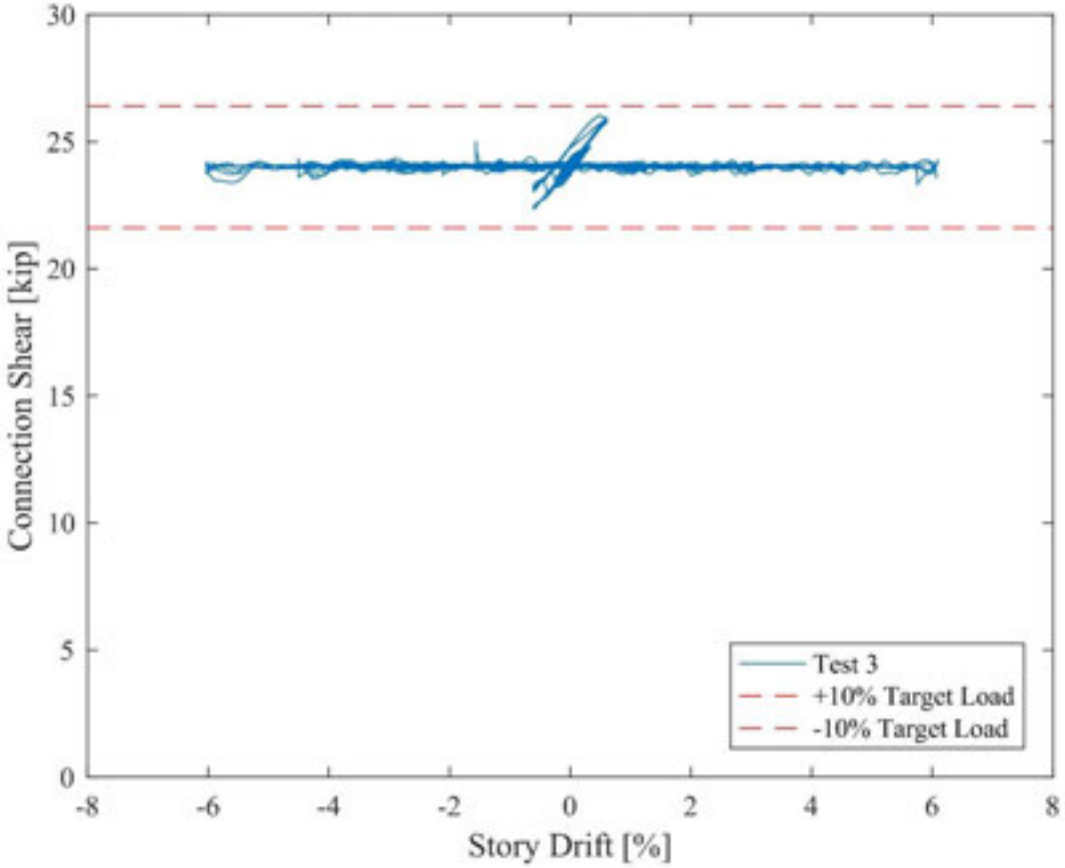

Figure 29 – Test 3 – Connection shear vs. story drift

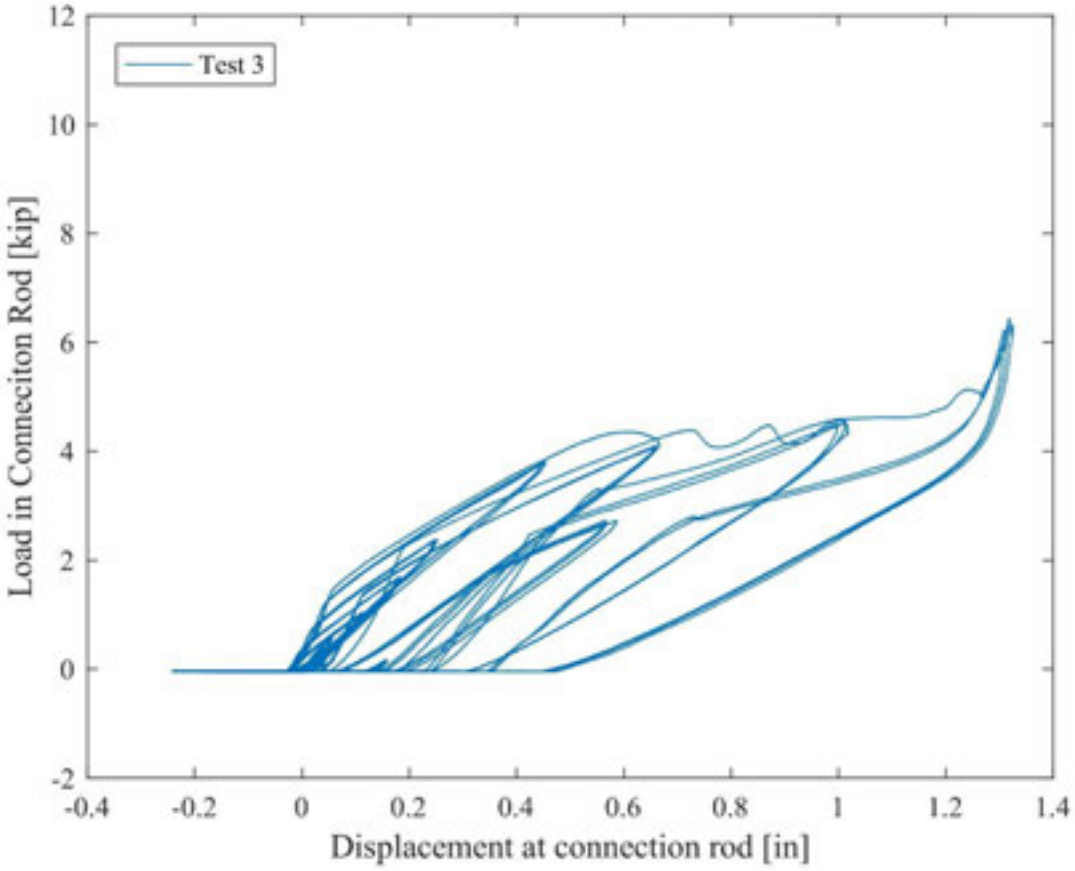

Figure 30 – Test 3 –Load in connection rod vs. displacement at connection rod

5.0 SUMMARY

Three separate tests of the BTC connection were successfully completed. Each of the three connections sustained the required 24-kip connection gravity shear load at displacement cycles up to 6% drift. No significant cracks or other major structural damage were observed in any of the test specimens throughout the entire displacement protocol. Nonlinear behavior was observed in the disc springs at displacements of 0.9% drift and above for Tests 1 and 2. The modified disc springs used in Test 3 displayed nonlinear behavior for drifts of 2.1% and above. As such, the disc springs used in Test 3 remain within the linear force-displacement range for DBE drift of 2%. Figure 31 shows an overlay of connection rod force-displacement curves from Tests 1, 2, and 3, illustrating how increasing the thickness and number of springs used in Test 3 expanded the linear range of the force-displacement relationship.

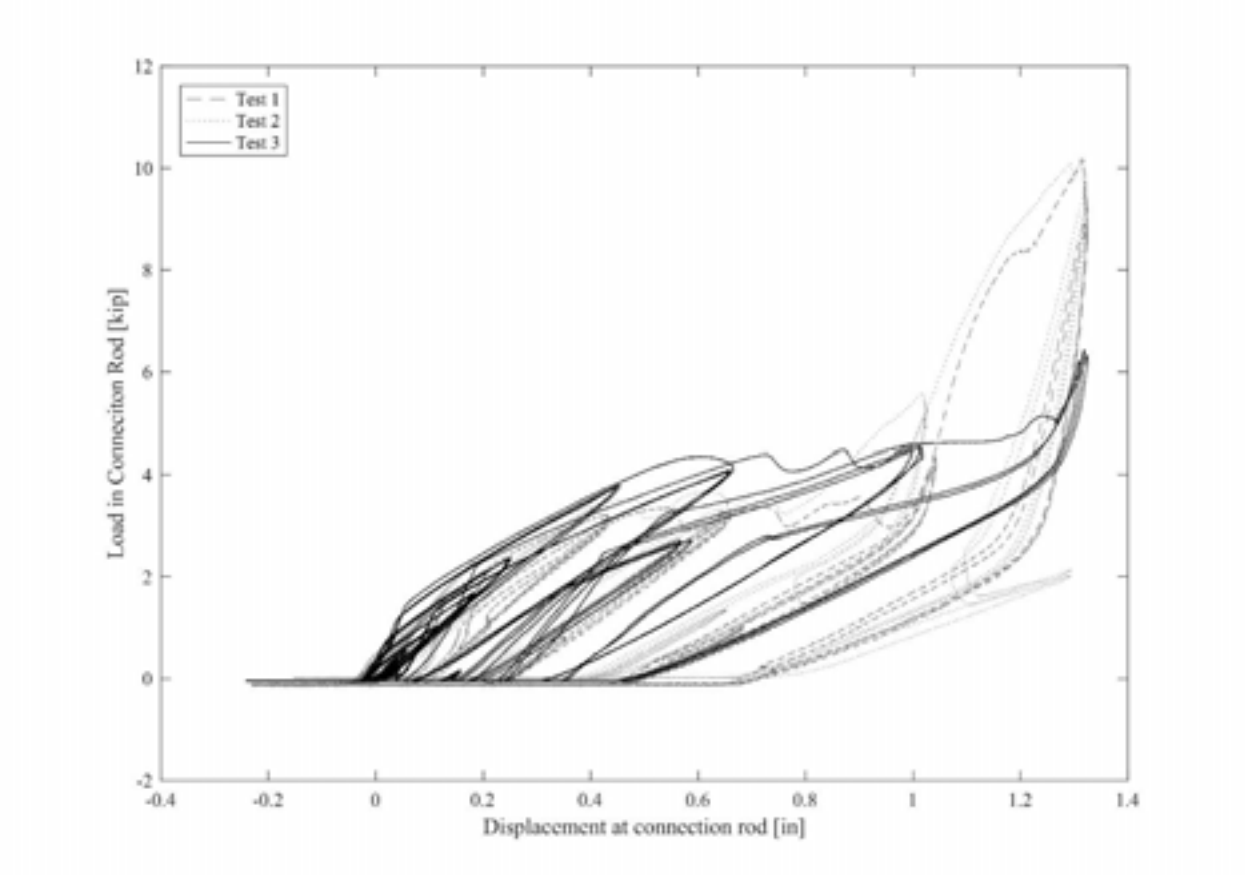

Figure 31 – Overlay of connection force-displacement curves from Tests 1, 2 and 3

APPENDIX A – TEST SETUP AND INSTRUMENTATION PLAN

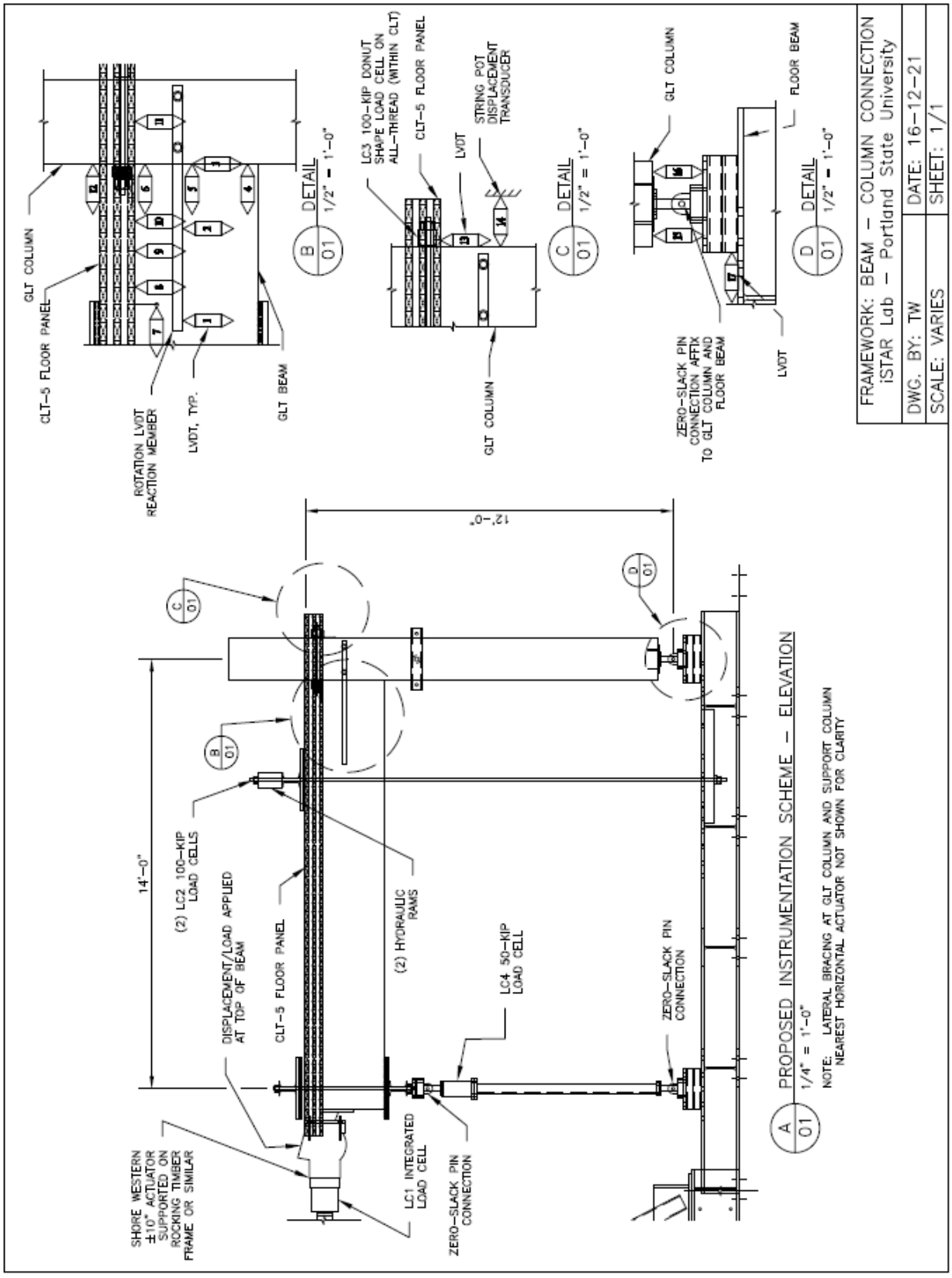

APPENDIX B – EXPERIMENTAL TESTING OBJECTIVES

kpff

Framework

an urban + rural ecology

Experimental Testing Objectives

April 20th 2016

KPFF Consulting Engineers
111 SW Fifth Avenue, Suite 2500
Portland, OR 97204
(503) 227-3251 | www.kpff.com

1.0 Introduction

1.1 Summary

The testing described in this report is pursued to facilitate the design of rocking CLT walls as part of the Framework Project in Portland, OR. Rocking cross-laminated timber (CLT) walls are a new, rapidly evolving technology for use in a building's lateral force-resisting system in regions of high seismicity. While the behavior of rocking systems has been well studied for precast concrete walls, the extension to timber wall buildings raises several additional issues. These are addressed through the testing proposed in this report and include:

- *CLT crushing tests* – These tests will define the nonlinear force-deformation relationship at the toe (compression-end) of the rocking walls, including damage states.
- *CLT wall panel tests* – These tests will define the flexural and shear stiffness of both a bare CLT panel and a CLT panel splice.
- *Glue-laminated timber (GLT) beam-to-column connection tests* – These tests will demonstrate that the gravity connection proposed can accommodate the seismic drift expected for the Framework Project.

1.2 Points of Contact

In discussing issues related to this experimental testing, the following persons shall be considered the primary points of contact:

Structural Engineer of Record Representatives	Eric McDonnell KPFF Consulting Engineers eric.mcdonnell@kpff.com Reid Zimmerman KPFF Consulting Engineers reid.zimmerman@kpff.com
Testing Agencies Representatives	Andre Barbosa Oregon State University andre.barbosa@oregonstate.edu Peter Dusicka Portland State University dusicka@pdx.edu
Material Supply/Fabrication Representative	Lucas Epp StructureCraft Builders Inc. lepp@structurecraft.com

1.3 Schedule

The following is the schedule for testing:

- TBD – Fully fabricated specimens to be delivered to testing agency.
- TBD – Testing completed and results provided to KPFF Consulting Engineers (electronic format is acceptable). Testing agency shall make every effort to supply results from test groups as soon as they become available.
- TBD – Draft report submitted to KPFF Consulting Engineers
- TBD – Comments on draft report provided to testing agency
- TBD – Final report submitted to KPFF Consulting Engineers

2.0 CLT Crushing Tests

2.1 Objective

The objective of the cross-laminated timber (CLT) crushing tests is to determine the stress-strain relationship of the CLT walls out to ultimate failure (i.e., strain at which strength loss falls below 20% of peak strength).

2.2 Specimens and Loading

The following is a description of the specimens and loading for the CLT crushing tests:

- Fully fabricated specimens to be provided and delivered at no cost to testing agency
- Monotonic, quasi-static loading to a deformation at which residual strength stabilizes; expected ultimate load is approximately 520k
- Uniform compression on 18in wide specimen of CLT5; specimen length of 5ft; specimen to be supported to prevent buckling
- Three (6) specimens of bare CLT5; three (6) specimens of CLT5 with self-tapping screws; where more than one CLT supplier is tested, specimen counts above shall be for each supplier

2.3 Deliverables

The following shall be provided to KPFF Consulting Engineers by the date indicated in Section 1.3. Where numerical data is requested, it shall be provided in Microsoft Excel or text format.

- Specimen naming convention consistent across all supplied information
- Measured dimensions and moisture content of specimens
- Photos of specimens from all four sides before and after testing
- Video with audio from both sides of specimen
- Load-deformation response of specimens with corrections applied (e.g., for test setup, actuator, etc.). The deformation at which (1) wood yielding is first visually observed, (2)

cracks or delaminations reach 1in in length, and (3) buckling of wood fibers is first visually observed should also be reported.

- Notes about (1) any unusual circumstances which occurred during setup or testing, and (2) any observations which may affect interpretation of results (e.g., presence of existing cracks, large knots, etc.).

3.0 CLT Wall Panel Tests

3.1 Objective

The objective of the CLT wall panel tests is to assess the material properties of a bare CLT wall panel, and a splice configuration in the built-up CLT wall panel. More specifically, the following are sought: (1) the equivalent linear flexural and shear stiffness of the bare CLT wall panels, and (2) the splice flexural and shear stiffness.

3.2 Specimens and Loading

The following is a description of the specimens and loading for the CLT wall panel tests:

- Fully fabricated specimens to be provided and delivered at no cost to testing agency. Note that post-tensioning cables/rods to be provided by testing agency.
- Cyclic, quasi-static loading in accordance with the abbreviated basic loading history in CUREE Publication No. W-02 except that trailing cycles shall be taken equal to the primary cycle (rather than 75% of it), testing to approximately 200k shear (400k point load); axial load on wall panel to be kept constant at approximately 375k.
- Two (2) 5'x20' CLT9 specimens, two (2) 5'x20' CLT9 specimen with HSK splices, and two (2) 5'x20' CLT9 specimen with project-specific design splice, where more than one CLT supplier is tested, specimen counts above shall be for each supplier; specimens configured as shown below:

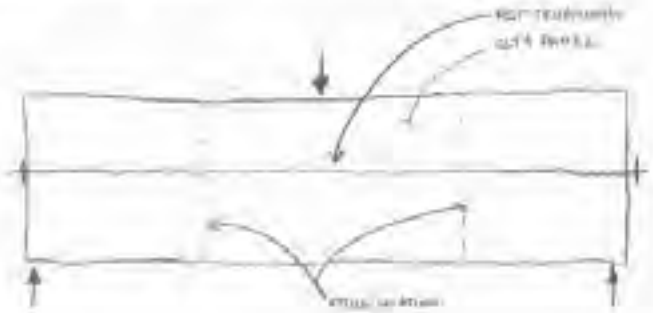

3.3 Deliverables

The following shall be provided to KPFF Consulting Engineers by the date indicated in Section 1.3. Where numerical data is requested, it shall be provided in Microsoft Excel or text format.

- Specimen naming convention consistent across all supplied information
- Measured dimensions and moisture content of specimens
- Photos of specimens from all four sides before and after testing within test setup
- Video with audio of each test
- Global load versus midpoint displacement response of specimens with corrections applied (e.g., for test setup, actuator, etc.).
- Equivalent elastic modulus, E_{eq}, and equivalent shear modulus, G_{eq} for each bare CLT test
- Shear load-shear deformation response and moment-rotation response of splice connections
- Notes about (1) any unusual circumstances which occurred during setup or testing, (2) any observations which may affect interpretation of results (e.g., presence of existing cracks, large knots, etc.), and (3) observation of any nonlinearity during tests (e.g., localized crushing at actuators, wood splitting, etc.).

4.0 GLT Beam to Column Connection Tests

4.1 Objective

The objective of the glulam timber (GLT) beam to column connection tests is to demonstrate that the proposed beam-to-column connection shown below is capable of withstanding cyclic deformations out to the drifts expected in the building at the risk-targeted maximum considered earthquake without loss of gravity-carrying capacity. This is often referred to as a deformation-compatibility check. The rotation at which damage occurs (but that does not necessarily affect gravity-carrying capacity) is also sought.

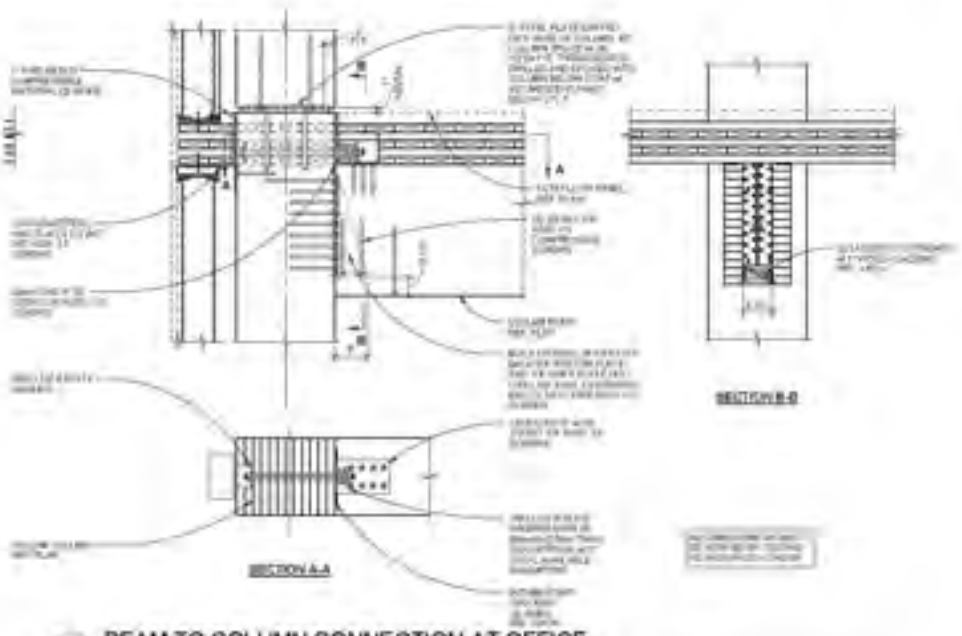

1 BEAM TO COLUMN CONNECTION-AT OFFICE

4.2 Specimens and Loading

The following is a description of the specimens and loading for the GLT beam-to-column connection tests:

- Fully fabricated specimens to be provided and delivered at no cost to testing agency
- Cyclic, quasi-static lateral loading in accordance with the abbreviated basic loading history in CUREE Publication No. W-02 except that trailing cycles shall be taken equal to the primary cycle (rather than 75% of it); testing shall be conducted to at least 6% drift, continuing to failure or the stroke capacity of the actuators; imposed shear load in beam to remain constant at 20k during cycling (corresponding to 1.32D + 0.5L); gravity loading in column need not be applied
- Full scale specimens of GLT 14¼in x 16½in column (14ft long) and GLT 12¼in x 24in beam (14ft long); no CLT floor panels to be included
- Three (3) specimens total

4.3 Deliverables

The following shall be provided to KPFF Consulting Engineers by the date indicated in Section 1.3. Where numerical data is requested, it shall be provided in Microsoft Excel or text format.

- Specimen naming convention consistent across all supplied information

- Measured dimensions and moisture content of specimens
- Photos of specimens from all four sides before and after testing within test setup
- Video with audio of each test
- Tip load versus deflection response of specimens with corrections applied (e.g., for test setup, actuator, etc.). The drift ratio at which visible damage is observed, if occurs, shall also be reported.
- Tip load versus connection rotation response of specimens with corrections applied (e.g., for test setup, actuator, etc.).
- Notes about (1) any unusual circumstances which occurred during setup or testing, (2) any observations which may affect interpretation of results (e.g., presence of existing cracks, large knots, etc.), and (3) observation of any nonlinearity during tests (e.g., localized crushing at actuators, cracking in beam or column etc.).

APPENDIX C – TEST SPECIMEN PHOTOS

Figure 32 – Pre-test facing east

Figure 33 – Pre-test facing north

Figure 34 – Pre-test facing west

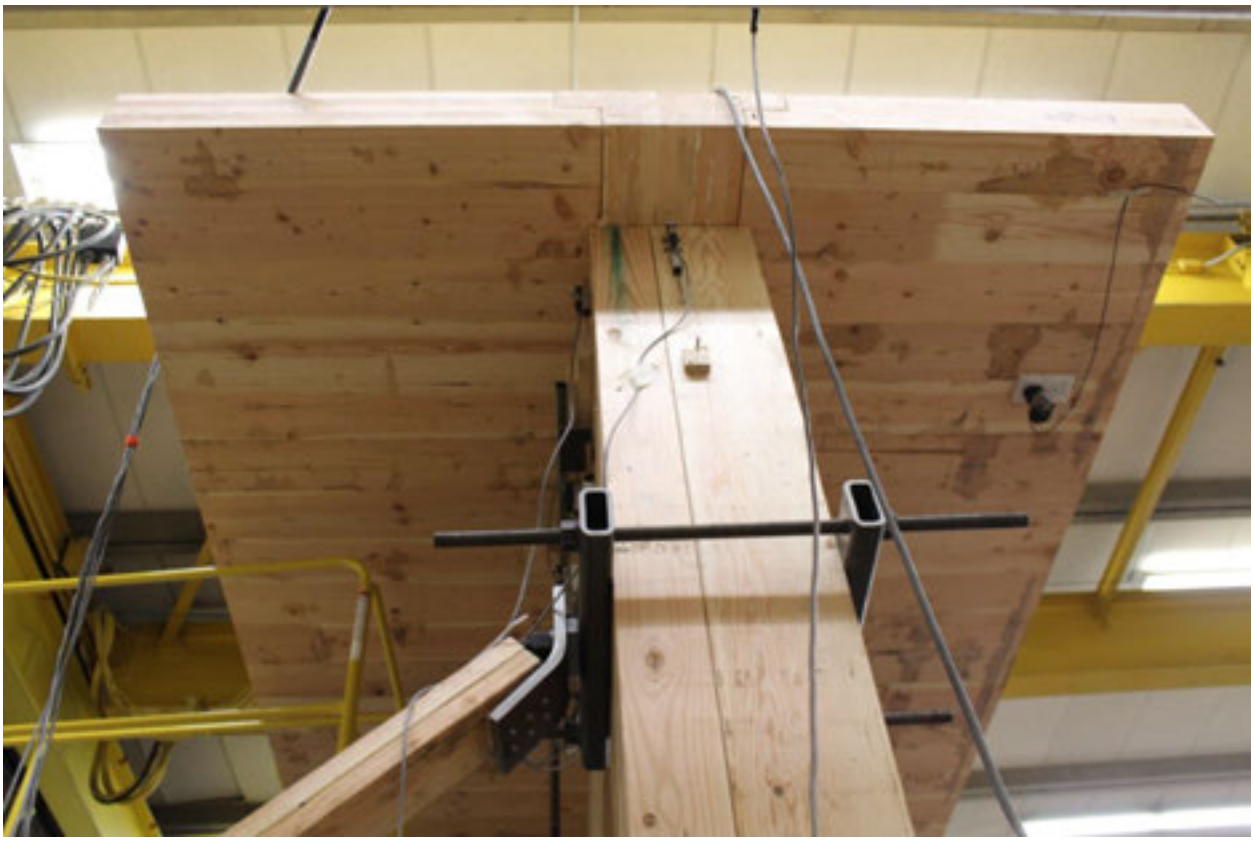

Figure 35 – Pre-test facing north

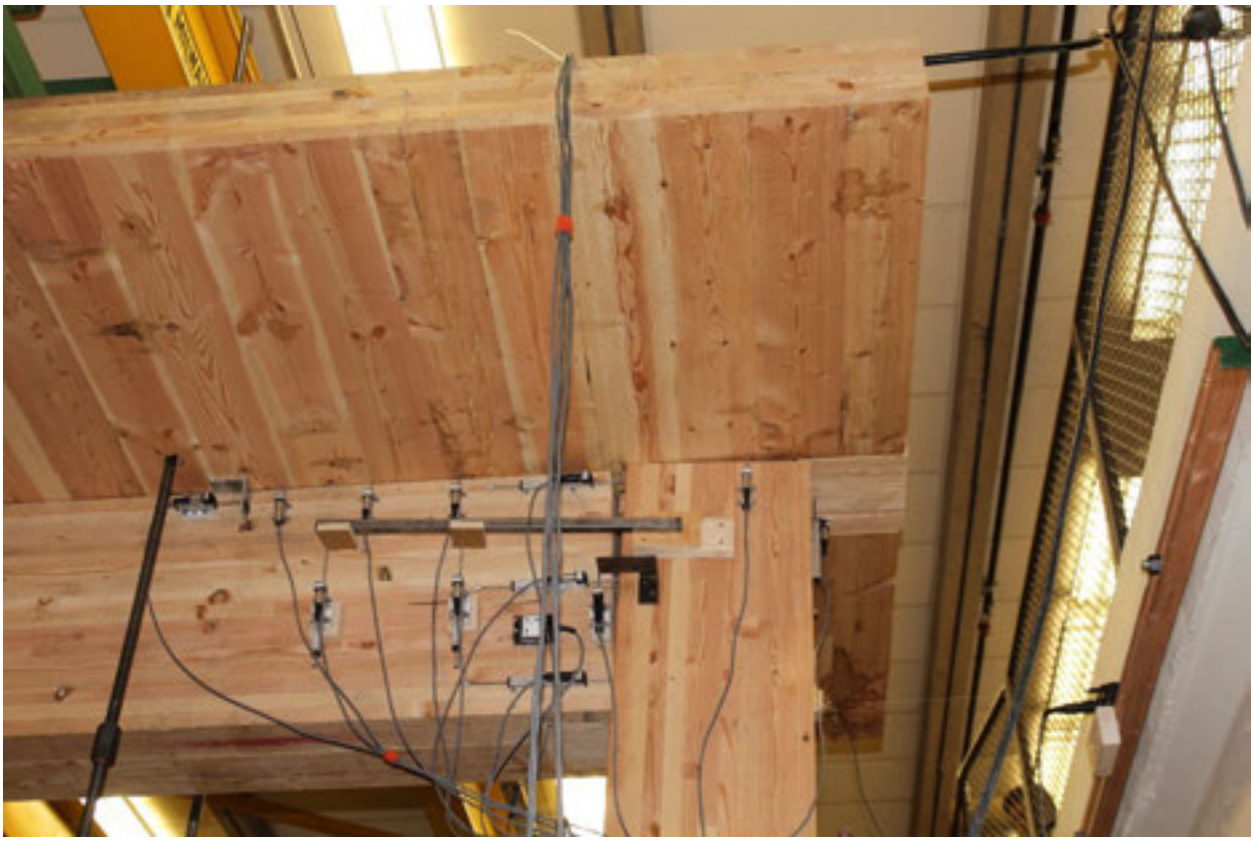

Figure 36 – End of test facing west

Figure 37 – End of test facing east